NPS-MR-95-001

NAVAL POSTGRADUATE SCHOOL
Monterey, California

SYSTEMATIC AND INTEGRATED APPROACH TO TROPICAL CYCLONE TRACK FORECASTING PART II: CLIMATOLOGY, REPRODUCIBILITY, AND REFINEMENT OF METEOROLOGICAL KNOWLEDGE BASE

by

Lester E. Carr, III, Mark A. Boothe, Sean R. White,
Chris S. Kent, and Russell L. Elsberry

September 1995

Prepared for: Office of Naval Research
Code 322MM, Arlington, VA 22217-5660

Naval Postgraduate School
Monterey, California 93943-5000

Rear Admiral M. J. Evans
Superintendent

Richard S. Elster
Provost

This report was prepared for the Joint Typhoon Warning Center (JTWC) at the Naval Pacific Meteorology and Oceanography Center (NPMOC) West, Guam and for the Alternate JTWC at NPMOC, Pearl Harbor, Hawaii. Funding was provided by the Office of Naval Research Marine Meteorology Program.

This report was prepared by:

REPORT DOCUMENTATION PAGE

Form Approved
OMB No. 0704-0188

1. AGENCY USE ONLY (Leave blank)	2. REPORT DATE	3. REPORT TYPE AND DATES COVERED
	September 1995	Interim 10/94 - 9/95

4. TITLE AND SUBTITLE Systematic and Integrated Approach to Tropical Cyclone Track Forecasting. Part II. Climatology, Reproducibility, and Refinement of Meteorological Knowledge Base

5. FUNDING NUMBERS

6. AUTHOR(S) Lester E. Carr, III, Mark A. Boothe, Sean R. White, Chris S. Kent, and Russell L. Elsberry

7. PERFORMING ORGANIZATION NAME(S) AND ADDRESS(ES)
Naval Postgraduate School
Department of Meteorology
589 Dyer Rd., Room 254
Monterey, CA 93943-5114

8. PERFORMING ORGANIZATION REPORT NUMBER

9. SPONSORING/MONITORING AGENCY NAME(S) AND ADDRESS(ES)
Office of Naval Research
Code 322MM
800 N. Quincy
Arlington, VA 22217-5000

10. SPONSORING/MONITORING AGENCY REPORT NUMBER

11. SUPPLEMENTARY NOTES The views expressed in this report are those of the author and do not reflect the official policy or position of the Department of Defense.

12a. DISTRIBUTION/AVAILABILITY STATEMENT
Approved for Public Release: Distribution Unlimited

12b. DISTRIBUTION CODE

13. ABSTRACT

This report continues the development of the Systematic Approach to tropical cyclone track forecasting by Carr and Elsberry (1994) with specific application to the western Pacific region. Five years (1989-93) of 12-h Naval Operational Global Atmospheric Prediction System (NOGAPS) analyses are examined for every tropical cyclone to establish a climatology of Environment Structure characterizations. Frequencies of the four Synoptic Patterns and the six Synoptic Regions are calculated, and characteristic tracks while in each of the Pattern/Region combinations are provided. Transition paths between the various Pattern/Region combinations are tabulated.

A four-year subset of NOGAPS analyses is used in a reproducibility test in which three trainees attempted to achieve the same Environment Structure assignments as an experienced forecaster. Approximately 81% of the Synoptic Patterns, 86% of the Synoptic Regions, and 77% of the Pattern/Region combinations were correctly assigned by the trainees. However, certain Pattern/Region combinations were found to be poorly identified, which indicated a need for some new training materials. Approximately 81% of the Pattern/Region transitions to a correct or similar combination were detected by the trainees. About 72% of these correct/similar transitions were identified within $\pm$ 12 h of the actual transition, and 88% were identified within $\pm$ 24 h. Certain transitions were consistently missed, which again indicates a need for improved descriptions and training.

Refinements of the Meteorological Knowledge Base of the Systematic Approach were made on the basis of the five-year climatology and reproducibility test. These refinements, which are summarized in Chapter 4.9, include new transitional mechanisms associated with Monsoon Gyre Formation and Dissipation and Reverse-oriented Trough Formation. A new conceptual model called Subtropical Ridge Modulation is defined in which superposition of a midlatitude trough or ridge may account for an Environment Structure transition.

To clarify the application to specific situations and to improve the recognition of transitions, probabilities or transitions from each Pattern/Region combination are provided from the five-year climatology. In addition, guidelines are tabulated for each transition in terms of the key indicators in the streamline/isotach analysis, satellite imagery, and track changes.

14. SUBJECT TERMS Tropical cyclone track forecasting
Tropical cyclone motion

15. NUMBER OF PAGES 96

16. PRICE CODE

17. SECURITY CLASSIFICATION OF REPORT	18. SECURITY CLASSIFICATION OF THIS PAGE	19. SECURITY CLASSIFICATION OF ABSTRACT	20. LIMITATION OF ABSTRACT
Unclassified	Unclassified	Unclassified	

TABLE OF CONTENTS

ABSTRACT

This report continues the development of the Systematic Approach to tropical cyclone track forecasting by Carr and Elsberry (1994) with specific application to the western Pacific region. Five years (1989-93) of 12-h Naval Operational Global Atmospheric Prediction System (NOGAPS) analyses are examined for every tropical cyclone to establish a climatology of Environment Structure characterizations. Frequencies of the four Synoptic Patterns and the six Synoptic Regions are calculated, and characteristic tracks while in each of the Pattern/Region combinations are provided. Transition paths between the various Pattern/Region combinations are tabulated.

A four-year subset of NOGAPS analyses is used in a reproducibility test in which three trainees attempted to achieve the same Environment Structure assignments as an experienced forecaster. Approximately 81% of the Synoptic Patterns, 86% of the Synoptic Regions, and 77% of the Pattern/Region combinations were correctly assigned by the trainees. However, certain Pattern/Region combinations were found to be poorly identified, which indicated a need for some new training materials. Approximately 81% of the Pattern/Region transitions to a correct or similar combination were detected by the trainees. About 72% of these correct/similar transitions were identified within $\pm$ 12 h of the actual transition, and 88% were identified within $\pm$ 24 h. Certain transitions were consistently missed, which again indicates a need for improved descriptions and training.

Refinements of the Meteorological Knowledge Base of the Systematic Approach were made on the basis of the five-year climatology and reproducibility test. These refinements, which are summarized in Chapter 4.9, include new transitional mechanisms associated with Monsoon Gyre Formation and Dissipation and Reverse-oriented Trough Formation. A new conceptual model called Subtropical Ridge Modulation is defined in which superposition of a midlatitude trough or ridge may account for an Environment Structure transition.

To clarify the application to specific situations and to improve the recognition of transitions, probabilities or transitions from each Pattern/Region combination are provided from the five-year climatology. In addition, guidelines are tabulated for each transition in terms of the key indicators in the streamline/isotach analysis, satellite imagery, and track changes.

ACKNOWLEDGMENTS

This research has been sponsored by the Office of Naval Research Marine Meteorology Program under the management of Robert F. Abbey, Jr. The authors gratefully acknowledge the crucial assistance and many valuable contributions made by personnel at the Naval Pacific Meteorology and Oceanography Center Pearl Harbor, Hawaii. Particular appreciation is extended to CAPT J. Etro for his ongoing support of this research project and for making available personnel and facilities at NPMOC West Guam/JTWC during the development of this research. Many thanks to LCDR E. Petzrick, Deputy Director JTWC, and to his relief LCDR M. Angove for their support of this project, and for handling the administrative details associated with the first author's visits to Guam. Mr. F. Wells and Mr. E. Fukada provided valuable comments and suggestions on the manuscript. NOGAPS analyses were provided by the Fleet Numerical Meteorology and Oceanography Center. Sean White (NOAA Corp) has participated as part of an educational program. Mrs. Penny Jones expertly typed the manuscript.

LIST OF FIGURES

LIST OF TABLES

1. Introduction

In a previous technical report, Carr and Elsberry (1994; hereafter CE) introduced the concept of a Systematic and Integrated Approach to Tropical Cyclone (TC) Track Forecasting, which will hereafter be referred to as the Systematic Approach. In short, the objective of the Systematic Approach is to enable the forecaster to formulate an official TC track forecast that consistently improves upon the accuracy of numerical and other objective TC motion forecast guidance, particularly in the minority of cases where the numerical model forecast errors are very large. The central premise of the Systematic Approach is that for the forecaster to "add value" to the available track forecast models he/she must have a reasonably comprehensive knowledge of how the forecast guidance tends to err in various recurring meteorological situations, and a consistent procedure for formulating the official track forecast to minimize errors.

After setting forth the motivation and methodological framework (CE Fig. 2.1) for the Systematic Approach, the bulk of CE was devoted to development of a set of conceptual models of Environment Structure, TC Structure, and TC-Environment Transformations (CE Fig. 2.1 and Tables 3.1-3.3). These conceptual models serve as a meteorological knowledge base for TC motion, and provide the underlying dynamical foundation of the Systematic Approach. A subsequent technical report will complete the initial introduction of the Systematic Approach by developing a second knowledge base of numerical TC forecast model traits and objective TC track forecast technique traits organized around the meteorological knowledge, and by illustrating the potential practical utility of the complete Systematic Approach via several representative case studies. Although such a technical report is currently under development, preparation of this interim report seemed desirable for the reasons set forth below.

Many of the dynamical processes and much of the nomenclature associated with the conceptual models of the meteorological knowledge base were introduced in CE. During the model-by-model development of the knowledge base, the emphasis was on acquainting forecasters with the key aspects of each model. No attempt was made to describe the range of possible and sometimes subtle ways the models must be applied to a wide variety of actual situations. In addition, the conceptual models of Environment Structure and structure change via TC-Environment Transformations were illustrated in CE using comparatively unambiguous real-world examples that were chosen to highlight a particular conceptual model and minimize the role of competing influences. Thus, the format of CE provides a somewhat simplified exposition of the meteorological knowledge base to facilitate assimilation of the key components by TC forecasters. In particular, CE does not provide climatological frequencies of various recurring conceptual model combinations nor a comprehensive view of the preferred paths of change among the model combinations.

Much emphasis was given in CE to developing a number of conceptual models for various modes of significant interaction between the circulation of the TC and the environment. In these so-called TC-Environment transformation models, the presence of

a TC may precipitate major changes or "transitions" in Environment Structure[1] that in turn result in substantial changes in the motion of that TC or other nearby TCs. Owing to space constraints, no discussion was included of important situations in which largely TC-independent evolutions of Environment Structure are the principal source of major changes in TC motion.

This report addresses the above issues that were not covered in CE. In Chapter 2, the results of using the Systematic Approach meteorological knowledge base to characterize a large number of TC motion scenarios in the western North Pacific is presented. Analysis of the resulting climatology will reveal such important facts as:

(i) the frequency of various combinations of the Synoptic Patterns and Regions that comprise the set of Environment Structure conceptual models, including year-to-year and season-to-season variability;

(ii) characteristic TC tracks associated with particular Pattern/Region combinations; and

(iii) the frequency of Environment Structure transitions between various combinations of Synoptic Patterns and Regions, as well as the range of characteristic TC track changes arising from the transitions.

Case studies presented in CE showed particularly distinct transitions in Environment Structure, e.g., when the TC-Environment transformation acts robustly and alone. However, environment transitions may be precluded, delayed, or terminate with a reversion to a previous Pattern/Region owing to competing influences such as concurrent TC-Environment transformations or Environmental Structure evolutions largely unrelated to the TC. The climatological analysis presented in Chapter 2 will also address the various types and frequencies of the recurring transitions.

Operational utilization of the meteorological knowledge base of the Systematic Approach presumes the forecaster will be able to identify the correct Synoptic Pattern and Region without the benefit of hindsight that is available to the researcher. The second objective of this report is to present in Chapter 3 the results of a "reproducibility test," in which three trainees apply the TC-Environment conceptual models and attempt to achieve the same classification as one of the developers of the Systematic Approach, who is an

---

[1] By contrast, most recent basic research into the processes affecting TC motion has been organized around the hypothesis that TC motion results from the superposition of: (i) a predominant, passive response of the TC to advection by a large-scale environment that evolves essentially independently of the TC; and (ii) a second-order propagation of the TC relative to that environmental advection.

experienced forecaster and was permitted to have recourse to hindsight. Such a test provides information such as:

(i) the relative difficulty of discerning various Synoptic Pattern/Region combinations, and discerning the type and timing of Environment Structure transitions between Patterns and between Regions within a Pattern;

(ii) ambiguities in the formulation and documentation of the various TC-Environment conceptual models when applied to a wide array of real-world situations; and

(iii) deficiencies in the training of the test participants, which need to be corrected to improve the utility of the Systematic Approach meteorological knowledge base to the operational forecaster.

The third objective of this report is to present a refined and more comprehensive view of the meteorological knowledge base of the Systematic Approach based on the insights gained from the climatological analysis and the reproducibility test. Included in this objective is the development of some operationally useful tools that will assist the forecaster in better understanding and applying the meteorological knowledge base of the Systematic Approach to a wide range of TC-Environment situations. The forecaster is first provided the range of climatologically recurring "paths" of Environment Structure transitions and associated TC track changes. However, the additional modes of Environmental Structure transitions have been identified through the climatological analysis in Chapter 2 will be described in Chapter 4. Case studies similar to those in CE will be provided to familiarize the forecaster with the general nature of these other modes of Environment Structure transitions and the associated TC track changes.

The second tool to be introduced in Chapter 5 will be a set of operationally relevant flow charts that will equip the forecaster with the ability to ascertain whether the TC-Environment situation is in the process of transitioning, and what the most probable transition should be given the present TC-Environment situation. Brief summaries will be included of the key processes and identifying attributes associated with the various TC-Environment structures, changes in those structures, and the underlying transitional mechanisms.

2. Climatology of Synoptic Patterns and Regions

(Principal Author, M. A. Boothe)

2.1 Introduction

The Environment Structure of the tropical western North Pacific tends to resemble one of four Synoptic Patterns defined (Table 2-1) in the Systematic and Integrated Approach to Tropical Cyclone Track Forecasting (hereafter Systematic Approach) of Carr and Elsberry (1994; hereafter CE). In addition, the tropical cyclone (TC) lies in a smaller Synoptic Region (Table 2-1) within the Synoptic Pattern, such that the environmental flow associated with this Synoptic Pattern/Region determines the storm's motion. The first objective of this chapter is to describe a climatological data base that has been developed in terms of the Synoptic Pattern/Region frequency of occurrence based on all western North Pacific TCs during 1989-1993. Various TC track characteristics for each Pattern/Region will also be presented. This climatological data base provides insights for assigning properly the present and future Environment Structure.

2.2 Data Base

L. Carr has examined five years (1989-93) of 12-h Naval Operational Global Atmospheric Prediction System (NOGAPS) 500 mb analyses of streamlines and isotachs for all dates *on which a TC existed* in the western North Pacific. Only storms of intensity equal

Table 2-1. Synoptic Pattern/Region combinations (with abbreviations) that characterize the Environment Structure in the Systematic Approach (see descriptions in CE).

Patterns	Regions
S - Standard	DR - Dominant Ridge WR - Weakened Ridge AW - Accelerating Westerlies
N - North Oriented	NO - North-Oriented AW - Accelerating Westerlies
G - Monsoon Gyre	DR - Dominant Ridge NO - North-Oriented AW - Accelerating Westerlies
M - Multiple TCs	NF - Northerly Flow SF - Southerly Flow

to or exceeding 25 kt (12 m s^{-1}) have been included in the data base. Synoptic Pattern/Region assignments have been made for each storm based on the NOGAPS analyses, visible and infrared satellite imagery, and the *complete* storm track. That is, L. Carr had the benefit of both the past and the future motion to ensure that these Pattern/Region assignments could serve as the best possible standard or benchmark for a "reproducibility test" to be described in Chapter 3. A total of 166 storms during the five years results in 2485 Pattern/Region assignments that constitute this climatological data base. When multiple storms exist, separate Pattern/Region assignments are made for each storm.

Evaluation of NOGAPS analyses has been limited to the 500 mb level (vice the optimum steering level for the TC intensity as recommended in CE) because only that level was immediately available for the entire 5-year period in the Naval Postgraduate School archives. This decision made it difficult to make an unambiguous Pattern/Region assignment on the basis of the NOGAPS analysis alone in a few situations involving weak TCs near the subtropical ridge axis or near other TCs. However, knowledge of the subsequent motion of the TC permitted a resolution of such ambiguities. For example, a situation involving a weak TC that is just equatorward of a thin subtropical ridge, which might be characterized equally well as S/DR or S/WR given only the 500 mb analysis, would be readily described as S/DR if the TC track over the next 12 h was west-northwest at a steady 10-12 kt (as opposed to a slowing and turn toward the north).

Changes in the TC Environment Structure may occur either due to large-scale forcing or owing to interactions with the TC. During such transitions, the Environment Structure has features of both the original Pattern/Region as well as the one toward which it is changing. These transitional situations have been recorded by assigning two Patterns and two Regions, with the original Pattern/Region always recorded first until the transition is complete.

2.3 Pattern and Region Frequencies

The first question to be addressed is: "For any given time, what are the odds that a TC will be in a particular Pattern/Region?" The resulting climatology is obtained by counting each of the 2485 map time assignments as one occurrence of the particular Pattern/Region. For transitional (dual assignment) situations, each Pattern/Region is counted as one half, so that the total number of cases remains as 2485.

2.3.1 Pattern Frequency

The cumulative frequency of TCs existing in the four Synoptic Patterns is shown in Fig. 2.1a. The Standard (S) Synoptic Pattern, which is characterized by a strong generally east-west oriented subtropical ridge with trade wind easterlies and monsoon (or near-equatorial) trough equatorward, is the most prevalent (58%) Pattern. This seemingly high percentage is not surprising when it is realized that TCs in the S/DR Pattern/Region can

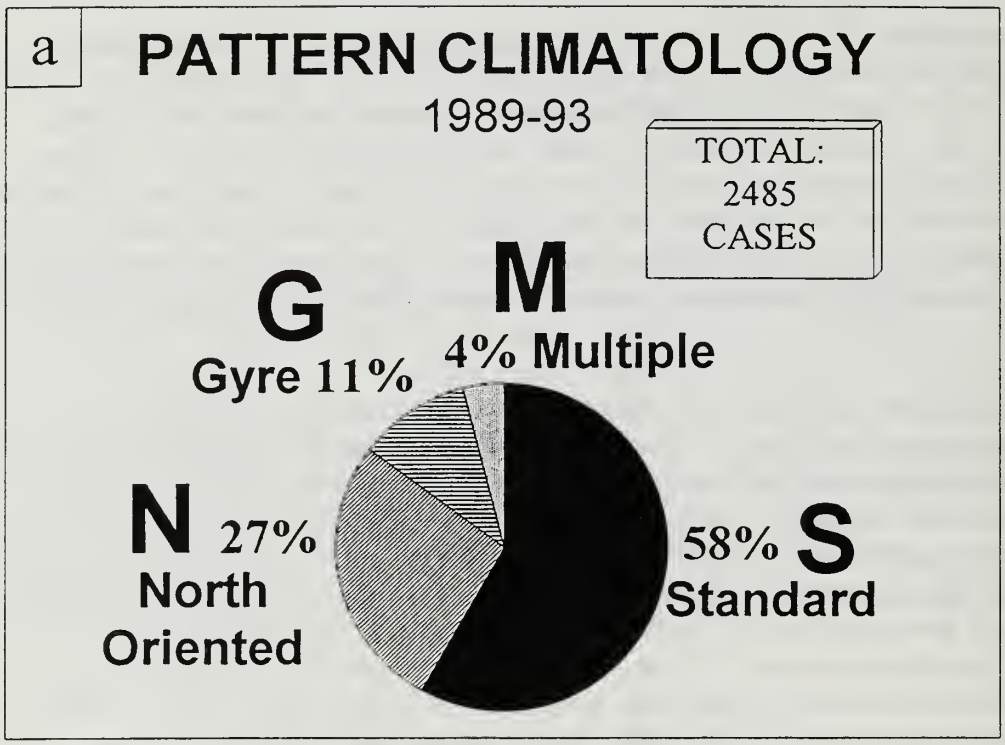

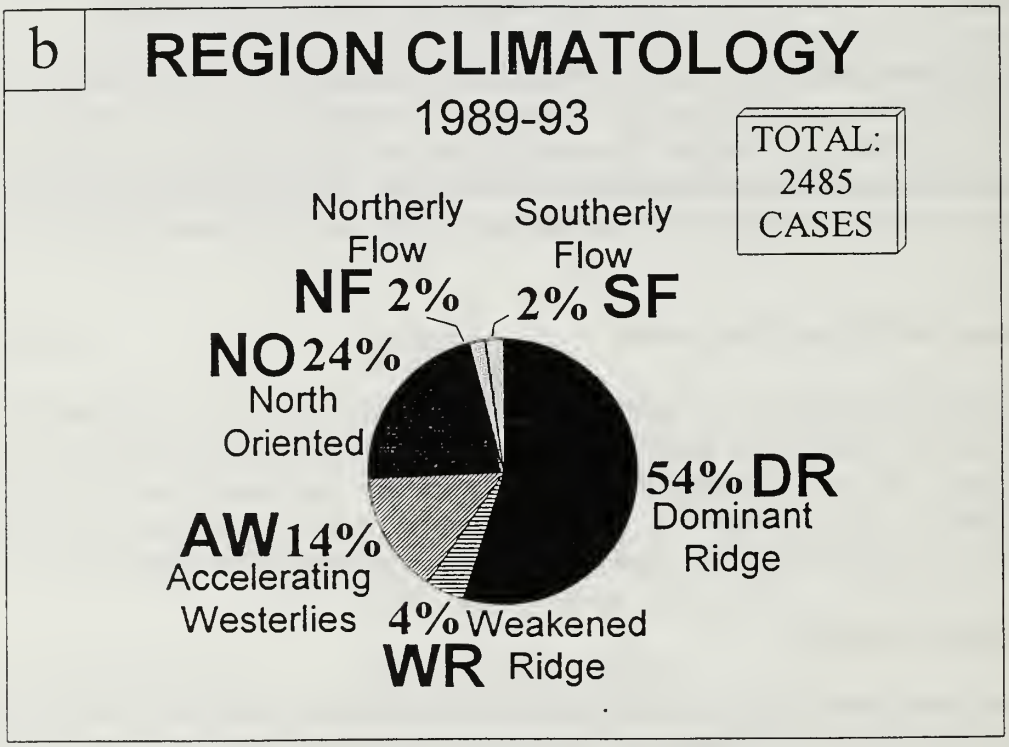

Fig. 2.1 Climatology of (a) Synoptic Patterns and (b) Synoptic Regions during 1989-1993 in the western North Pacific.

remain equatorward of the subtropical ridge all their lives and produce long straight-running tracks. In 27% of the 2485 cases, the TC is in a north-oriented (N) Pattern with ridging east of the storm, which then places the TC in a southerly environmental flow. Cases in which the TC is under the influence of a monsoon gyre (G) or multiple (M) TCs represent only 11% and 4%, respectively, of the five-year sample.

2.3.2 Region Frequency

Tracks of TCs in different Synoptic Patterns are expected to differ because the large-scale environment flows are different. However, each Synoptic Pattern has two or three associated subareas that are called Synoptic Regions (see CE). Three of these Synoptic Regions are used in more than one Synoptic Pattern because similar flows exist within these smaller areas. For example, the Dominant Ridge (DR) Region is characterized by easterly flow south of the strong subtropical ridge in the Standard (S) Pattern or is located northwest of the gyre in the Gyre (G) Pattern. The DR Region comprises over half (54%) of all classifications (Fig. 2.1b). The second most common (24%) Synoptic Region is the North-Oriented (NO), which exists in the N and G Patterns. A TC may also move northward within the S pattern as it is recurving around the subtropical ridge in the Weakened Ridge (WR) Region, which is a relatively small subarea of only the S Pattern. The small area of the WR Region means that the recurving TC will spend little time in this region, which is indicated in Fig. 2.1b by the small number of cases (4%). Although the Accelerating Westerlies (AW) Region exists in three of the four Synoptic Patterns, TCs are generally moving rapidly in the AW Region and thus constitute only 14% of the cases. In addition, these TCs are often sheared apart and quickly dissipate. Finally, the M Pattern northerly flow (NF) and southerly flow (SF) Regions each contribute about 2% of the cases, and thus are rather rare events.

2.3.3 Pattern/Region Frequency

Although flows in similar Synoptic Regions of different Synoptic Patterns will be similar, the storm tracks may be slightly different because of the different large-scale environmental forcing. For example, the environmental flow in both S/DR and G/DR is essentially easterly. However, the presence of the gyre to the southeast in the G/DR Pattern/Region may tend to drive TCs slightly toward the southwest. Hence, a census of specific Pattern/Region combinations (Fig. 2.2) is necessary.

The S/DR combination is the most frequent at 50.8%, N/NO has the second highest frequency at 17.5%, and all others are less than 10%. It is somewhat surprising that a larger (9.4%) percentage of cases in the Accelerating Westerlies (AW) Region are associated with a North-Oriented (N) Pattern, rather than as S/AW in the S Pattern in a typical recurvature sequence. One explanation is that although Environment Structure may start out Standard, the TC modifies it to the N Pattern so that it ends up moving into the N/AW rather than the S/AW combination. However, rarely does the Environment Structure change such that a TC initially in a N Pattern eventually reaches the midlatitudes by entering the S/AW combination. Another explanation might be that those TCs in the S/AW are moving more rapidly (and thus contribute fewer cases) than in the N/AW Region.

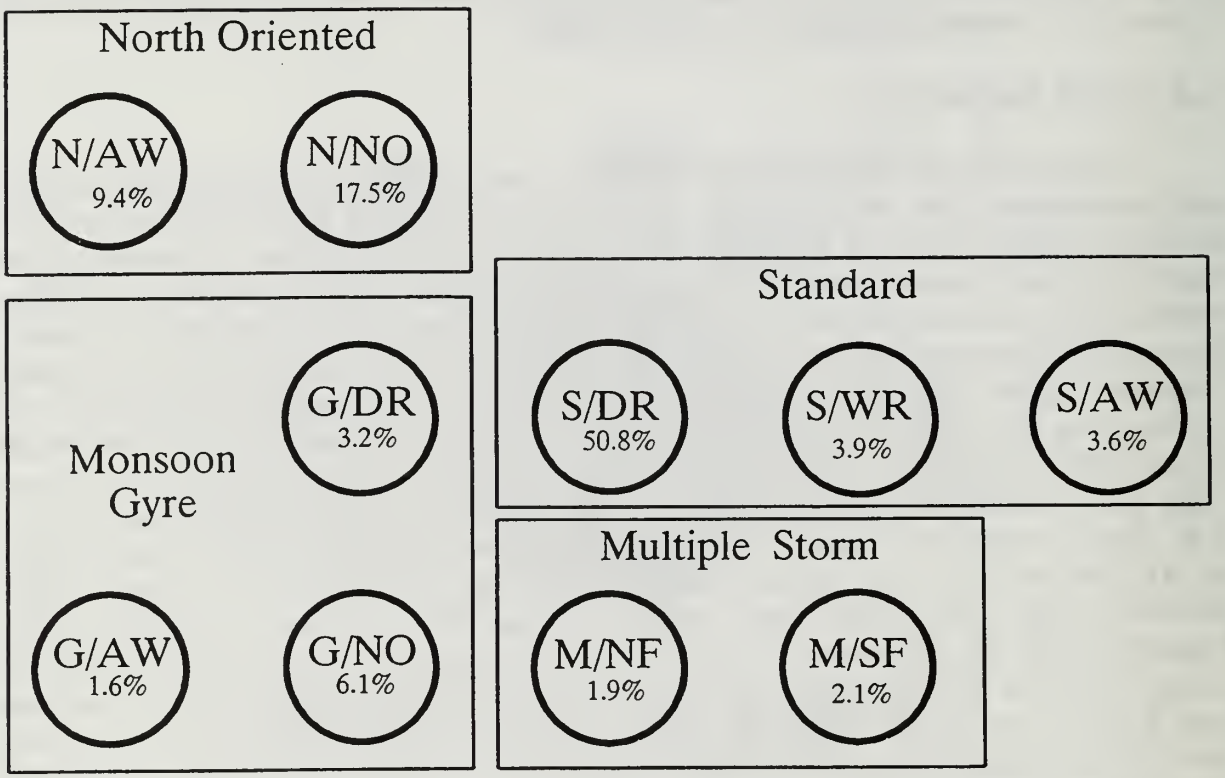

Fig. 2.2 Climatology of Synoptic Pattern/Region combinations in the western North Pacific during 1989-1993.

In the monsoon gyre (G) Pattern, most of the cases (6.1% of overall sample) are tracking northward in the NO Region. Then 3.2% cases are found in the G/DR Region, in which the TC has rotated around to the northern portion of the gyre and is moving generally westward. Only 1.6% of the sample are in the G/AW Region in which the TC is likely to dissipate or move rapidly out of the domain. Because of the different lengths of time that the TCs continue to exist, the percentages in G/DR versus G/AW does not indicate the fractions of storms that continue around the monsoon gyre versus escape into the westerlies.

Table 2-2 (a) Number of times (regardless of duration) the storms are in the Synoptic Pattern/Region without counting transitions. Number of storms that were in the Pattern/Region combination (b) excluding and (c) including dual assignments.

a

		%
S/DR	158	38.1
S/WR	33	8
S/AW	22	5.3
N/NO	81	19.5
N/AW	47	11.3
G/NO	30	7.2
G/DR	14	3.4
G/AW	11	2.7
M/NF	9	2.2
M/SF	10	2.4
	415	

b

		% 166 TCs
S/DR	138	83.1
S/WR	31	18.7
S/AW	22	13.3
N/NO	79	47.6
N/AW	47	28.3
G/NO	30	18.1
G/DR	14	8.4
G/AW	11	6.6
M/NF	9	5.4
M/SF	10	6
	391	

c

		% 166 TCs
S/DR	142	85.5
S/WR	36	21.7
S/AW	23	13.3
N/NO	94	56.6
N/AW	55	33.1
G/NO	30	18.1
G/DR	15	9
G/AW	12	7.2
M/NF	11	6.6
M/SF	17	10.2
	435	

Simple percentages of the overall sample of assignments do not take into account that TCs spend different lengths of time in each Pattern/Region because each combination has a different areal extent, TCs travel at different speeds in each Pattern/Region, and some synoptic situations are self-destructive. Hence, Synoptic Pattern/Region combinations that occur frequently, but last for only a short time, may be under-represented. In this five-year data base of 166 storms, 415 separate Pattern/Region assignments were made (Table 2-2a), regardless of the length of time spent in the Pattern/Region. Some assignments persist for over a week, as in the case of long straight runners, and others exist for just one map time (12 h). In Table 2-2a, each of these situations is counted as a single Pattern/Region occurrence. Compared with the count of each analysis time in Fig. 2.2, S/DR has a large reduction from 50.8% of all maps down to 38.1% of the occurrences. The other nine Pattern/Region combinations all have increased frequencies, particularly the S/WR, which rises from 4.0% to 8.0%. In both analysis counts and occurrences, the S/DR, N/NO, and N/AW are the most common Pattern/Region combinations.

Another useful question may be: "How many storms experience each Pattern/Region combination?" (Table 2-2b). Of the 166 storms in the five-year database, a large majority (138 or 83.1%) lie in the S/DR Pattern/Region at some point in their lives. Almost half (47.6%) of all storms are in N/NO at some time. If dual assignment cases in which the storm does not complete a transition to the Pattern/Region are also considered, then the count in every Pattern/Region either rises (e.g., S/DR increases to 142 or 85.5%) or remains the same (Table 2-2c).

2.3.4 Seasonal Variations

As the large-scale environment changes with the seasons, the Synoptic Pattern classifications (based upon the original method of counting each map time) also have

seasonal trends (Fig. 2.3a). For this five-year period, TCs are observed in every month except February. Whereas storms exist in either the S or the N Patterns throughout the year, the G and M Patterns tend to be confined to limited periods. The N Pattern exhibits a nearly Gaussian distribution for much of the year with a maximum in late August/early September. Whereas the S Pattern tends to have a similar distribution, a relative minimum clearly exists in September (and perhaps into October), with another late season maximum in November. The monsoon gyre (G) Pattern is only observed from June to November during this five-year period, and the frequency distribution is near-Gaussian with a maximum in August. Although multiple (M) storm Pattern cases exist from April to December, the number of cases is so small that the seasonal distribution is not well defined.

During January-May, the ratio of S to N Pattern classifications remains nearly constant, with the S Pattern roughly four times as likely as N (Fig. 2.3b). Presumably, it is the maxima of the G and N Patterns in August and September respectively, that leads to the relative minimum in S during that period. Again, the different lengths of time that a TC persists in each Pattern makes the interpretation less certain.

2.4 Tracks

Summaries of TC tracks in each Pattern/Region are used to illustrate some dramatic differences in motion, which emphasize the importance of assigning accurately the Environment Structure in the Systematic Approach. The S Pattern tracks (Fig. 2.4) are generally as expected. Long, generally east-to-west tracks in the trade wind easterlies are associated with the S/DR combination (Fig. 2.4c). A few tracks in the S/DR combination do have southward motion that is likely caused by an indirect influence of a nearby TC. Short northward tracks are associated with the S/WR combination as TCs move through the ridge (Fig. 2.4b), and then accelerate toward the northeast into the midlatitude westerlies in the S/AW combination (Fig. 2.4a).

The ridge to the southeast of the TCs in the N (here the N1 and N2 Synoptic Patterns of CE have been combined) Pattern causes early (low latitude) recurvature of mature storms or initial northward motion of developing storms (Fig. 2.5b). These TCs are often still far south of midlatitude westerlies when they enter the N/NO combination. The ridging associated with Rossby wave dispersion in a TC also tends to follow the TC as it travels north, which causes the poleward motion to persist and retards the development of eastward motion. Hence, TCs in N/NO (Fig. 2.5b) have longer tracks than those moving through subtropical ridge breaks in S/WR (Fig. 2.4b). Also, the more complicated interaction between a TC and the ridging in N/NO can cause sinusoidal "S" tracks as in Fig. 2.5b.

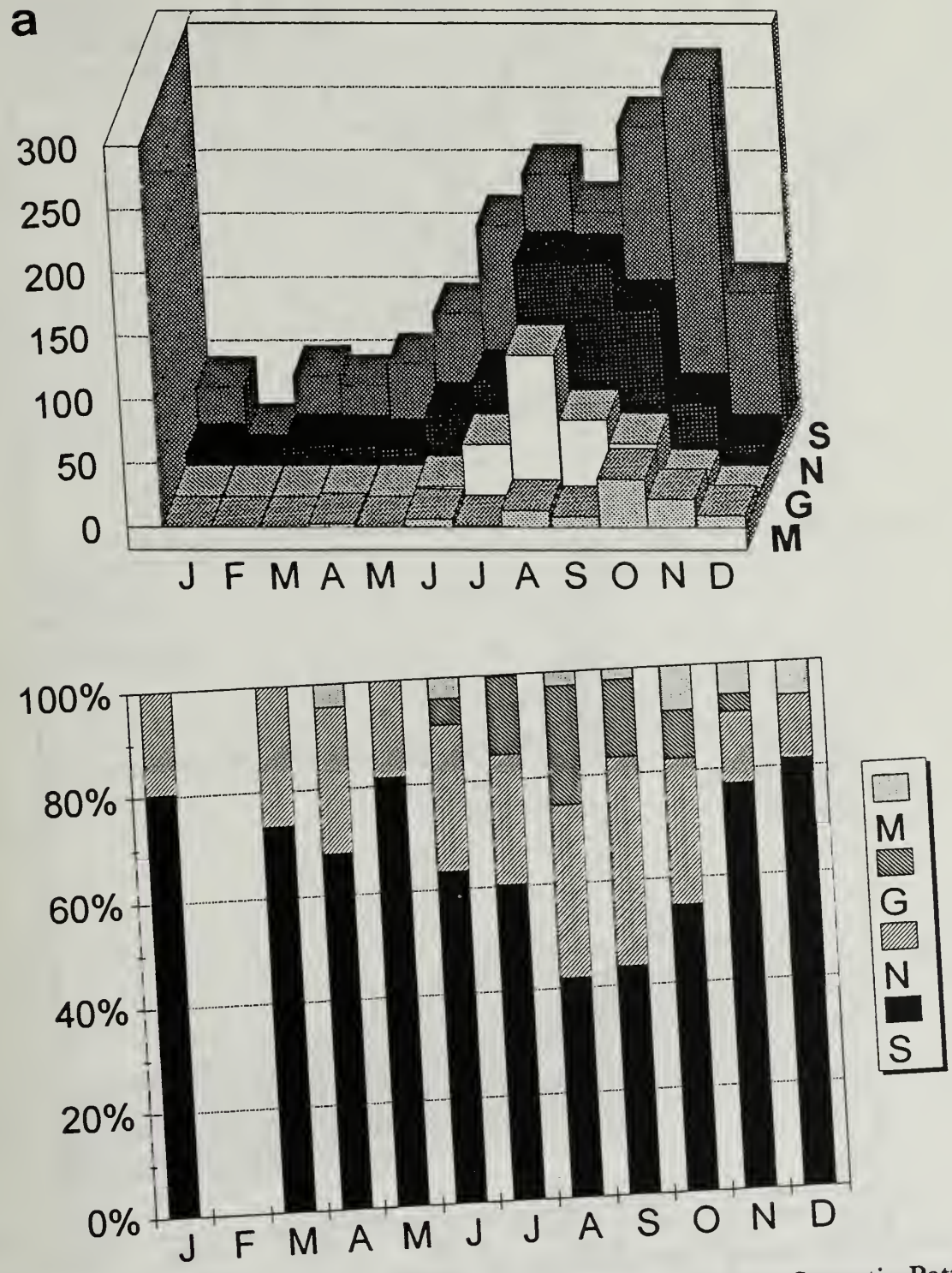

Fig. 2.3 Monthly (a) occurrences and (b) percent frequency of the Synoptic Patterns in western North Pacific TCs during 1989-1993.

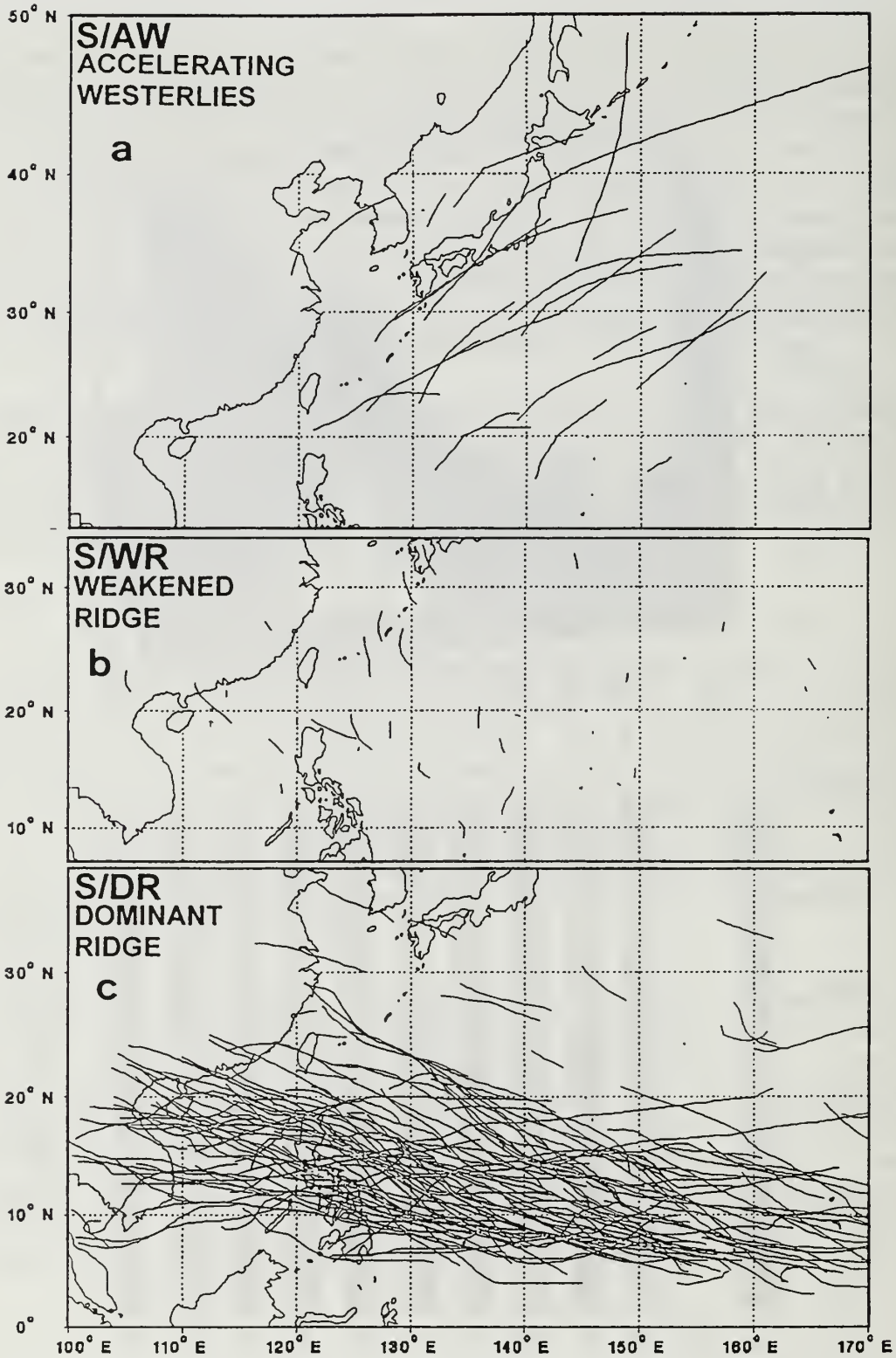

Fig. 2.4 Storm tracks during 1989-1993 while the storm is in the Standard Pattern and the (a) Accelerating Westerlies, (b) Weakened Ridge, and (c) Dominant Ridge Regions. Periods of dual assignments are omitted.

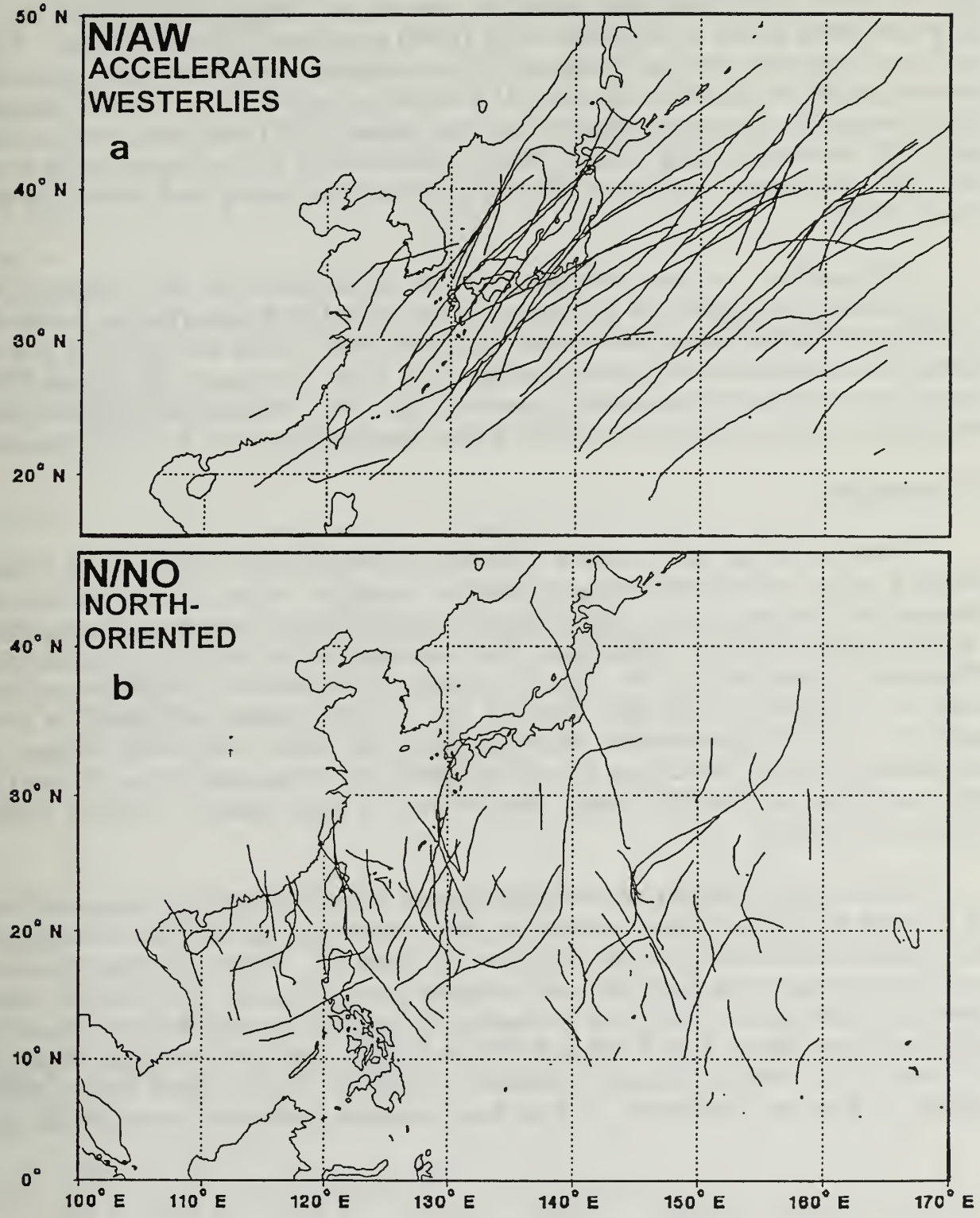

Fig. 2.5 Storm tracks as in Fig. 2.4, except in the North-oriented Pattern and the (a) Accelerating Westerlies and (b) North-oriented Regions.

Most tracks in the G/NO combination have cyclonically curved paths as the TCs form and move counterclockwise around the east side of a monsoon gyre (Fig. 2.6c). A bifurcation often occurs as the storm in the G/NO combination moves poleward. If the storm is able to break through a weakness in the subtropical ridge, recurvature occurs and the storm makes the transition into the G/AW combination (Fig. 2.6a). If the TC does not break through the subtropical ridge and the gyre persists, the TC will move westward into the G/DR combination (Fig. 2.6b). Under the influence of the subtropical ridge to the NNW and the monsoon gyre to the SE, these TCs may have a long track toward the west or even WSW.

Although few in number, the tracks of TCs in the M Pattern are also consistent (Fig. 2.7). Northward propagation of the western TC in the M/NF Pattern/Region is retarded enough by the northerly flow between the ridge to the west and the eastern TC to give the western TC a southward component of motion (Fig. 2.7b). Conversely, TCs in the M/SF Region have a northward component of motion (Fig. 2.7a). Although not illustrated here, these storms tend to approach recurvature without slowing down as in the typical situation.

2.5 Transitions

Tracks of storms that remain in a particular Pattern/Region are expected to have persistent paths until an Environment Structure transition occurs. Thus, the greatest challenge for a forecaster is to recognize when the Environment Structure will change, which is then expected to lead to a significant track deviation from a persistence forecast (e.g., differences in tracks in Figs. 2.4 - 2.7). Transitions of Environment Structure occur as a result of transitional mechanisms (see CE Fig. 3.4 and related discussion) in three categories: (i) TC-Environment transformations (CE Table 3-3); (ii) changes in Environment Structure that do not principally depend on the presence of the TC; and (iii) simple advection of the TC through (and/or out of) some Synoptic Patterns by the environment steering.

Based on this 5-year sample, each Environment Structure transition is associated with one or more[1] of the transitional mechanisms that are shown in Fig. 2.8. The definitions of the transition mechanism acronyms are shown in Table 2-3. Notice that more than one transitional mechanism is listed for some transition paths in Fig. 2.8. For example, either a Beta Effect Propagation (BEP) or a Subtropical Ridge Modification (SRM) may cause the same transitional effects from S/DR to S/WR to S/AW. The N/NO to S/DR transition may occur from Tropical Cyclone Interaction (TCI4), a Vertical Wind Shear (VWS) situation, or from the SRM effect. In both these examples, midlatitude waves modify the

[1] Although these assessments were carefully based on the dynamical concepts, case studies, and transformation indicators (see CE p. 178-183), subjectivity in making some of these assessments is acknowledged.

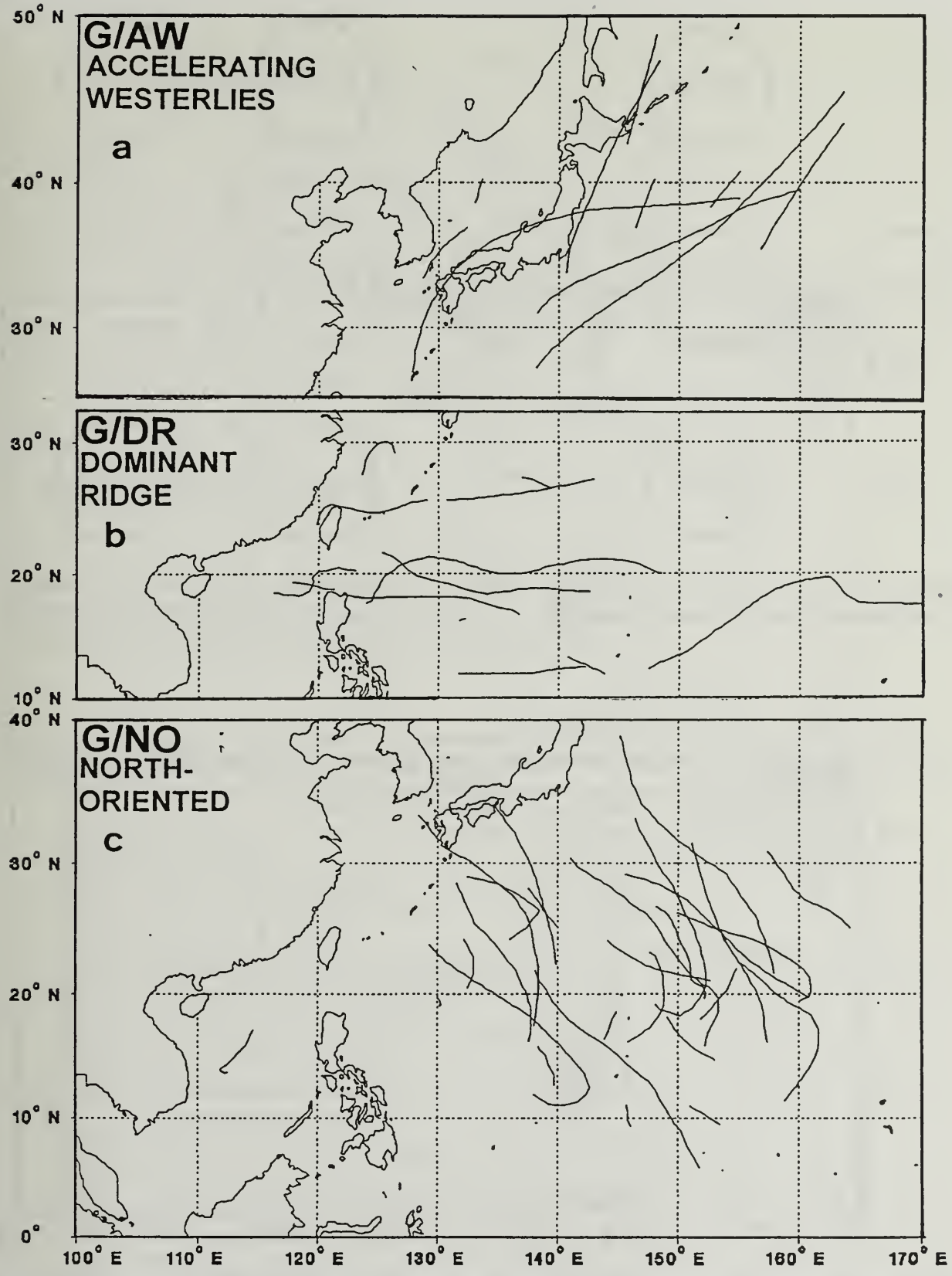

Fig. 2.6 Storm tracks as in Fig. 2.4, except in the monsoon gyre Pattern and the (a) Accelerating Westerlies, (b) Dominant Ridge, and (c) North-oriented Regions.

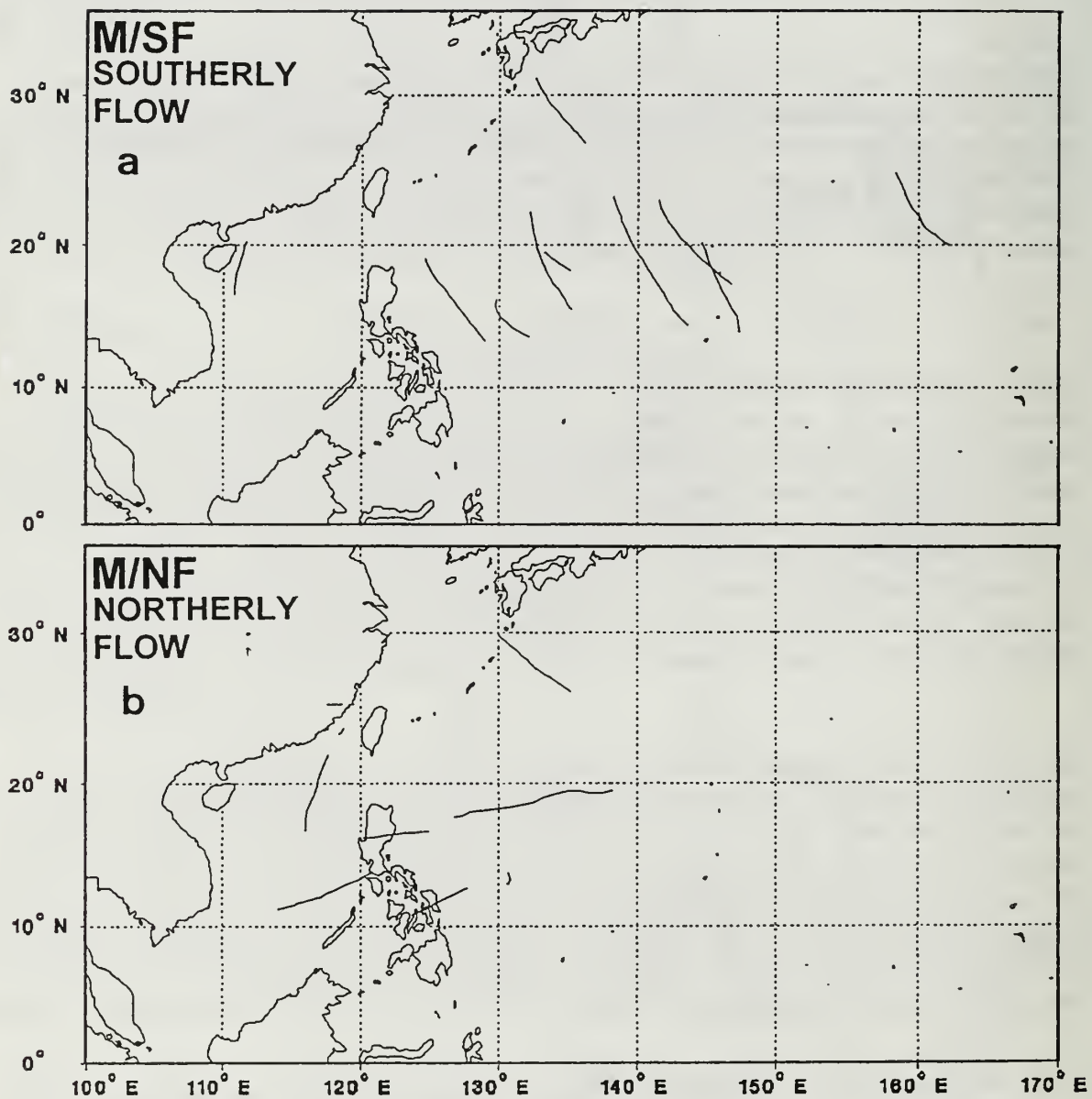

Fig. 2.7 Storm tracks as in Fig. 2.4, except in the multiple storm Pattern and the (a) Southerly Flow, and (b) Northerly Flow Regions.

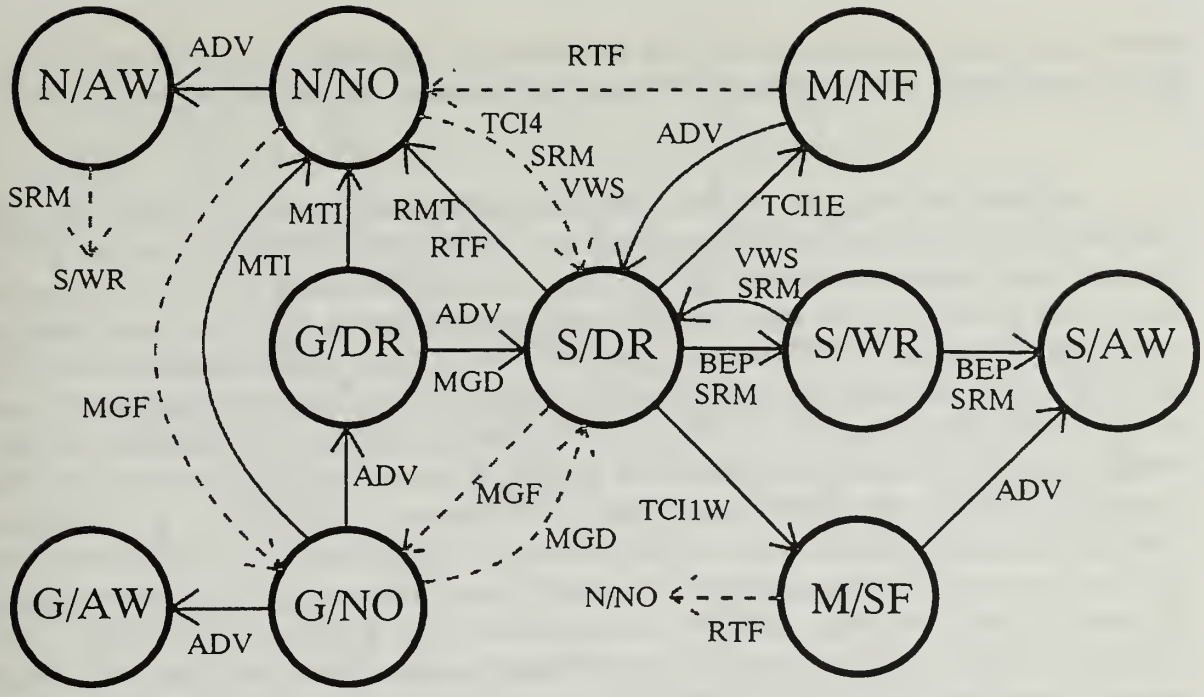

Figure 2.8 Transition mechanisms (see Table 2-3 for definitions of acronyms) between Synoptic Pattern/Regions defined in Table 2.1. The solid (dashed) transitions have (have not) been previously described by CE (see text).

Table 2-3 Definitions of the transitional mechanism acronyms appearing in Fig. 2.8.

Transitional Mechanisms Nomenclature		
Acronym	Meaning	Applicable CE transition schematic
BEP	Beta Effect Propagation	Fig. 3.38
VWS	Vertical Wind Shear	Fig. 3.46
RMT	Ridge Modification by a "Large" TC	Fig. 3.52
MTI	Monsoon Gyre-TC Interaction	Fig. 3.68
TCI1	Formation of a M Pattern	Fig. 3.77
TCI4	Weakening of another TC's Beta-induced ridging	not illustrated
ADV	Advection by Pattern Steering Flow	Fig. 3.52, 3.68, 3.77
RTF	Reverse-oriented Trough Formation	not illustrated
MGF	Monsoon Gyre Formation	not illustrated
MGD	Monsoon Gyre Dissipation	not illustrated
SRM	Subtropical Ridge Modulation by Midlatitude Waves	not illustrated

subtropical ridge circulation and thus influence TC recurvature or non-recurvature. This SRM transitional mechanism will be described in more detail in Chapter 4.

Although a majority of the transition paths (solid arrows) in Fig. 2.8 have been discussed and illustrated in CE (see their Figs. 3.38, 3.46, 3.52, 3.68, and 3.77), a minority of transitions (dashed arrows in Fig. 2.8) have not been discussed in CE. In some situations, one of the previously discussed transitional mechanisms is found to precipitate another transition. Examples of this category include: (i) N/NO-S/DR transitions in response to the VWS TC-Environment transformation, which CE had previously associated only with the S/WR-S/DR transition; (ii) N/NO-S/DR transitions in response to the TC14 transformation, which CE had previously viewed to be only an inhibitor of the S/DR-N/NO transition; and (iii) the transitions from the M Pattern in response to a Reverse-oriented Trough Formation (RTF), which will be shown in Chapter 4 to be a variation of the RMT-TC Environment transformation. A second (new) category of transition paths involve Monsoon Gyre Formation (MGF) or Monsoon Gyre Dissipation (MGD). The MGF transition simply reflects that a TC may form concomitantly with the MG, rather than forming after the MG is already well developed, which is the only scenario implied in the CE Fig. 3.12 and associated discussion. Similarly, it was found in the five-year sample that a MG may dissipate independent of the TC. More discussion of these variations of the transitional mechanisms in Fig. 2.8 will be given in Chapter 4.

The number of occurrences of "recurring" transitions between the ten Pattern/Region combinations, and the number of storms that never experience a transition, during the five-year period are shown in Fig. 2.9. A total of 248 "complete" transitions occur. Here, the term "complete" is used to exclude those periods of dual Synoptic Pattern/Region assignments in which it appears a transition is approaching, but an actual change of either the Region, or the Pattern, or both does not occur. The term "recurring" implies that such a transition occurs more than once. Considering only recurring transitions reduces the number of transitions only slightly to 239, which is 96% of the total. Notice that the number of transitions entering a Pattern/Region does not necessarily equal those that are exiting. This difference is because TCs can develop or dissipate within any one of the ten Pattern/Region combinations. Examples of cases that undergo some of the newly defined transitions (shown by the dashed arrows in Fig. 2.9) will be described in Chapter 4.

As indicated by the numbers in Table 2-2a, most TCs have at least one transition from one Pattern/Region combination to another during their lifetimes. That is, 415 separate Pattern/Region assignments are made for only 166 storms. Of the 166 storms in the data base, only 43 (26%) remained in just one Pattern/Region while above 25 kt intensity. These TCs are depicted in Fig. 2.9 by numbers within the Pattern/Region circle. Most (39) of these cases were straight-runners in the S/DR Region in which the storms remained in the trade wind easterlies equatorward of a persistent subtropical ridge. The other four cases were all weak, short-lived storms (1.5 - 2 days). Three of these made cyclonic turns around the east side of monsoon gyres in the G/NO Region, while the fourth

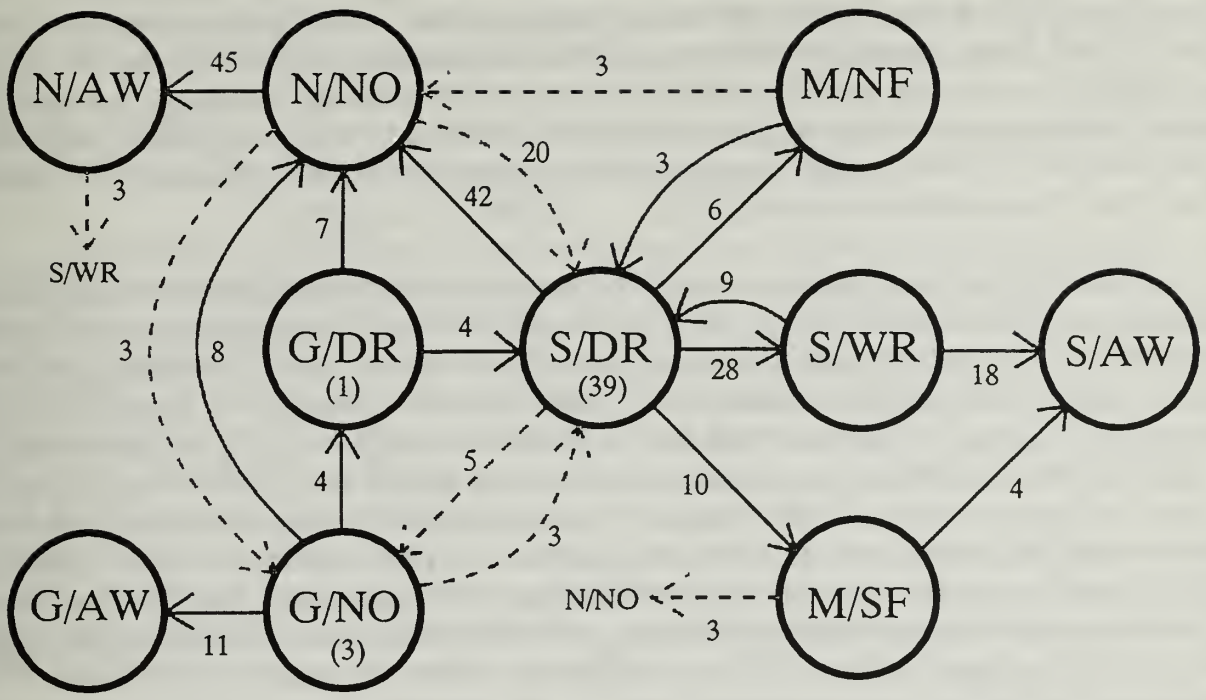

Fig. 2.9 Recurring (i.e., more than one occurrence) transitions between Synoptic Pattern/Regions for intensity $\geq$ 25 kt. Number within each circle indicates storm remained in that Pattern/Region throughout the life cycle. The total number of transitions is 239. Solid transition lines are those discussed in CE, and dashed transition lines have not been previously discussed.

intensified to 25 kt (12 m s^{-1}) upon entering the G/DR Region from the G/NO Region and persisted there for the remaining two days with an intensity equal to or greater than 25 kt.

An example of a series of transitions in which a TC remains within the same Synoptic Pattern is a typical recurvature case (S/DR --> S/WR --> S/AW). A TC propagates from the DR Region to the WR Region in a poleward transition relatively often (28: 11.7% of 239 total; 30.8% of 91 leaving S/DR). TCs that continue to recurve then move into the AW Region (18: 7.5% of 239 total; 66.7% leaving S/WR). However, a ridge sometimes builds in the midlatitudes north of a TC in the WR Region that inhibits its recurvature into the westerlies (the SRM transition in Fig. 2.8). The TC may then be forced south and re-enter the DR Region, which results in a "stair-step" track. Such a process accounts for four of the nine S/WR-->S/DR "return" transitions. Three of the remaining five return transitions also made stair-step tracks due to vertical wind shear caused by late season northeasterly low-level flow (the VWS transition in Fig. 2.8). The remaining two return transitions originate in N1/AW, and they are discussed below.

The most common (42: 17.6% of 239; 46.2% leaving S/DR) transition that a TC makes from S/DR is into N/NO, which is a change of the entire Synoptic Pattern. Most (32 of 42) of these transitions involve a RMT transformation in which the TC is the controlling factor, in that the TC modifies its environment enough to change the Synoptic Pattern. Hence, more storms tend to recurve into N/AW (45: 18.8% of 239; 66.2% leaving N/NO) via this TC-Environment transformation as opposed to passing around the ridge as in the typical recurvature scenario (S/DR -- > S/WR -- > S/AW).

Although the most frequent transition from the N/NO combination is to N/AW, a TC moving northward in N/NO is not a guarantee that it will transition into the N/AW combination. A relatively large fraction of cases (20: 8.4% of 239; 29.4% leaving N/NO) actually return to the S/DR combination. This is another example of a transition not described in CE that led to the inclusion of dashed lines in Fig. 2.8. If a TC enters N/NO at a low latitude, the Environment Structure may change substantially before the TC reaches the accelerating westerlies. Half of these 20 returns to S/DR occur when the peripheral southeastern ridge, which was strong enough to force the storm northward at low latitudes, becomes weaker relative to the subtropical ridge. Consequently, the TC track turns westward as the dominant flow becomes the easterlies south of the stronger ridge. Eight of the remaining returns from N/NO to S/DR are caused by another TC via the TCI4 transformation (another new transition; see Fig. 2.8) in which the second storm to the east weakens the peripheral ridge to the southeast of the first TC. The remaining two cases involve off-season storms in which vertical wind shear (VWS) results in a lower steering level and the TC turns westward or even southwestward under the influence of the lower tropospheric subtropical ridge.

The most frequent transition from G/NO is to G/AW (11: 4.6% of 239; 42.3% leaving G/NO) in which the TC moves poleward out of the gyre. The more frequent transitions to G/AW versus to G/DR in Fig. 2.9 may seem to be inconsistent with the smaller number of G/AW combinations versus G/DR in Fig. 2.2. However, this difference in numbers of analyses is related to the longer persistence times in G/DR, whereas the storms in G/AW tend to dissipate. If the transition from G/NO is considered to be a bifurcation between a poleward or a westward track, it is significant that the transition to G/AW is almost three times as likely as a transition to G/DR. The second most frequent transition from G/NO is to the N/NO combination, which does not involve a significant track change, since both combinations have poleward tracks. In these eight cases (3.3% of 239; 30.8% leaving G/NO), the transition to a N Pattern occurs as the gyre and the TC circulations combine. Seven of these transitions involve a MTI transformation, which is a merger of the TC and gyre. Although much less common (4: 1.7% of 239; 15.4% leaving G/NO), the third most frequent G/NO transition is to the G/DR combination in which the TC rotates around to the western side of the gyre and into easterlies. A similar transition from G/NO to a westward track in the S/DR combination occurs in three cases (1.3% of total; 11.5% leaving G/NO. In this scenario, the gyre dissipates (labelled as MGD in Fig. 2.8) and leaves the TC in the easterly flow of the S/DR combination.

Finally, a TC in the G/DR combination within easterly flow to the northwest of a gyre may or may not escape the gyre circulation. Gyres may intensify or move westward with the TC. For example, the transition involving a MTI transformation to N/NO, in which the gyre to the east coalesces with the TC, is more common (7: 2.9% of total; 63.6% leaving G/DR) than the scenario in which the TC simply advects westward away from the gyre and into S/DR (4: 1.7% of total; 36.4% leaving G/DR).

TCs enter the G Pattern via only two scenarios. The more common (5: 2.1% of 239; 62.5% entering G/NO) scenario involves a TC that transitions from S/DR via advection into the eastern edge of a preexisting or developing gyre (G/NO). This transition often occurs when the TC is weak and the adjacent gyre circulation is strong enough to influence the TC. Recall that this data base only includes TCs with an intensity of at least 25 kt. For TCs of intensity less than 25 kt, the S/DR -- > G/NO transition is the most common (9). Therefore, the S/DR -- > G/NO transition is actually more common than Fig. 2.8 implies, and the forecaster must anticipate such a transition early in a TC life cycle. The less common (3 cases: 1.3% of total; 37.5% entering G/NO) transition into the G Pattern occurs when a strong gyre develops (labelled as MGF in Fig. 2.8) to the west of a TC in the N/NO combination, and the southerly flow on the gyre's eastern edge becomes the steering for the TC. Only subtle changes in track would be anticipated since the Regions remain as NO.

An Environment Structure change to the Multiple (M) Pattern originates from only the S/DR Pattern/Region. All six (2.5% of total; 6.6% leaving S/DR) transitions to M/NF, and all ten (4.2% of total; 11.0% leaving S/DR) transitions to M/SF, involve a storm originally in S/DR. Storms in either M/NF or M/SF can undergo the transition to N/NO (three cases each) if the two closely positioned storms produce enough RMT-type ridging to the southeast to change to the N Synoptic Pattern, which is referred to as RTF in Fig. 2.8. Another transition occurs when the eastern TC, which is located in southerly flow between the western TC and the subtropical ridge to the northeast, is accelerated directly into S/AW (4 cases: 1.7% of total; 57.1% leaving M/SF). As the two storms separate, the western TC in M/NF typically (3 cases, 1.3% of total) returns to S/DR.

Finally, storms that move into an Accelerating Westerlies (AW) Region rarely return to another Pattern/Region. The common scenario is the TC is advected quickly away and dissipates. Of the 78 cases that enter the three AW Regions, only three (1.3% of total; 3.8% from AW) return. These three cases involve weak storms that enter the AW of a weakening reverse-oriented monsoon trough N Pattern at a relatively low latitude. The subtropical ridge builds to the north (labelled as SRM in Fig. 2.8) of the TC, and the TC transitions to S/WR, and in two cases a further transition to S/DR occurs. However, such cases are rare, and the vast majority of storms in AW move into the midlatitudes and dissipate.

3. Reproducibility Test

(Primary authors: Sean White and Chris Kent)

3.1 Introduction

The Synoptic Patterns and Regions developed in the Systematic Approach of Carr and Elsberry (1994; hereafter CE) were the focus of this reproducibility test. The primary goal of conducting this reproducibility test was to ascertain whether trainees could determine the correct Synoptic Patterns/Regions listed in Table 2-1, because correct identification of these Patterns/Regions is an essential step in the application of the Systematic Approach. Another objective was that a study of the incorrect identifications by the trainees would highlight deficiencies in the descriptions of the Patterns/Regions or in the training phase of the program. That is, trainee misconceptions, difficulty in identifying Patterns/Regions, and misclassifications based on the conceptual models were anticipated, and do not necessarily indicate the knowledge base of the Systematic Approach is flawed. Rather, it may simply indicate deficiencies in the descriptions of the conceptual model(s), or in the training phase.

3.2 Training

The three trainees had no previous tropical cyclone forecast experience. Their instruction in the Systematic Approach was to first read a draft version of CE. After each assigned reading, discussions were conducted to ensure the trainees possessed a thorough understanding of the material. Feedback and questions from the trainees contributed to improvements in the descriptions in the final version of CE. Also, some training aids were introduced and flow charts (discussed later) were produced through this training phase that emphasized the salient points of and interrelationships among the Synoptic Patterns/Regions.

The second phase of the training began with some relatively easy storms from 1989; and the trainees were allowed to work together to apply the conceptual models of the Systematic Approach. Upon completion, a detailed debrief was conducted with the instructor that reinforced the principles. The trainees then moved on to another set of 1989 cases where they worked independently. This second set of cases was to establish whether the trainees were adequately trained to proceed with the reproducibility test. Again, an extensive debrief was conducted to intercompare Pattern/Region assignments, and where differences existed, to review each individual's reasoning. After this second set of cases was completed, a determination was made to proceed to the actual reproducibility test.

3.3 Reproducibility Test of Pattern/Region Assignments

Trainees were presented with operational 500 mb analyses from Fleet Numerical Meteorology and Oceanography Center (FNMOC). On these charts, the warning and

past 12-, 24-, and 36-h positions, translation speeds, and intensities had been plotted (Fig. 3.1). Geostationary satellite infrared (IR) imagery was also provided twice a day (but no animation was provided as would be available in an operational center). The primary purposes of the satellite imagery were to establish the position of the TC in the synoptic circulation (monsoon gyre, reverse-oriented monsoon trough, etc) and to make a rough estimate of the TC size from the overall cloud shield.

Some special circumstances of this reproducibility test make it a "lower bound" of what might be expected from a training program for forecasters. As noted above, two of these trainees have no operational forecasting experience, and the third trainee has no tropical cyclone forecasting experience. On the one hand, these trainees were provided a single storm at a time in an isolated work environment, so they did not have the pressures of real-time operations. On the other hand, the trainees individually made their Synoptic Pattern/Region assignments (and were not allowed to go back and change an assignment when new evidence appeared), so they did not have the benefit of feedback from other forecasters or a lead forecaster as in a "team" operation.

The test was for all western North Pacific tropical cyclones from June-October during 1990 (except August-September), 1991 (except July), 1992, and 1993. This reproducibility test consists of only a subset of the five-year period (1989-1993) involved in the climatological summary of the Synoptic Pattern/Region assignments described in Chapter 2. Each of the three trainees generally proceeded chronologically from the 1990 cases through to the 1993 cases. The experience gained by each trainee might show improvement in their overall ability to assign correct Synoptic Patterns/Regions as the test continued. However, the entire sample of four years was completed with no feedback on intermediate years.

The identifications made by each trainee were compared to the assignments by an experienced forecaster (L. Carr) who is the principal author of the Systematic Approach. In addition to having personally forecast many of these storms, L. Carr also had the benefit of the complete storm track, the entire set of satellite imagery, and future analyses. Thus, he had the benefit of hindsight that the trainees were not allowed. Consequently, L. Carr's assignments of the Synoptic Pattern/Region are considered to be the " benchmark."

First, the methods utilized in determining the number of correct identifications will be examined. Various measures of reproducibility will be examined, and interpretations of the scores will be provided. Finally, these results will be discussed with a view towards producing improved training materials and the "fine tuning" of the conceptual models presented in the Systematic Approach.

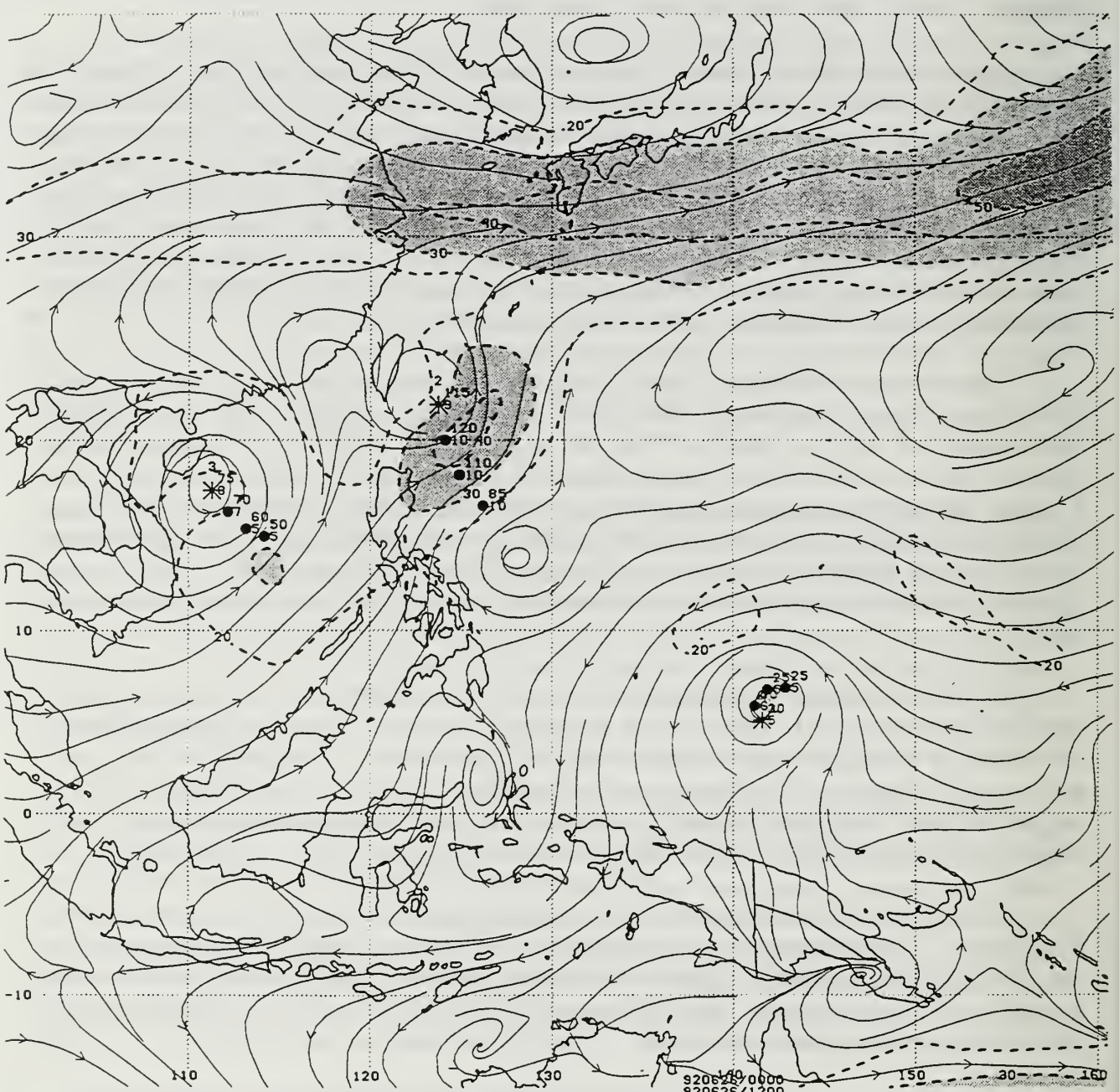

Fig. 3.1 Example of 500 mb streamline and isotach (10 kt interval; light shading > 30 kt, and heavy shading > 50 kt) analysis with present (dot) and past 12-, 24-, and 36-h storm positions.

3.3.1 Method of Scoring. The first goal of the reproducibility test is to assess how successfully each trainee identified the Synoptic Patterns, the Synoptic Regions, and then the combined Pattern/Region. This section contains a description of the methods utilized in assigning either correct or incorrect Pattern/Region identifications by the trainees.

The Synoptic Pattern/Region combinations possible under the Systematic Approach and their associated abbreviations are listed in Table 2-1. Descriptions of these Patterns and Regions are given in CE. In particular, notice in Table 2-1 that the N Pattern is a combination of the N1 and the N2 Patterns of CE. The reasons for this combination based on this reproducibility test are given below.

Hypothetical examples of the classifications of the Synoptic Patterns/Regions by the experienced forecaster (henceforth the benchmark) and by a trainee are shown in Table 3-1. While not actual classifications for a particular storm, the classifications are created to provide an example of the number of possible combinations. Each successive line is numbered (1-5) to provide easy reference and counts as either correct or incorrect.

Notice in Table 3-1 that two Pattern/Region assignments are given for entries 3-5. Such a dual assignment indicates that some aspects of both Patterns/Regions are present. This commonly occurs prior to a transition from one Pattern to another Pattern or from one Region to another Region within the same Pattern. Whereas it may seem to be more desirable to force a single Pattern/Region assignment, such dual assignments recognize that the Tropical Cyclone (TC)-Environment Structure is a continuum (see CE). Furthermore, potential inaccuracies in TC positions or in the FNMOC analyses make it desirable to allow for some ambiguity in the specifications of the Pattern/Region.

An important distinction is made here relative to the procedure in Chapter 2, where the climatology data base counts line 3 of Table 3-1 as an "occurrence" by assigning 0.5 for both the S and the N Patterns, an "occurrence" of 0.5 for both the DR and the NO Regions,

Table 3-1. Five examples of possible assignments of Synoptic Pattern (first letter; see symbol definitions in Table 2-1) /Region (second letter) for benchmark (L. Carr) and a trainee. These fields are created only to serve as an example of possible combinations of benchmark and trainee assignments.

	Benchmark	Trainee
1.	S/DR	S/DR
2.	S/DR	S/DR
3.	S/DR N/NO	S/DR
4.	S/DR N/NO	N/NO
5.	N/NO S/DR	G/NO S/DR

and 0.5 for both the S/DR and the N/NO Pattern/Region combinations. However, such an equal handling of the dual Pattern/Region assignments is not necessarily appropriate for scoring in the reproducibility test. The interpretation of dual assignments by L. Carr and the trainees was not the same (this aspect was not anticipated so a common interpretation was not established prior to the reproducibility test; it is recommended that a standard procedure should be addressed by an operational center), which caused some difficulty in adopting a scoring system. L. Carr's interpretation was that the order of the letters should imply the likely direction of the transition, rather than implying that the environment structure conformed better to the first letter listed. Unfortunately, each of the trainees had a different interpretation, or did not utilize the dual assignments with the same intent. Whereas one trainee felt that a clear (single) designation of the Pattern/Region was required (or at least highly desirable), another trainee frequently utilized dual assignments (and thus might be viewed as "gaming" the scoring system). The third trainee was intermediate between these extremes.

Given the desire for a binary scoring scheme (correct=1 and incorrect=0), the dual Pattern/Region assignments introduce an arbitrariness into the scoring. Consider first only the Pattern (first letter) assignments in the examples in Table 3-1. Three criteria are used in the scoring system:

i) assigning correct (score=1) when the trainee Pattern assignment is the same as the single benchmark assignment as shown in lines 1 and 2, or if the trainee Pattern assignment agrees with the first of the dual benchmark assignments as shown in line 3;

ii) assigning correct (score=1) if the trainee Pattern assignment agrees with either the first or second dual benchmark assignments, as shown in line 4; and

iii) assigning correct (score=1) if the first or second trainee Pattern assignments agrees with either of the dual benchmark assignments, as shown in line 5.

The Region and Pattern/Region scoring also utilized the same three criteria as illustrated above for scoring the Pattern assignments. Each of these three criteria (i-iii), in the order listed, provides more leeway in determining correct assignments. For example, criteria i) allows for a correct assignment without considering a dual assignment by either the benchmark or the trainee, whereas criteria ii) and iii) allow for a correct assignment while considering dual assignments by both benchmark and trainee.

Although the scoring was initially conducted considering only Pattern/Region combinations under criteria i), subsequent scoring utilized criteria ii) and iii). Thus, a somewhat liberal scoring system was adopted in view of the lack of an agreed practice or interpretation of dual assignments prior to the beginning of the reproducibility test. Also, when the scoring methods outlined by criteria ii) and iii) were used, the Pattern/Region

combinations were subdivided into Pattern only, Region only, and Pattern/Region scores, which results in three different measures of reproducibility.

The analysis of assignment differences between the benchmark and the trainees immediately revealed a difference in interpretations of the N1 and N2 Synoptic Patterns. The key difference is the size of the TC and thus whether the ridging to the east and equatorward of the TC will tend to translate poleward with the TC and delay recurvature (see CE). That is, the sometimes subtle distinctions between the N1 and the N2 Patterns caused the trainees considerable difficulties. In fact, one trainee systematically reversed the assignments of the N1 and N2 Patterns. Upon examination of the training materials, the definitions provided the trainees, and the realization that only subtle differences exist between the N1 and the N2 Patterns, the decision was made to combine the N1 and the N2 Patterns into the N Pattern. Whereas this does result in the "artificial" inflation of the final scores, the purpose of the reproducibility test was to determine the trainee's ability to recognize the different Synoptic Patterns/Regions, not to distinguish between two subtly different Patterns. In this regard, this aspect of the reproducibility reveals more about the shortfalls in either the training or the definitions. Some additional aspects concerning the enhancements made to the training and definitions will be examined in a subsequent section.

These various measures of reproducibility (emanating from the subdivision of the Pattern/Region combinations) and the subsequent interpretations will be examined for each of the Synoptic Patterns, Regions, and Pattern/Region combinations.

3.3.2 Reproducibility test of Patterns only. This first test documents the trainee's ability to identify correctly the Patterns (large-scale Environmental Structure) within the context of the Systematic Approach. Pattern recognition involves correct determinations of the existence and orientation of the large-scale environment (synoptic features) surrounding the TC. These synoptic features are a key element of the TC-Environment conceptual model and the subsequent TC tracks according to CE.

The percent correct identifications of each trainee (A-C) for a four-year (1990-1993) total for each of the four Synoptic Patterns is shown in Table 3-2. The high percent (greater than 90%) correct identifications for the S Pattern is due to the frequency of occurrence (58.2%) and the ease of recognizing this Pattern. Notice the percent range for the three trainees is quite small (about +/- 1.5%) for the S Pattern.

The N Pattern, which is the second most frequent (28.2%) Pattern, has a substantially decreased number of correct identifications by the trainees. For example, trainee C detected this pattern in only 43.4% of the cases. Since no yearly or other mid-term review was allowed in this reproducibility test, no opportunity was available to correct trainee C's anomalous N Pattern tendencies until the end of the test. In a typical operational environment, this anomaly would have been detected and probably corrected.

Table 3-2. Percent correct identifications for each trainee (A-C) for the four-year (1990-1993) total for each of the four Synoptic Patterns. The right column lists each trainee's overall percent correct identifications. The combined row shows percent correct for all three trainees combined. Below this row is the combined number of Patterns found in the four-year sample. In parentheses is the frequency of each Pattern for the four years.

		SYNOPTIC PATTERNS				
		S	N	G	M	OVERALL
	A	93.6	84.6	61.0	79.5	87.6
TRAINEES	B	91.4	78.2	35.4	45.9	80.8
	C	94.2	43.4	42.0	86.3	75.2
Combined		93.1	69.1	46.0	72.4	81.2
		834.5	405	144	50.5	1434
		(58.2)	(28.2)	(10.1)	(3.5)	

Several factors are believed to be involved in the degraded performance in recognizing the N Pattern. This is a more difficult Environmental Structure to recognize than the S Pattern. One difficulty is to recognize the frequent transitions from S to N Patterns via the Ridge Modification by a large TC (RMT) transformation mechanism. The N Pattern environmental features outlined in CE require closer scrutiny of the large-scale synoptic features, while also considering the effects on the environment of the imbedded TC. On the one hand, a TC that is not influencing its surroundings would make identification of the Synoptic Pattern relatively easy, provided the two can be separated. On the other hand, the possibility that a TC is interacting or providing influence may make separating the TC and its environment difficult, and thus make determination of the large-scale Environmental Structure (Pattern) more difficult.

Although the N Pattern was more difficult to recognize than the S Pattern, the test still resulted in a combined correct total of 69.1%. Trainee C revealed that during the RMT transition this trainee held back from allowing the S to transition to the N Pattern because the TC did not exhibit a northeast track. Trainee C attributed northeast TC motion to the N Pattern due to the orientation presented by the initial schematic N Pattern conceptual model provided during the training phase. The TC motion in most of the N Patterns, falsely identified by trainee C as the S Pattern, exhibited predominant northerly TC motion.

Trainee C identified this northerly motion as the S Pattern with significant RMT as described in CE. This tendency to stay longer in the S Pattern is reflected in this trainee obtaining the highest four-year total of correct S Pattern identifications. Whereas trainees A and B more frequently allowed this RMT transition and thus correctly identified more N Patterns, trainee C delayed or missed the N Pattern transition due to the predominant northerly TC motion (trainee C expected the TC motion to be northeasterly) and reliance on the RMT to account for the substantial ridging to the east and equatorward of the TC. In Chapter 4 the description of the N Pattern has been broadened to include northwesterly through east-northeasterly TC environmental steering.

The G Pattern had a much smaller frequency of occurrence (10.1%) than the S and N Patterns and was recognized by the trainees at the lowest combined four-year total (46.0%) of any of the four Synoptic Patterns. This is thought to be caused by the unfamiliarity of the trainees with the Environmental Structure of the G Pattern because the training with the 1989 sample cases did not emphasize the G Pattern as much as was possible.

In more than half of the four-year cases, the trainees incorrectly identified the G Pattern as the N Pattern. CE state that the G Pattern contains a prominent north-south oriented ridge circulation to the east of the Monsoon Gyre. However, the N Pattern also has significant ridging to the east, so trainees not recognizing these subtle differences in the Environmental Structure from the analyzed maps would be unlikely to look for evidence of the G Pattern's presence contained in the satellite IR imagery. Supporting evidence of a G Pattern is provided in the satellite imagery in terms of a partial or complete, quasi-circular, and rather large- scale, ring of convective clouds.

As the trainees progressed through the sample (years 1990-1992), their overall yearly percent correct identifications improved (not shown). For 1993, this was not the case as the percent correct identifications fell substantially. This decrease is in part due to the increased frequency of the G Pattern for the 1993 season. Although the ability of the trainees to recognize the G Pattern (about 50% of the time) is not too discouraging in view of its low frequency of occurrence, improvement in recognition of the G Pattern is desirable due to the anomalous TC tracks that are produced. The trainee's difficulty in recognizing the G Pattern demonstrates the need for greater emphasis during the training phase of the environmental characteristics and the supporting evidence that is found in the satellite imagery associated with the G Pattern.

A low frequency of occurrence is not the only factor contributing to a degradation in recognition of the Synoptic Patterns. Although the M Pattern frequency of occurrence is only 3.5%, the trainees' four-year combined percent correct identifications of the M Pattern was 72.4% (Table 3-2). Detection and recognition of the M Pattern is easy with the characteristic features set forth in CE. An example is the TC Interaction (TCI1) model, which is the TC-environment transformation that describes the approach of one TC to another TC. Once the M Pattern is established, the key requirements are that the two TCs

are in proximity and that one TC or the other be sufficiently close to a significant ridge axis. This type of Synoptic Pattern combined with the significant TC track deviations that are associated with the M Pattern allow for comparatively easy recognition.

Whereas trainees A and C achieved relatively high (at or above 80%) correct identifications for the M Pattern, trainee B had significantly less (45.9%) correct identifications. In most of the M Pattern cases in the sample, significant TC track deviations did occur owing to the northerly or southerly environmental flow patterns described in CE. Trainee B did not attribute the TC-Interaction (TCI1) to the observed TC track deviations. Rather, trainee B utilized other TC-Environment models or combinations of these models as described in the many TC-Environment transformations found in CE. Trainee B's results showed no persistent tendencies (the incorrect Synoptic Patterns chosen to explain the M Pattern were randomly dispersed throughout the sample years). Once again, trainee B's tendency to mischaracterize M Patterns would likely have been detected in an operational setting, and would have been corrected.

3.3.3 Reproducibility test of Regions only. This second test documents the trainee's ability to identify correctly the Regions within the context of the Systematic Approach. Synoptic Region recognition is a crucial factor in the Systematic Approach because it is these regions that classify the areas within the Synoptic Pattern that are related to the environmental steering imposed on TCs.

The percent correct identifications of each trainee (A-C) for a four-year (1990-1993) total for each of the six Synoptic Regions is shown in Table 3-3. Notice the overall combined total for the Regions (86%) is above that for the Patterns (81.2%).

The trainees' highest combined four-year percent correct (94.5%) identifications was for the DR Region because the DR Region is easily recognized. The WR Region was the least recognizable Region, as the trainee's combined percent correct identifications for the WR Region was only 59.2%. The short time the TC remains in the WR Region is thought to be the contributing factor that explains the trainees' reduced ability to recognize the WR Region.

A TC may enter the WR Region from the S Pattern through two situations. The first situation occurs after leaving the DR Region and before entering the AW Region during recurvature. The second situation occurs after leaving the DR Region and before returning to it during a "stair-step" track maneuver. One aspect of the Systematic Approach is that transitions may occur through a TC-Environment transformation. As stated earlier, the TC-Environment transformation process is a continuum and thus the transition from one Region to another Region may not be recognized in a frame by frame reference (12 h intervals as was the case for this reproducibility test).

Table 3-3. Percent correct identifications for each trainee (A-C) for the four-year (1990-1993) total for each of the six Synoptic Regions. The right column lists each trainee's overall percent correct identifications. The combined row shows percent correct for all three trainees combined. Below this row is the combined number of Regions found in the four-year sample. In parentheses is the frequency of each Region for the four years.

		SYNOPTIC REGIONS						
		DR	WR	AW	NO	NF	SF	OVERALL
TRAINEES	A	94.0	61.5	92.5	90.1	81.0	80.0	91.6
	B	96.5	20.8	77.0	67.4	25.0	61.9	84.0
	C	93.1	80.0	81.1	53.9	82.6	79.3	81.2
	Combined	94.5	59.2	83.5	70.3	66.7	74.7	86
		802.5	36	164	381	23	27.5	1434
		(56.0)	(2.5)	(11.4)	(26.6)	(1.6)	(1.9)	

As such, a TC in transition from the DR Region to the WR Region and then either to the AW Region (recurvature) or back to the DR Region (stair-step) is in a constant state of transition. The time a TC is in a WR Region and not experiencing tendencies toward another transition could be quite short. Thus, the opportunity to characterize the environment associated with the WR Region is limited due to the short time that a TC is in the WR Region. Trainee B's low percent correct (20.8%) identification for the WR Region is thought to be due to this time constraint. This time constraint coupled with the less distinct circulation features describing the WR Region make this Region difficult to recognize.

The trainees' combined percent correct identifications for the AW Region was 83.5% (Table 3-3). The easily recognizable features of this Region in any of the S, N, or G Patterns allowed the trainees to recognize the AW Region despite the relatively small frequency of occurrence of 11.4%. The trainees' percent correct identifications in the NO Region (70.3%) is very similar (within 1%) to their percent correct identifications in the N Pattern (69.1%). Although the trainees' individual percent correct identifications for the NO Region (Table 3-3) do vary relative to those for the N Pattern (Table 3-2), the recognition factors listed above for distinguishing the N and the G Patterns are considered to explain the reduction in the percent correct identifications for the NO Region.

Even though both the NF and the SF Regions of the M Synoptic Pattern were represented at less than 2% frequency for the four-year sample, the trainees' combined percent correct identifications for both the NF and the SF Regions were near 70% (+/- 5%). As mentioned above, the M Pattern is easily recognized and thus so are the SF and the NF Regions. On the one hand, trainees A and C had percent correct identifications for the M Pattern that are similar to the percent correct identifications the trainees achieved for both the NF and the SF Regions. The M Pattern (Table 2-1) can only be associated with one or the other of these Regions. On the other hand, trainee B's significant difference between the percent correct identifications for the NF and the SF Regions suggests something other than the time factor may be involved in trainee B's ability to recognize the NF or the SF Regions. The discussion above regarding trainee B's tendency to mischaracterize M Patterns also applies here.

Trainee B had considerable difficulty in recognizing the NF Region (Table 3-3) because he did not recognize the equatorward motion of the TC as a characteristic of the M Pattern. If such a recognition failure would have existed in operational forecasting situations, it would have been noticed and measures would have been taken to correct anomalous Region assignments.

In general, the percent correct identifications for the Synoptic Regions is above that for the Synoptic Patterns. The importance of the Synoptic Region in describing the TC environmental steering suggests that recognizing the correct Region is more important than recognizing the correct Pattern. That is, an incorrect Pattern assignment with a correct Region assignment would still describe the essential environmental steering affecting a TC. However, the successful application of the Systematic Approach will require correct Pattern and Region identifications to enable the forecaster to recognize correctly the crucial TC-Environment transformations. These Pattern/Region combinations are discussed in the next subsection and the TC-Environment transformations found in this reproducibility test case are discussed in Chapter 3.4.

3.3.4 Reproducibility test of Pattern/Region combinations. This third test documents the trainees' ability to identify correctly the Pattern/Region combinations. Recognition of these Patterns/Regions constitutes the backbone of the Systematic Approach in producing an improvement over present predictive TC track techniques. Although the reproducibility tests of Patterns only and Regions only are valuable in highlighting the environmental features the trainees had difficulty recognizing, they do not reflect the true overall ability of the trainees in determining the correct Pattern/Region combinations.

The percent correct identifications of each trainee (A-C) for a four-year (1990-1993) total for each of the ten possible Synoptic Pattern/Region combinations is shown in Table 3-4. Notice the unusually low percent correct (8.8%) identification for trainee B for the S/AW combination.

Table 3-4. Percent correct identifications for each trainee (A-C) for the four-year (1990-1993) total for each of the ten Synoptic Pattern/Region combinations. The right column lists each trainee's overall percent correct identifications. The combined row shows percent correct for all three trainees combined. Below this row is the combined number of Pattern/Region combinations found in the four-year sample. In parentheses is the frequency of each Pattern/Region combination for the four years.

		SYNOPTIC PATTERNS/REGIONS					
		S/DR	S/WR	S/AW	N/NO	N/AW	
	A	93.3	64.1	51.7	83.2	74.2	
TRAINEES	B	94.7	16.7	8.8	70.8	71.3	
	C	93.0	78.8	47.4	40.6	22.2	
	Combined	93.6	53.3	35.6	65.0	56.7	
		773	36	25.5	289.5	115.5	
		(54.0)	(2.5)	(1.8)	(20.2)	(8.0)	
		G/NO	G/DR	G/AW	M/NF	M/SF	OVERALL
	A	69.9	44.4	25.0	82.6	75.0	84.6
TRAINEES	B	29.3	35.5	23.8	25.0	59.1	76.9
	C	42.4	27.6	40.0	82.6	79.3	71.2
	Combined	47.8	34.4	29.5	66.7	72.0	77.5
		91.5	29.5	23.0	23.0	27.5	1434
		(6.5)	(2.0)	(1.6)	(1.6)	(1.9)	

A simple combination of the Synoptic Pattern (Table 3-2) and the Synoptic Region (Table 3-3) test results does not explain the trainees' results for the Synoptic Pattern/Region combinations. This is because of the method of scoring, in particular criteria iii) in Section 3.3.1 that allows a correct assignment if it agrees with either one of the dual assignments that is regarded as the benchmark. Trainee B's 8.8% correct identifications for the S/AW combination does not appear to be consistent with the 77% correct identifications for the AW Region. This can occur because criteria iii) allows a high AW Region only assignment, but then has a low Pattern/Region combination score because the correct Pattern was not also identified with these AW Region assignments. Therefore, a trainee with a large percent correct identification in either the Patterns only or the Regions only may have a decreased ability in a particular Pattern/Region combination due to the scoring when dual assignments are made.

The combined percent correct identifications of the S/DR Pattern/Region combination by the trainees was 93.6%. As stated above, the S Pattern and the DR Region are both easily identifiable. The trainees' combined percent identifications for the rare (2.5%) S/WR combination was 53.3%. Trainee B demonstrated the lowest ability for this Pattern/Region combination because of the reasons stated above under the WR Region description.

The last S Pattern/Region is the S/AW combination. The trainees' combined (35.6%) correct identifications for the S/AW combination is lower than would be expected given the ease of identification for both the S Pattern (Table 3-2) and the AW Region (Table 3-3). Similarly, the G/AW Pattern/Region combination has a low percent correct identifications, even though the G Pattern (Table 3-2) and the AW Region (Table 3-3) have higher percent correct identifications. The ease in recognizing the AW Region as a TC turns to the north was offset by the lack of discernment by the trainees of the G Pattern (being mistaken for the N Pattern or S Pattern) resulting in lower scores in the Pattern/Region combinations.

With the exception of trainee C, the trainees' ability in the N/NO combination, which is the second most common Pattern/Region combination, was comparable to the trainees' ability within the N Pattern and the NO Region. Trainee's A and B percent correct identifications were similar to the combined (65%) correct identification for all the trainees. Trainee C only had a 40.6% correct identification of the N/NO combination due to trainee C's anomalous N Pattern identifications described above. The N/AW combination, which is the third most frequent Pattern/Region (8.0%), was correctly identified in 56.7% of the cases. Although trainee C was able to recognize well the AW Region (Table 3-3), the excessive S Pattern assignments by trainee C explains the misidentification of the N/AW combination as a S/AW combination, which resulted in trainee C achieving only a 22.2% correct identification for the N/AW combination.

Only a 47.8% correct identification was achieved by the trainees for the G/NO combination. The difficulties experienced by the trainees in recognizing the G Pattern

resulted in lower than desired abilities in identifying the G/NO combination as well as the low 34.4% and 29.5% correct identifications for the G/DR and the G/AW combinations, respectively. Once again, training for the G Pattern needs to be given greater emphasis to improve the correct identification of this Pattern.

Finally, the M/NF and the M/SF Pattern/Region combinations received relatively high combined percent correct identifications of 66.7% and 72%, respectively (Table 3-4). As noted above, trainee B had difficulty with the M/NF Pattern/Region combination. The percent correct identifications by trainee B for the M/NF (25%) and the M/SF (59.1%) are due to the anomalous M Pattern tendencies of trainee B.

The overall combined correct percent identifications for the trainees was 77.5% for the Synoptic Pattern/Region (Table 3-4). The special circumstances of this reproducibility test make it a "lower bound" of the Pattern/Regions to be expected in operation. This ability of trainees without previous tropical cyclone forecasting experience to recognize these Patterns/Regions reinforces the validity of the Systematic Approach. This test is important to application of the Systematic Approach because this component involves subjective thought processes in the recognition and assignment of the Pattern/Region combination.

3.3.5 Revised Training. As indicated in Section 3.2, the training for this reproducibility test of recognizing the TC-Environment situation occurred as the CE report on the Systematic Approach was being finalized. One of the new training tools that was developed during the reproducibility test will be described here, with the intent that this tool be incorporated into the future training. Next, some proposed enhancements to be made to the training will be described based on the lessons learned during the reproducibility test. Two sources were utilized to apply the principles of the Systematic Approach to the TC-Environment situation. The first of these was the FNMOC analyses with the past tracks superposed (Fig. 3.1). The second was the geostationary satellite infrared imagery that was utilized both as a validation of the features in the numerical analyses and to provide additional information on the TC-Environment situation.

To assist in distinguishing between the S and N Patterns, the following procedure is proposed for annotating the FNMOC analysis:

i) denote the current position of the TC with a red TC symbol;

ii) denote the axis of the subtropical ridge in the vicinity of the TC using a brown sawtooth line;

iii) denote the axis of a peripheral ridge to the south through east of the TC by a brown sawtooth line; and

iv) draw in blue a streamline beginning at the midpoint of a line that extends south-southeast from the TC to the axis of the peripheral ridge and ends

where the streamline reaches a longitude that is either 10° east or west of the longitude of the TC.

Step iv) in this procedure is used to determine whether a TC in the Standard (S) Pattern/ Dominant Ridge (DR) Region is approaching the Ridge Modification by a large Typhoon (RMT) transformation to a North-Oriented (N) Pattern/ North-Oriented (NO) Region. The S/DR and the N/NO Pattern/Region combinations account for 74.1% of all the Pattern/Region combinations. Drawing the streamline described in step iv) facilitates identification of the transition between these two Pattern/Region combinations via the RMT transformation. In other words, this streamline identifies the influence imposed on the TC by the Environmental Structure, and as such, enables identification of the TC-Environment Structure.

As an example, consider the FNMOC 500 mb streamline analyses in Fig. 3.2. In panel a), the defining streamline starts at the midpoint of the TC and the peripheral ridge, extends northward and then westward to end at a longitude 10° west of the TC. Consequently, this represents a S/DR Pattern/Region. In panel b), the streamline extends northward, somewhat westward, and finishes eastward of the TC. Notice that the streamline *does* pass through the longitude of the TC, which indicates that a RMT transformation for the S/DR transition to the N/NO Pattern/Region is in progress. In panel c), the streamline denotes the transition to the N/NO Pattern/Region combination is completed because it *does not* pass west of the longitude of the TC from its beginning to end. Finally, panel d) has a streamline similar to the streamline in panel c), except that the additional information from the storm path indicating a significant increase in the TC translation speed suggests placing this TC-Environment Structure in the N/AW Pattern/Region combination.

Geostationary satellite infrared imagery was utilized to validate the FNMOC analyses and provide additional information on the TC-Environment Structure, i.e., the Synoptic Patterns and Regions. Specific indicators of TC-Environment Structures or Transformations that are determined from the satellite imagery include: i) size of the TC; ii) existence of a "wave-train" convective pattern to the southeast of the TC; and iii) indication of a monsoon gyre.

The size of the TC and the extent of the subtropical ridge poleward and/or eastward of the TC are factors considered in evaluating the possibility of the RMT transformation. Relatively large TCs can be expected to exhibit larger and stronger peripheral ridging to the southeast due to Rossby wave dispersion. If this peripheral ridging is significantly large relative to the subtropical ridge, the RMT transformation may occur (see description in CE). The information provided by the satellite imagery in conjunction with the streamline analysis described as step iv) above provides supporting evidence for the transition of the TC-Environment Structure.

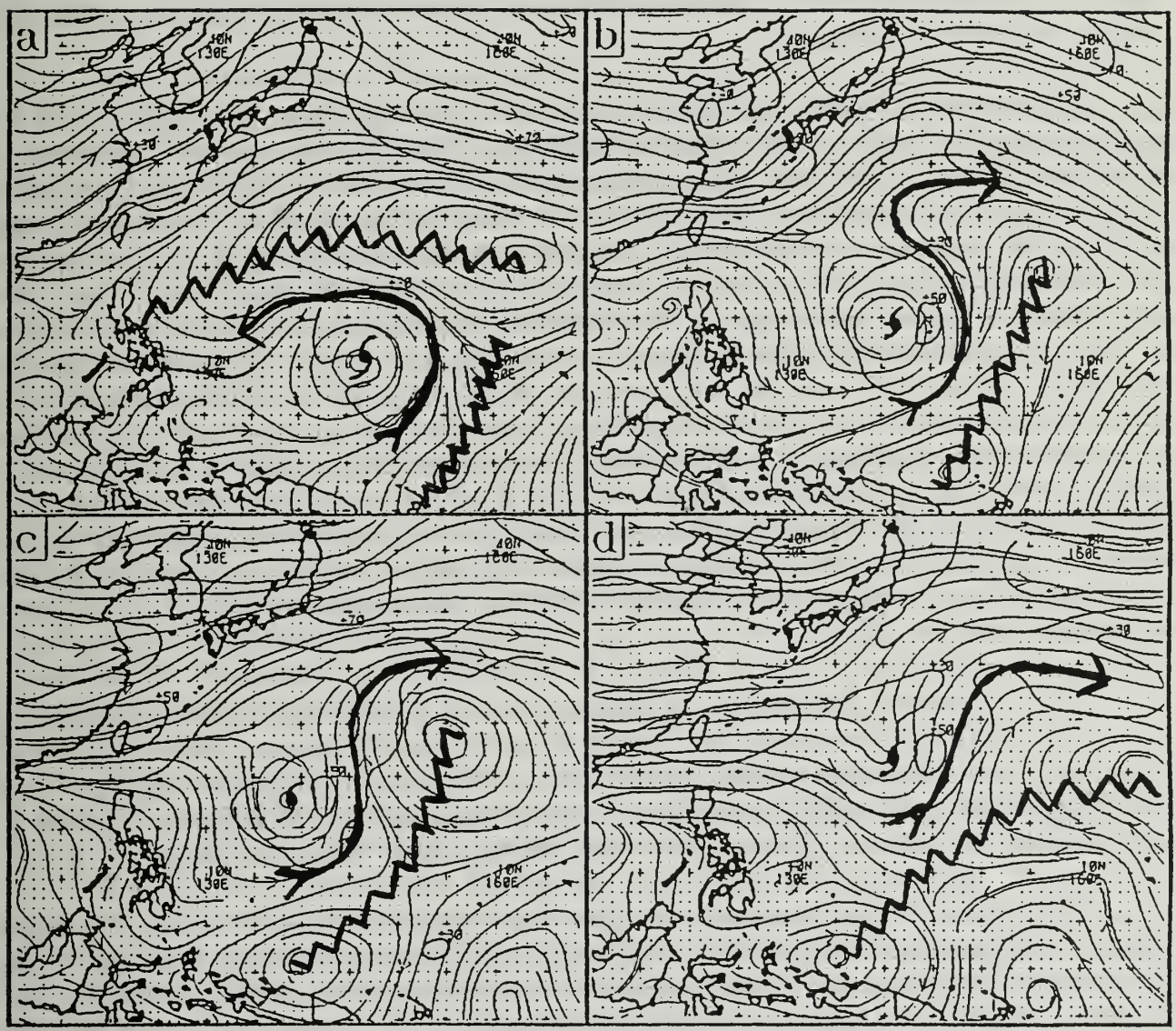

Fig. 3.2 FNMOC 500 mb streamline and isotach (kt) analyses at 0000 UTC for (a) 27 November 1991, (b) 28 November, (c) 29 November, and (d) 30 November during Supertyphoon Yuri. Each analysis is annotated with a defining streamline used to determine if a transition from S/DR is in progress (panel b) or is complete (panels c and d).

The "wave-train" pattern is the distinct cloud max-min-max pattern of convection that includes the TC and extends to the southeast. This easily recognized pattern allows identification of the existence of Rossby wave dispersion and also provides information on the possibility of a RMT transformation. However, caution must be exercised on relying only on the "wave-train" convective pattern to signify Rossby wave dispersion with its potential for the RMT transformation. A cloud max-min-max pattern is also evident when a second TC approaches from the east toward a TC. The subsidence induced between these two TCs may also produce a cloud max-min-max pattern similar to that generated by a single comparatively large TC.

The Gyre (G) Pattern definitions and the associated Regions as explained in CE were not applied well in this reproducibility test. That is, the trainees' frequency of detection of the G Pattern was only 46.0% (Table 3-2). A better or more consistent use of satellite imagery in detection of the G Pattern is the major impetus for this revised training section. The importance of utilizing the geostationary satellite imagery in conjunction with the FNMOC analyses in validating "large-scale" synoptic features cannot be over-emphasized. CE state one premise of the Systematic Approach is to introduce the element of human reasoning based on a dynamic, meteorological knowledge base so that the numerical guidance is not the only source of information to the forecaster. The geostationary satellite imagery allows forecasters to develop a conceptual model independent of the numerical analyses. A subtle point in the Systematic Approach is the forecaster's ability to separate the individual effects of the TC from the environment and vice versa. In other words, a forecaster must be able to envision the synoptic environment without the TC present. As with the other Synoptic Pattern conceptual models, the forecaster must recognize that actual G Patterns depicted in FNMOC analyses may vary from the idealized schematics found in CE.

The G Synoptic Pattern may be distinguished in geostationary satellite imagery by the extensive, deep convection that occurs in the confluent region between the large monsoon gyre and the ridge circulation to the east. This convection is further characterized by CE as partial or complete, quasi-circular, and comparatively large scale as it tends to wrap around the monsoon gyre and take on a characteristic "fish-hook" shape.

One trainee having incorrectly assigned the N Synoptic Pattern for the G Synoptic Pattern in more than half the cases is attributed to the similar north-south oriented ridging to the east of both of these Synoptic Patterns in the idealized conceptual models in CE. Whereas this similarity makes it difficult to distinguish the N and the G Synoptic Patterns from the FNMOC analyses alone, the differences are more pronounced in geostationary satellite imagery. As in the G Synoptic Pattern characteristics outlined above, the N Synoptic Pattern does have the extensive, deep convection to the east due to the confluence with the peripheral ridge. Unlike the G Synoptic Pattern, the N Synoptic Pattern does not have the partial or complete, quasi-circular convection. A more consistent use of the geostationary satellite imagery in conjunction with the FNMOC analyses should allow the forecaster to assign the correct TC-Environment Structure. The deficiencies revealed by the

reproducibility test emphasize the importance of utilizing concurrently these sources of information.

Additional discussion of "lessons learned" from the reproducibility test will be given in Chapters 4 and 5.

3.4 Reproducibility Test of Pattern/Region Transitions

3.4.1. Introduction. Whereas properly identifying the correct Synoptic Pattern and Region is important, of even greater importance is the proper recognition of when a cyclone transitions from one Synoptic Pattern/Region combination to another. Because such transitions will normally lead to significant changes in the track of the cyclone, recognition of an upcoming transition and the timing of that transition are tantamount to accurate track forecasts. It is in this area of reducing potential forecast errors associated with changing storm motion that the Systematic Approach can be most useful in its application. The hypothesis is that a properly equipped forecaster can anticipate the Synoptic Pattern/Region transition and select (reject) the objective aid guidance that agrees (disagrees) with the anticipated transition (CE).

3.4.2. Definitions. Before examining the results of the reproducibility test involving the three trainees, some terminology must be defined to give the reader the proper understanding. The first term to be defined is transition. As defined by CE, a transition may involve a change from one Synoptic Pattern to another, or from one Region to another region within the same Pattern. As discussed in Chapter 3.3.1, the benchmark assignment is not always a single Pattern and Region. In those cases in which dual Pattern/Region combinations were assigned (see Table 3-1 in Chapter 3.3.1), the definition of a transition becomes more complicated.

Table 3-5 contains four sequences of Pattern/Region combinations. Case 1 is an example of how a Region transition from Dominant Ridge (DR) to Weakened Ridge (WR) appears to begin, and the trainee might have even implied by the reversed sequence WR/DR in the third line that the Region was more like a WR than a DR. However, the effects forcing these Region changes in Case 1 then cease, and the original Pattern/Region combination is again assigned. Thus, this is *not* considered to be a Region transition because the WR Region never existed as a single entry. Whereas such a definition of a non-transition may appear to be arbitrary, it was judged to be an appropriate choice for this test in which the meaning and interpretation (especially of the ordering of letters) of dual assignments had not been agreed upon in advance for this reproducibility test.

Table 3-5. Four examples of Synoptic Pattern (first column; symbols defined in Table 2-1) and Synoptic Region (second column) sequences in time that illustrate definitions of transitions (see text).

CASE 1		CASE 2		CASE 3		CASE 4	
S	DR	S	DR	S	DR	S	DR
S	DR/WR	N	NO	S/N	DR/NO	S	DR/WR
S	WR/DR			N/S	NO/DR	S	WR/DR
S	DR			N	NO	S/N	WR/NO

Case 2 in Table 3-5 is an example of a direct transition in both Pattern and Region with no intermediate combinations. Here, the occurrence and the timing of the transition are obvious. Case 3 involves two intermediate combinations. The transition is considered to have occurred when the N/NO Pattern/Region combination appears as a single entry. That is, an Environment Structure that was clearly one Pattern/Region has clearly become a different Environment Structure. Even though the ordering of the letters has changed from line 2 to line 3 of Case 3, this is *not* considered to be an indication of a transition. This is because the experienced forecaster (L. Carr) and the three trainees did not agree in advance that the order of the letters in a dual assignment would have such a meaning. Notice that only the Pattern might have changed with a similar Region (e.g., S/DR transition to G/DR, or a G/NO to a N/NO), or only the Region may have changed within the same Pattern (e.g., S WR/DR becoming S/WR after earlier having been S/DR). In Case 3, the transition is clear because both the Pattern and Region have changed.

Case 4 in Table 3-5 is an example of a convoluted transition. This sequence includes both the DR and WR Regions of the S Pattern in the second and third lines. As in the first three lines of Case 1, a transition is *not* considered to have occurred from the original S/DR to a single entry representing the change to the WR Region (recall the order of listing of two regions is not considered to have special meaning). A transition is considered to have occurred at the fourth line because the original (DR) Region is no longer one of the Region combinations.

As in Section 3.3.1, designing a scoring method is difficult for such transitions involving multiple Patterns/Regions and dual assignments on the part of the experienced forecaster and each of the three trainees. A *fully correct* transition requires that the trainee assignments have a sequence from the benchmark Pattern/Region to the new Pattern/Region. A *similar* transition is defined as occurring if the trainee begins the sequence in the benchmark Pattern and Region, but transitions to a Pattern/Region that has a similar track change of the tropical cyclone (i.e., S/DR → N/NO; S/DR → S/WR; S/DR → M/SF; S/DR → G/NO). These four examples all will result in a cyclone track change from westward or northwestward to a northward or northeastward track. The AW region is unique because of the typical speed of the cyclone while in this region, which precludes any other region from being considered as "similar."

The terms *miss* and *false* are also defined for use in scoring the transitions. A *miss* is when the benchmark has a transition and the trainee does not have either the *correct* or a *similar* transition. The term *false* is used when the benchmark does not have a transition and the trainee does indicate a transition occurred.

The final definitions are two types of *flip-flops*. The first type of *flip-flop* is the trainee assigns a transition from the benchmark Pattern/Region to either the correct or a similar Pattern/Region, but his sequence of assignments passes through a Pattern/Region that was not involved in the actual transition. An example of such a transition is S/DR → N/NO followed by N/NO → S/WR when the correct transition was S/DR → S/WR. This type of *flip-flop* results not only in a *flip-flop* being scored, but also a similar transition will have been scored because the S/DR → N/NO is a similar transition to the S/DR → S/WR. This flip-flop will be referred to as a *similar flip-flop* for discussion purposes. The second type of *flip-flop* is when an unnecessary transition from the benchmark Pattern/Region to a second, and incorrect, Pattern/Region is indicated by the trainee. That is, the trainee recognizes his transition was temporary or not necessary and then changes back to the correct Pattern/Region. This is simply called an *out/back flip-flop*.

The final terms to be defined are the use of the words *early* and *late* in reference to the timing of the transition. A trainee-identified transition that occurs before the benchmark transition is considered to be early. The late transition is when the trainee's identified transition happens after the transition of the benchmark. As the analyses were only supplied every 12 h, all timing increments are in 12-h periods.

3.4.3. Method of Scoring. The reproducibility test for the transitions has the goal of assessing how successfully each trainee identified a transition was occurring and the timing of the transition. The definitions described in 3.4.2 are used for the scoring. The number of correct and similar transitions is the most important result, because it indicates that the trainees were able to recognize that a transition in the Environment Structure was occurring that would be expected to trigger a track change.

The importance of the transitions is amplified when one considers there were 141 transitions in 85 tropical cyclones, or 1.66 transitions per storm, contained in the reproducibility test data set. Even if a storm did not experience a transition, the Environment Structure may seem to approach a transition for some interval. Thus, it is also important to not have a large number of false transitions or out/back flip-flops, which might lead to windshield-wiper track direction forecasts. Misses, false, and flip-flop transitions are viewed with varying degrees of importance with respect to the reproducibility test. The missed and false transitions are of the greatest importance because the trainee did not see the transition occur or thought he saw a transition that did not actually occur. These problems will be used to help identify deficiencies in the training procedures to improve the training provided to future users of the Systematic Approach.

The scoring results are summarized in Table 3-6 by individual year and a 4-y combined total. The numbers of transitions in 1990 through 1993 are 15, 34, 60, and 32, respectively. The tables have a combined total of 423 transitions since each of the three trainees should have detected 141 transitions. That is, the combined sums for the individual years will be 45, 102, 180, and 96, respectively. Unless otherwise identified, all future references to the number of transitions for the individual years and combined 4-y total will be the total for all three trainees.

3.4.4. Transition Tests. The 4-y combined scores will be discussed first, and followed by the discussion of the items of interest in the individual years.

i) 4-y Combined. A combined total of 423 transitions should have been detected by the three trainees in the 4-y combined data set. Of the 423 transitions, 204 (48.2%) were correctly identified by the trainees and an additional 138 (32.6%) similar transtions were identified. Summing these two transitions, 80.9% of the 423 transitions for the 4-y combined were identified by the trainees. Thus, the trainees missed only 81 (19.1%) of the transitions. Furthermore, an additional 26 (6.1%) false transitions were classified by the trainees, and there were 64 (15.1%) flip-flops by the trainees.

A review of the missed transitions was done to see if there was a Pattern or Region that was continually missed by the trainees. A percentage of missed Patterns was computed by dividing the number of times the Pattern was missed by the number of times the Pattern occurred in a transition. Each transition has two Patterns and two Regions so a total of 846 double-sided Pattern/Region transitions were counted. Transitions from the S Pattern were missed 68 of 342 times (19.9%), from the N Pattern were missed 51 of 336 times (15.2%), from the G Pattern were missed 35 of 123 times (28.5%), and from the M Pattern were missed 8 of 45 times (17.8%). Similarly, no Region transition was missed significantly more than the other Regions. Transitions from the NO Region were missed 66 of 318 (20.8%), DR was missed 49 of 255 (19.2%), WR was missed 20 of 84 (23.8%), AW was missed 19 of 144 (13.2%), NF was missed 5 of 21 (23.8%), and SF was missed 3 of 24 (12.5%).

Table 3-6 Combined numbers of transitions that should have been detected by the three trainees and separation into correct, similar, missed, false and flip-flops for each year and the 4-y combined total.

Year (Transitions)	Correct	Similar	Combined	Missed	False	Flip-flop
1990 (45)	28	13	41	4	3	9
1991 (102)	42	40	82	20	12	17
1992 (180)	92	52	144	36	6	24
1993 (96)	42	33	75	21	5	14
Combined (423)	204 (48.2%)	138 (32.6%)	342 (80.9%)	81 (19.1%)	26 (6.1%)	64 (15.1%)

When the Pattern/Region combinations were examined, the transitions involving G/DR and S/AW were missed 10 percent more frequently than any other combination. The G/DR was missed 12 of the 27 times (44.4%) it occurred in a transition, and S/AW was missed 11 of 30 times (36.7%). The least missed Pattern/Region combination was N/AW. It was missed only 5 of 93 times (5.4%).

Of the 81 misses in Table 3-6, seven cases involved all three trainees missing the transition (a total of 21 misses). In all seven cases, the transition was to another Pattern/Region that has a storm movement that was similar to what it was before the transition: three were transitions from G/NO to N/NO; two were S/WR to N/NO; one was S/WR to S/AW; and one was S/DR to G/DR. An additional 30 of the 81 misses involved 15 cases where two of the trainees missed the transition.

The 54 false transitions were examined in a similar way to the missed transitions. The false transitions did not involve any Pattern, Region, or Pattern/Region combination significantly more often than the others. At 13 of 123 (10.6%), the G Pattern was the most frequent false transition Pattern identified by the trainees. The Region with the largest number of false transitions was the SF Region at 3 of 24 (12.5%). The M/SF was also the worst Pattern/Region combination for falsely identified transitions.

The three trainees had a total of 64 flip-flops for the 4-y combined data set. Of these flip-flops, 27 (42.2%) were typed as similar flip-flops in that the trainee began in the correct or similar Pattern/Region combination, sequenced through a Pattern/Region not involved in the actual transition, and ended with the correct or similar Pattern/Region. An additional 29 (45.3%) of the flip-flops were of the out/back type in that the trainee did an unnecessary transition from the benchmark, recognized the mistake, and transitioned back to the correct Pattern/Region. The average time period the trainee took to perform the out/back flip-flop was 30 h.

ii) Timing. Another important result is the trainee's timing of the transition compared to the benchmark. While identifying that a transition is occurring is extremely important, correctly timing the transition is also of importance. Helping the forecaster properly identify the timing of the transition is a goal of the Systematic Approach training.

Figure 3.3 contains a histogram of the 342 correctly and similarly identified transitions for the three trainees for the 4-y combined data set. These correct or similar transitions were identified "on time" in 118 cases. However, one transition was identified 120 h late. Of the 342 correct/similar transitions, 245 (71.6%) were identified either 12 h late, on time, or 12 h early. These 245 well-timed transitions represent 58% of all the transitions that occurred in the 4-y combined data set. The timing distribution of the trainees is slightly shifted toward the late identifications. This is understandable considering the trainees did not have the opportunity of looking backward and correcting for a missed transition.

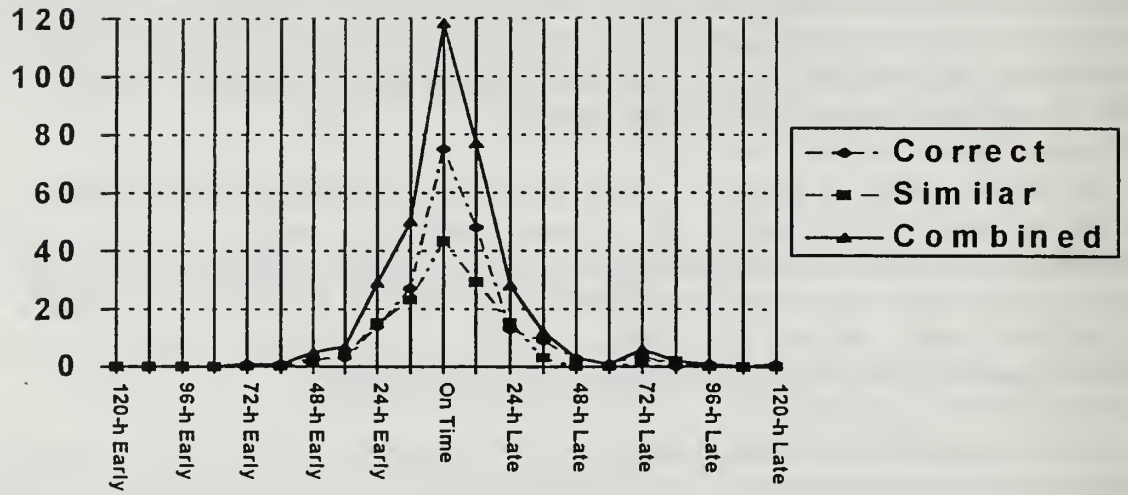

Figure 3.3 Histogram of timing of correct and similar transitions identified by the three trainees for the 4-y combined data set.

If the "acceptable" timing window for transitions is expanded to ±24 h, the number of correct/similar transitions is 302. This expanded window would result in 88.3% of the 342 transitions being identified as correct/similar transitions.

iii) 1990. A total of 45 transitions occurred in the 13 tropical cyclones in the 1990 data set. This year had the highest percentage of correct transitions with 62.2%. The year also had the best combined percentage of transitions with 41 (91.1%) being identified. Only 4 transitions (8.8%) were missed, which makes 1990 the lowest percentage of misses by over 10 percentage points. On the other hand, the percentage of flip-flops was higher.

iv) 1991. A total of 102 transitions occurred in 19 tropical cyclones. The scores for the trainees were similar to the scores for the 4-y combined data set. However, the highest percent of false transitions was recorded in this year.

v) 1992. With 180 transitions that occurred during 28 tropical cyclones, this was the most active transition year of the four, and alone accounted for 42.6% of all transitions. The scores for 1992 were very close to the average scores for the four years. The only significant deviation was that the number of false transitions was about one half of the average.

vi) 1993. This year included 25 tropical cyclones and 96 transitions. The scores for the year were similar to the four-year combined averages. The percentage of misses was slightly higher at 21.9% compared to the average of 19.1%.

4. Refinement of the Meteorological Knowledge Base

(Primary author: L. E. Carr, III)

4.1 Background

Carr and Elsberry (1994; hereafter CE) described the roles of the Environment and the TC in governing TC motion (schematically illustrated in CE Figs. 3.3 and 3.4) via specific conceptual models (listed in Tables 3.1 - 3.3 of CE). The TC-Environment conceptual models in CE were based in large measure on the first author's operational experience forecasting TCs during the 1990 and 1991 western North Pacific seasons. The completion of the five-year climatology described in Chapter 2, and the reproducibility test in Chapter 3, have provided a more systematic evaluation of the set of TC-Environment conceptual models proposed in CE. This chapter summarizes some of the more important results from this evaluation.

The consensus of the Systematic Approach developers (Carr and Elsberry) and reproducibility test trainees (Boothe, Kent, and White) is that the set of TC-Environment conceptual models proposed by CE are sufficient to characterize nearly all the variations of TC-Environment Structure that occur in the western North Pacific basin. However, a number of refinements are suggested to:

(i) provide additional emphasis regarding various details and inferences from the TC-Environment conceptual model set that were robustly verified and have potentially great forecasting utility;

(ii) revise and clarify the descriptions of some of the TC-Environment conceptual models;

(iii) document additional and sometimes complex transitional situations that are not explicitly mentioned in CE;

(iv) provide additional guidance for distinguishing between Pattern/Region combinations that have similar appearances in the NOGAPS analyses and satellite imagery; and

(v) provide more structured guidance to increase the timeliness of detecting that a transition in Environment Structure is taking place and to increase the probability of characterizing correctly that transition to a new Pattern/Region combination.

This chapter will address the first four issues above, including the introduction of two new conceptual models of Environment Structure transitions. The Reverse-oriented Trough Formation (RTF) occurs in association with two (or more) adjacent TCs. In the Subtropical Ridge Modulation (SRM), the transition is primarily related to midlatitude troughs and

ridges. Issue (v) in the above list will be addressed in Chapter 5.

4.2 S Pattern-related refinements

Three variations of the Standard (S) Pattern schematic were identified by CE (see their list on p. 26). It was noted that longitudinal variations (hereafter slope) of the subtropical ridge axis are correlated with variations in the generally westward direction of motion for TCs in the Dominant Ridge (DR) Region. For example, the west-southwest (WSW) track direction of Typhoon Ed (Fig. 3.18a in CE) is consistent with the east-northeast (ENE)-to-WSW slope of the subtropical ridge axis (Fig. 3.6b in CE). The smaller than average size of Ed is an important factor in this close agreement between the WSW track and ridge slope since the beta-effect propagation (BEP) speed of small TCs is usually negligible compared to the speed of environmental steering in the DR Region (see CE Fig. 3.9 and discussion of Ed on p. 77). Such agreement should not be expected with larger TCs, in which the BEP will tend to move the TC poleward into, and sometimes through (recall CE Fig. 3.51 and related discussion), the subtropical ridge regardless of the ridge axis slope. The five-year climatology confirms the prevalence of the S/DR combination and that important track variations about the generally westward tracks may be detected based on the past and forecast slope of the ridge axis.

A particularly useful expectation is that a non-climatological south-of-west track will be followed by small TCs when a ENE-to-WSW ridge axis slope is expected to persist. An illustration of this valuable relationship is provided here for Tropical Storm Winona (Figs. 4.1 and 4.2), which maintained a "compact" size throughout its existence (ATCR 1989, p. 33-36). Notice that a persistent ENE-to-WSW ridge axis slope is evident in the NOGAPS analyses during 16-20 January 1989 (Fig. 4.1), and that the storm position to the NNW of the NOGAPS-analyzed circulation center in Fig. 4.1c further supports the presence of east-northeasterly environmental steering. Although the track direction of Winona is persistently WSW (Fig. 4.2a), the JTWC forecasts tend to be more poleward with increasing forecast interval, which results in a right-of-track bias (Fig. 4.2b).[1] The 60 n mi forecast error at 24 h is actually a significant error for a small TC, as it potentially may be the difference between a direct hit and insignificant wind damage.

The case of Supertyphoon Gordon is another example that only smaller-than-average TCs will likely track south-of-west in the DR Region south of a ENE-to-WSW sloping ridge (Fig. 4.3). The WSW track of Gordon during 10-13 July 1989 changes to WNW during

---

[1] As will be shown in the Objective Aid Traits Knowledge Base in a subsequent report, the character of the JTWC forecast in Fig. 4.2b is indicative of a tendency to follow the consensus of the numerical and objective guidance, which tends to be more representative of the motion traits of average or larger TCs that thus tend to propagate more to the northwest than small TCs.

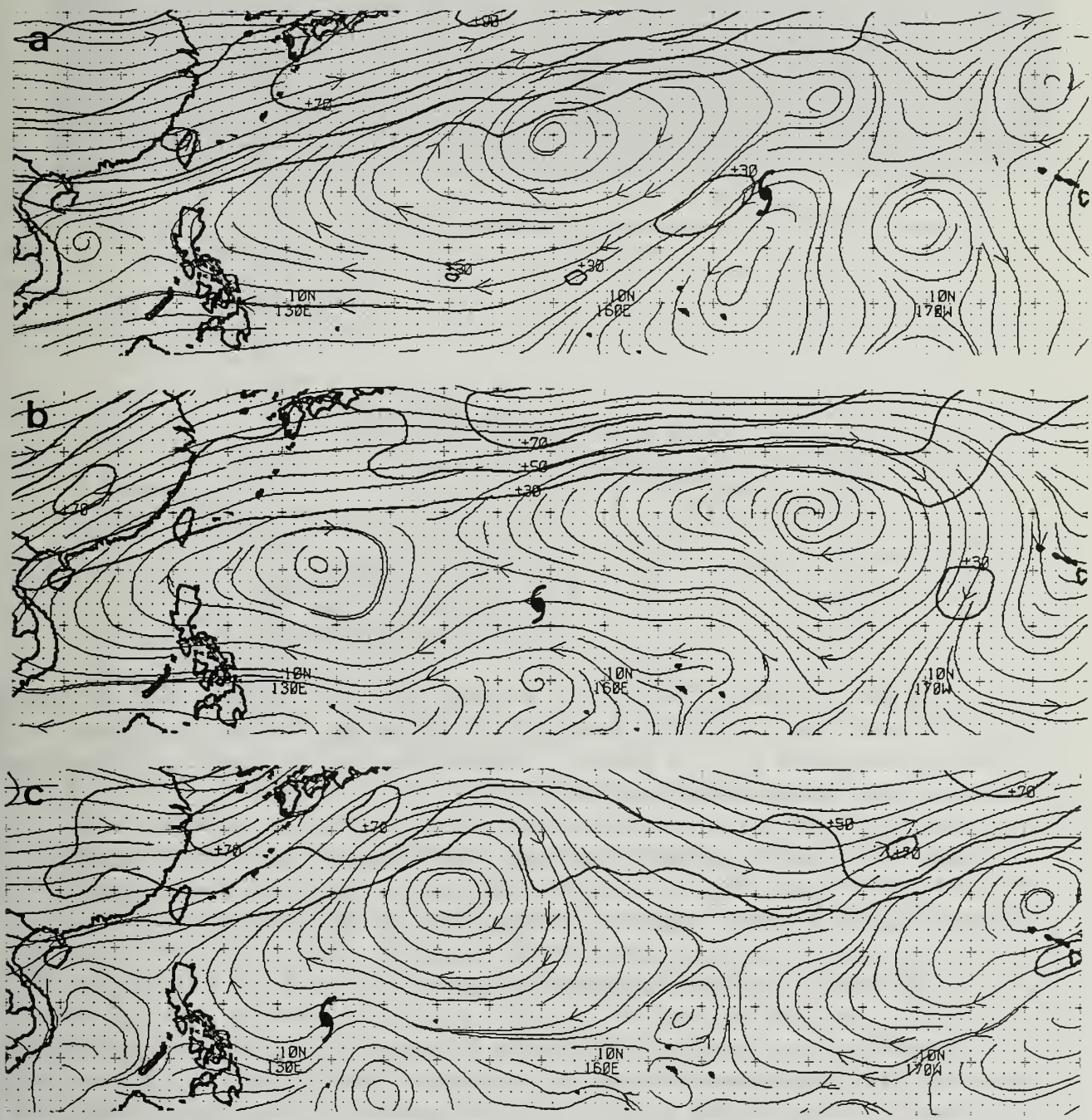

Fig. 4.1 Streamline (thin) and isotach (heavy; contour interval of 20 kt beginning at 30 kt) analyses at 500 mb from NOGAPS at 0000 UTC on (a) 16, (b) 18, and (c) 20 January 1989 during TS Winona (TC symbol).

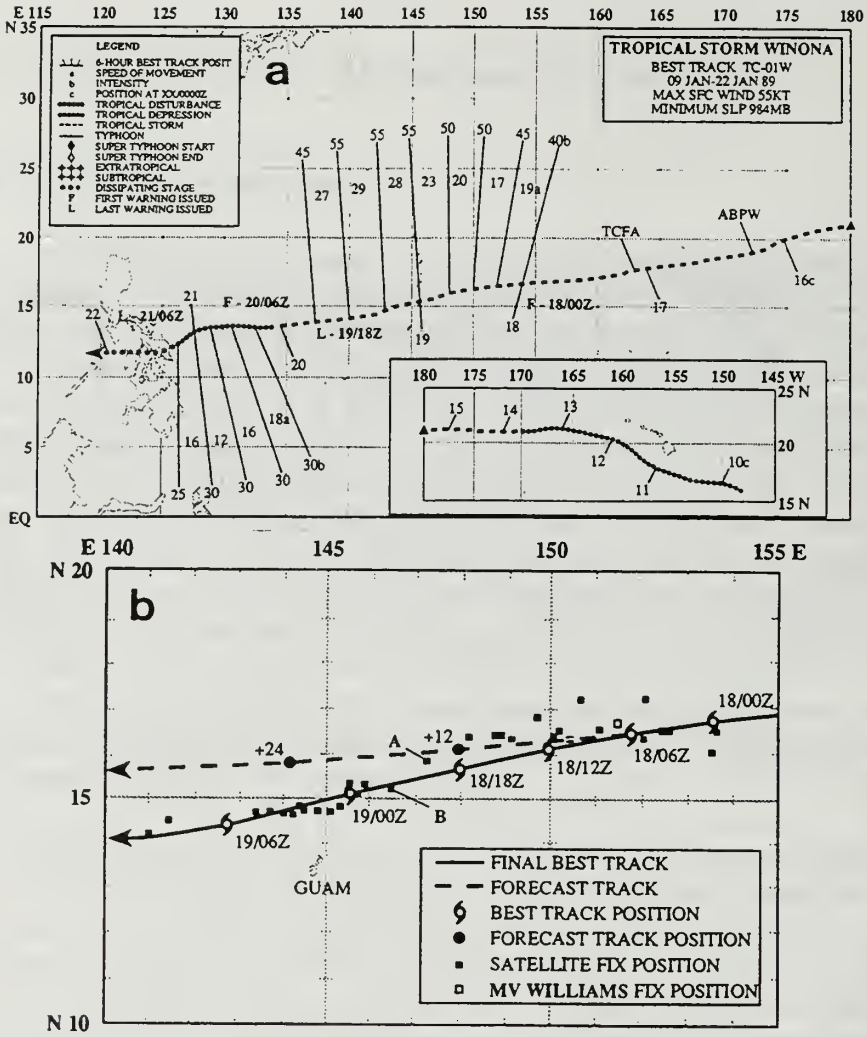

Fig. 4.2 (a) Best track from JTWC for TS Winona during 9-22 January 1989. (b) Example of a JTWC track forecast (dashed) from 06 UTC 18 January and best track from 00 UTC 18 January through 06 UTC 19 January. Notice how close this small storm approached Guam compared to the forecast (ATCR 1989).

14-19 July 1989 (Fig. 4.3c) despite a sloping ridge structure (not shown) similar to that associated with Winona (Fig. 4.1). The key difference is that Gordon was a small TC (Fig. 4.3b) until 13 July and was larger-than-average size after 15 July (Fig. 4.3a).

4.3 S/WR and N/NO Pattern/Region Ambiguity

One lesson from the reproducibility test (Chapter 3) is that the decision whether to characterize the Environment Structure in terms of the S/WR Pattern/Region combination versus the N/NO combination tends to be problematic. In the troublesome cases, the TC is equatorward of the subtropical ridge axis, and is typically larger-than-average in size, and this is associated with peripheral ridging (perhaps amplifying) to the southeast. Initially, this peripheral ridging may *not* be accompanied by an erosion of the subtropical ridge poleward

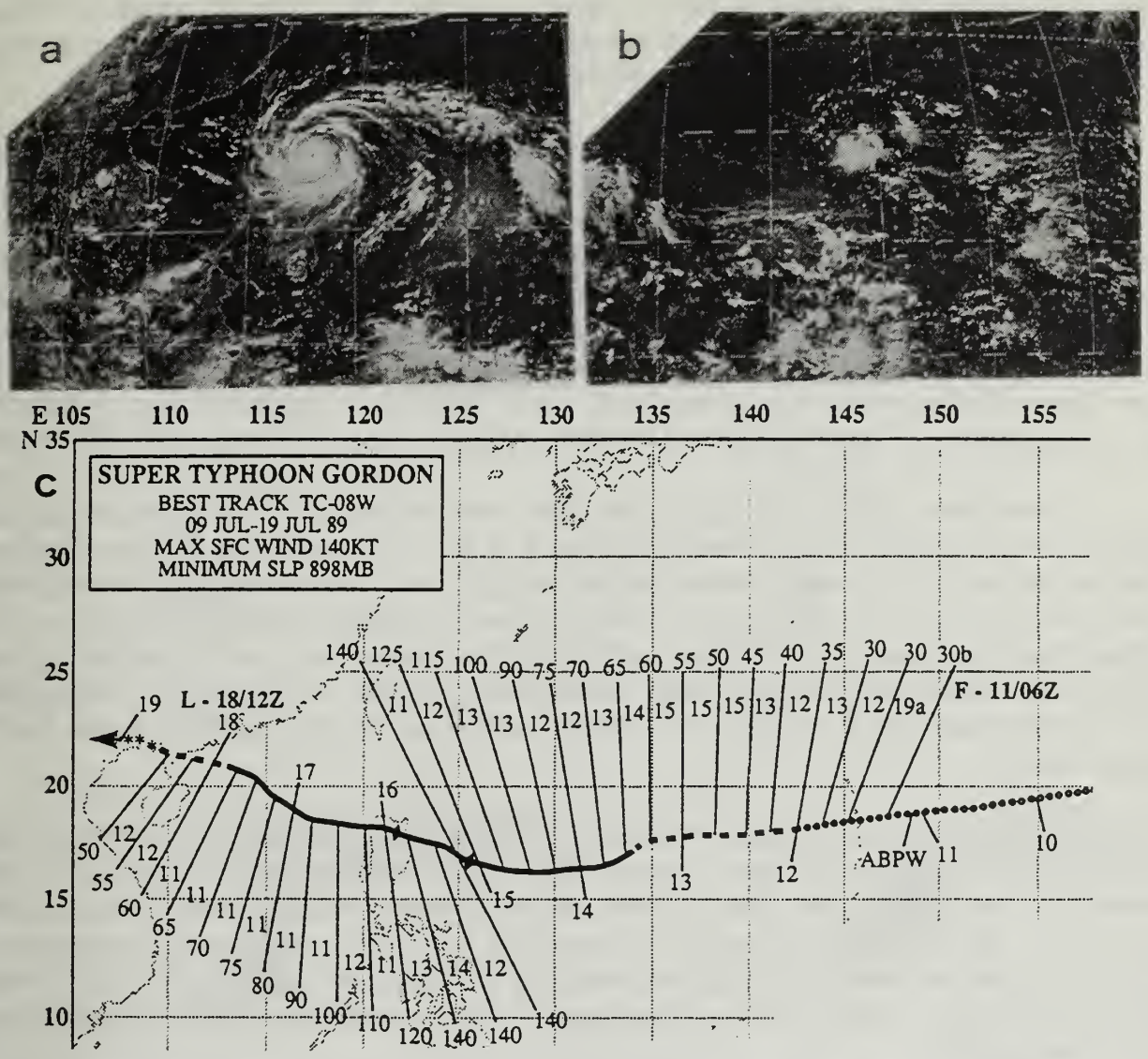

Fig. 4.3 Satellite images on (a) 15 July and (b) 11 July 1989 illustrate the increased size of ST Gordon in time. (c) Best track of ST Gordon from 9-19 July 1989 illustrating the south of west track prior to 14 July and the north of west track after 1200 UTC 14 July.

of the TC, or by an attendant shift of the isotach maximum from say the north-northeast to the east of the storm position. Thus, the Pattern/Region is characterized as S/DR. As the TC approaches a break in the subtropical ridge associated with a midlatitude trough, the decreasing height gradient to the north, perhaps combined with the slowly amplifying height gradient to the southeast, may result in a distinct shift of the isotach maximum to the east. Such a shift, in combination with the break in the subtropical ridge to the north and the peripheral ridging to the southeast, reasonably satisfies the N2 Pattern schematic of CE. Such a scenario may be characterized in three ways with almost equal justification: (i) as a transition from S/DR to S/WR by a significantly propagating TC that only subsequently appears to transition suddenly to N/NO as the ridge weakness is approached; (ii) as a transition from S/DR to N/NO that did not occur until the TC moved close to the break

in the subtropical ridge, which is thus a matter of timing (i.e., rate of peripheral ridge development versus rate of approach of the ridge break); or (iii) as a brief transition from S/DR to S/WR followed by a S/WR to N/NO transition.

An example in which the three trainees chose option (i) and the master developer of the Systematic Approach chose option (ii) is shown in Fig. 4.4 for Supertyphoon Yancy during August/September 1993. Notice the distinct isotach shift and the increase in prominence of the peripheral ridging southeast of Yancy from 1200 UTC 31 August to 1200 UTC 1 September (Figs. 4.4a and b, respectively), which led the master developer to assign a N/NO combination. It should be noted that the master developer's characterization was influenced by knowledge (not available to the trainees) that the peripheral ridging would follow Yancy during recurvature (Fig. 4.4e). Such behavior is indicative of a N Pattern, whereas a gradual turn toward the east is more typical in the AW Region of a S Pattern.

In retrospect, this ambiguity should have been expected. The principal feature associated with a RMT-induced transition from a S to N Pattern is just a more vigorous version of the peripheral ridging that accompanies BEP and is associated with Rossby wave dispersion (recall CE Appendices D and F). Since modelling results indicate that this peripheral ridging depends on TC size, and TC size is a continuum, it is not surprising that certain combinations of subtropical ridge structure and TC size would result in a marginal RMT-induced transition from the S to N Pattern when the TC approaches a break in the subtropical ridge.

Although this scenario generated many misclassifications in the reproducibility test, it is emphasized that the TC track change after such a sudden transition to the N/NO combination does not depart greatly from the recurvature track in a persistent S/AW combination. For example, the track of Yancy (Fig. 4.4e) has a more typical recurvature track (e.g., Typhoon Hattie; CE Fig. 3.41) than do the tracks of Typhoons Page or Yvette with their anomalous poleward turns immediately following recurvature (CE Figs. 3.53 and 3.57, respectively).

4.4 N Pattern-related refinements

In CE, two North-oriented (N) Synoptic Patterns were defined. N1 Pattern (CE Fig. 3.7a) is a manifestation of the formation in a reverse-oriented monsoon trough, and involves a smaller TC that moves through the pattern. The N2 Pattern (CE Fig. 3.7b) is generated by a single, and usually larger-than-average TC, as a result of strong Rossby wave dispersion peripheral ridging to the southeast of the TC (as a result, the peripheral ridge in the N2 Pattern tends to move poleward with the TC). During the development of the 5-year climatology, many variations on these proposed N Pattern types were observed. That is, a continuum of patterns was found that adequately satisfy the basic defining characteristic of the N type: anomalous ridging along the south through east periphery of the TC (or TCs) that is providing the primary impetus to TC motion. Among the range of possibilities are:

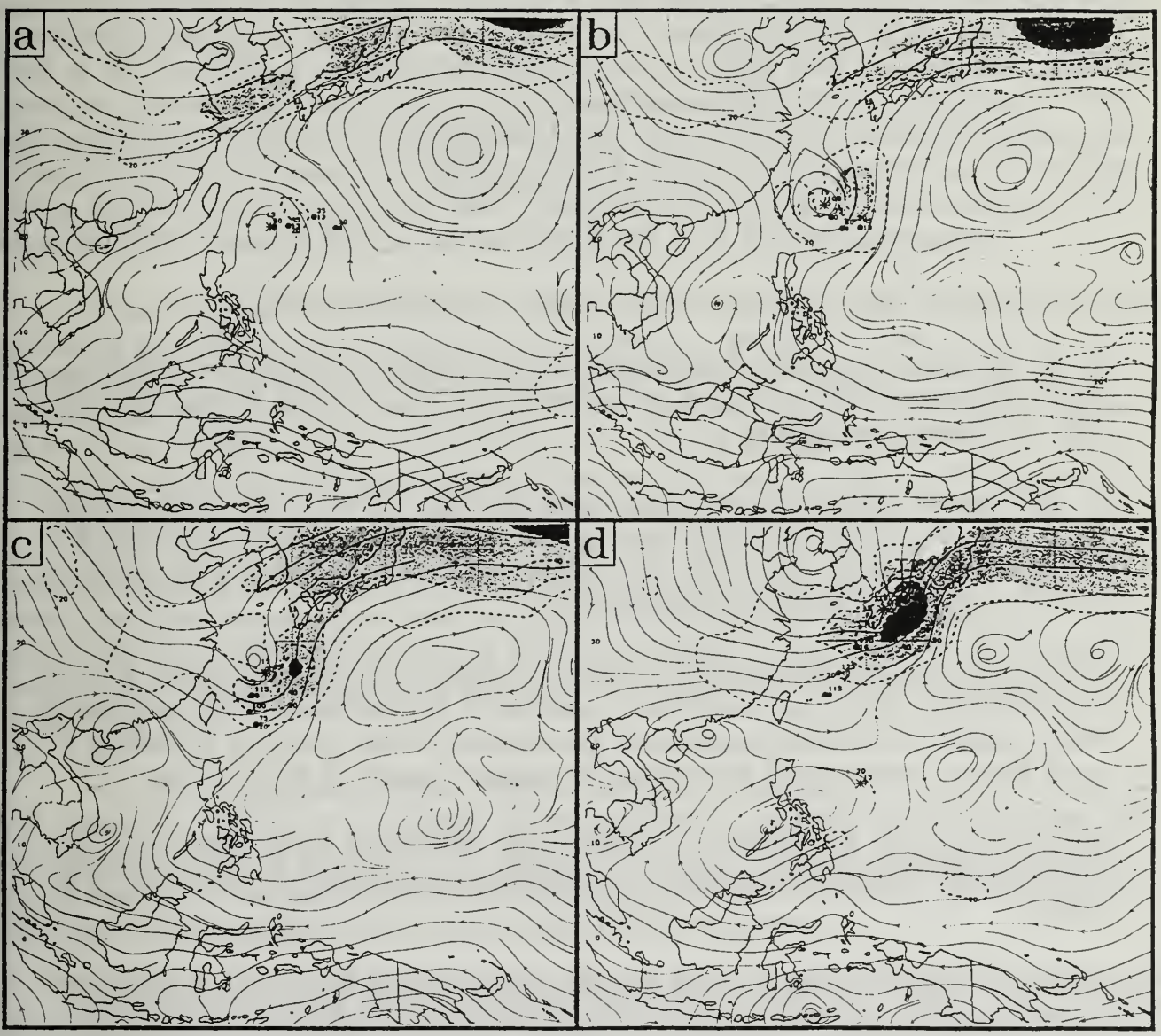

Fig. 4.4 Streamline and isotach (dashed; contour interval of 10 kt beginning at 20 kt with shading beyond 30 kt) analysis from NOGAPS at 12 UTC on (a) 31 August, (b) 1 September, (c) 2 September, and (d) 3 September 1993. Present (asterisk) and past 12-, 24-, and 36-h positions of ST Yancy are shown.

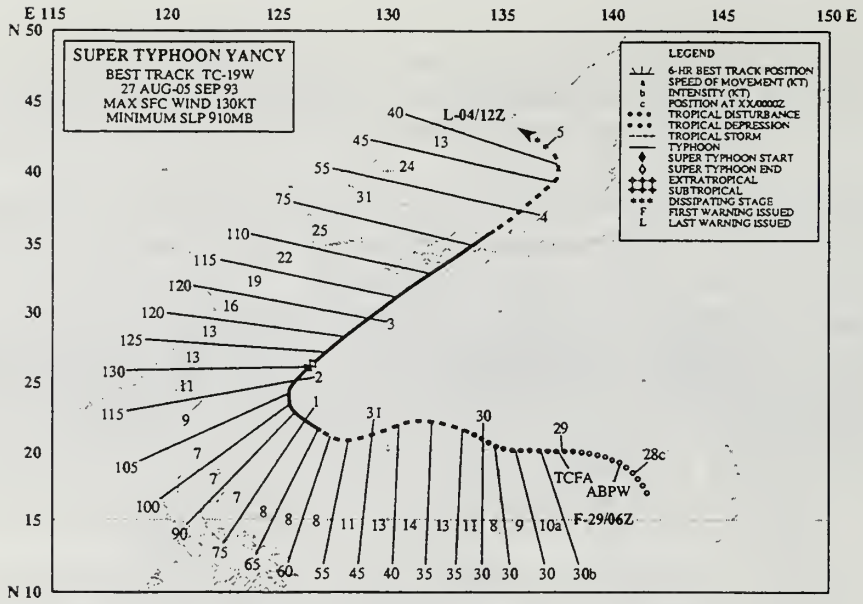

Fig. 4.4(e) Best track for ST Yancy during 27 August - 5 September 1993.

(i) N pattern development in response to the combined Rossby wave dispersion effects of multiple TCs, which will be addressed in Chapter 4.7 in terms of the new RTF transitional mechanism;

(ii) wide variations in the slope of the peripheral ridge with associated influences on TC motion (e.g., ENE TC motion in response to anomalous ridging to the south that has a nearly zonal orientation, in contrast to the more poleward motion implied in the N1 and N2 Pattern schematics in CE);

(iii) variations in the relationship between the movement of the embedded TC and the peripheral ridge (e.g., sometimes a portion of the peripheral ridge associated with a single TC will break away and drift southwest, which leads to a weakening of the N Pattern, and perhaps a transition to another (usually S) Pattern; and

(iv) changes in the Environment Structure from resembling N1 to more like N2 as a developing TC circulation appears to modify the character of the N pattern in its vicinity.

These variations observed in the five-year sample will henceforth be viewed as extensions and refinements of the proposed N pattern conceptual model as presented in CE to more adequately reflect reality. Reference to two explicit types of N Patterns (i.e., N1 and N2) will no longer be made. Rather the basic N Pattern type will be viewed as arising from a range of circumstances that cause attendant variations in the appearance of the pattern.

4.5 G Pattern-related refinements

4.5.1 Impact of rapid monsoon gyre (MG) movement. The implication from the G Pattern conceptual model in CE (see their Fig. 3.12 and accompanying discussion) is that TCs forming to the southeast of the MG will subsequently follow cyclonically curved, and predominantly poleward-oriented, tracks around the eastern semicircle of the MG at a rate roughly equivalent to the MG tangential wind speeds at the location of the TC. A tacit assumption is that the translation of the MG is small compared to the MG tangential wind speed at the location of the TC. In all the TC-MG case studies in CE, the impact on TC track of MG movement was relatively minor and the tracks have the expected cyclonic curvature. For example, the MG has minimal translation relative to the cyclonically curved, poleward-oriented tracks of Nancy and Owen (Fig. 3.89 in CE), and the highly circular track of Peggy (Fig. 3.92). Similarly, the cyclonically curved, poleward-oriented track of Tip (Fig. 3.69 in CE) from 9-11 September 1989 is consistent with the slow poleward drift of the associated MG center as Tip and the MG coalesced via a MTI transformation.

In several cases in the five-year climatological data base, the translation of the associated MG was roughly as fast as the movement of the TC. In such situations, the expected cyclonic curvature of the TC track may be greatly reduced or even absent. For example, the MG circulation in the August 1991 case involving TD 15W moves so fast to the west that TD 15W effectively retrogrades from the DR Region of the G Pattern during 25 and 26 August (Figs. 4.5a-b) to the transition zone between the DR and NO Regions by 27 August (Fig. 4.5c). As a result of this rapid westward movement of the MG, the track of TD 15W is more zonally-oriented rather than poleward-oriented and is slightly anticyclonic during the period (Fig. 4.5e). In the case involving Tropical Storm Val, the MG moves north-northwestward essentially as fast as Val during 24-26 September (Figs. 4.6a-c). As a result, Val remains roughly east of the MG's position, and the track of Val during 24-26 September is more poleward than zonally oriented, and is sinuous rather than cyclonically curved (Fig. 4.6e).

Very little is presently known about the processes associated with MG development and movement. Thus, no dynamically-based guidance is available to the forecaster for anticipating in advance whether a MG will move rapidly or be quasi-stationary throughout its existence. MG motion does seem to exhibit persistence; that is, rapid or quasi-stationary MGs tend to remain that way for most or all of their existence.

4.5.2 Monsoon Gyre Formation (MGF) recognition. During the reproducibility test, the trainees had considerable difficulty recognizing when the TC-Environment Structure conformed to the G Pattern (only a 46% average success rate according to Table 3-2). The principal cause of this problem was that CE did not address a transition of Environment Structure into a G Pattern as a result of Monsoon Gyre Formation (MGF) (see Fig. 2.8). In particular, the trainees indicated a need for guidance in recognizing MGF as it is occurring. In CE, it was tacitly assumed that the TC forms within the pre-existing MG and will have characteristic tracks in response to advection by the MG circulation. Since MG

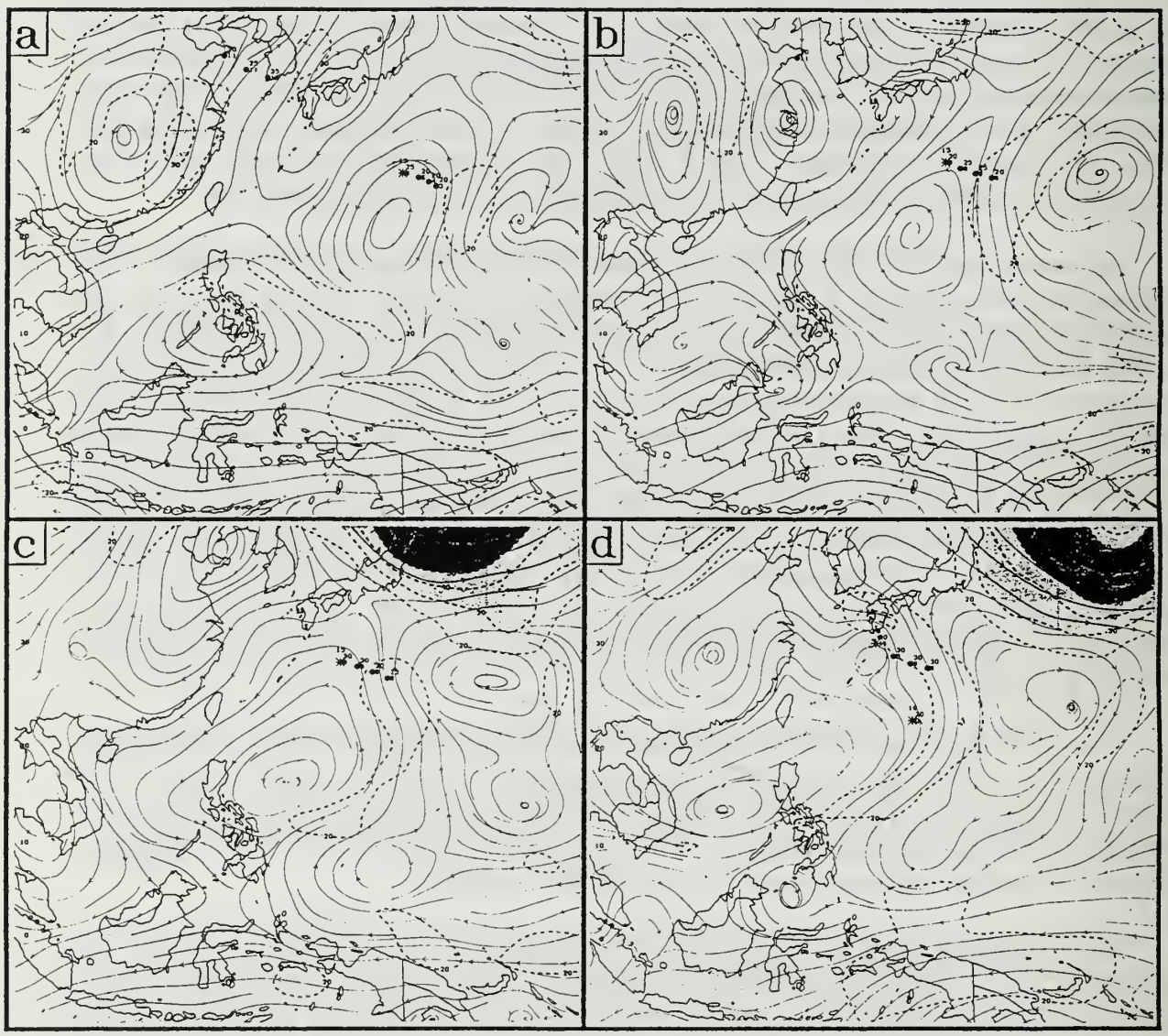

Fig. 4.5 As in Fig. 4.4, except for TD 15W during (a) 25, (b) 26, (c) 27, and (d) 28 August 1991.

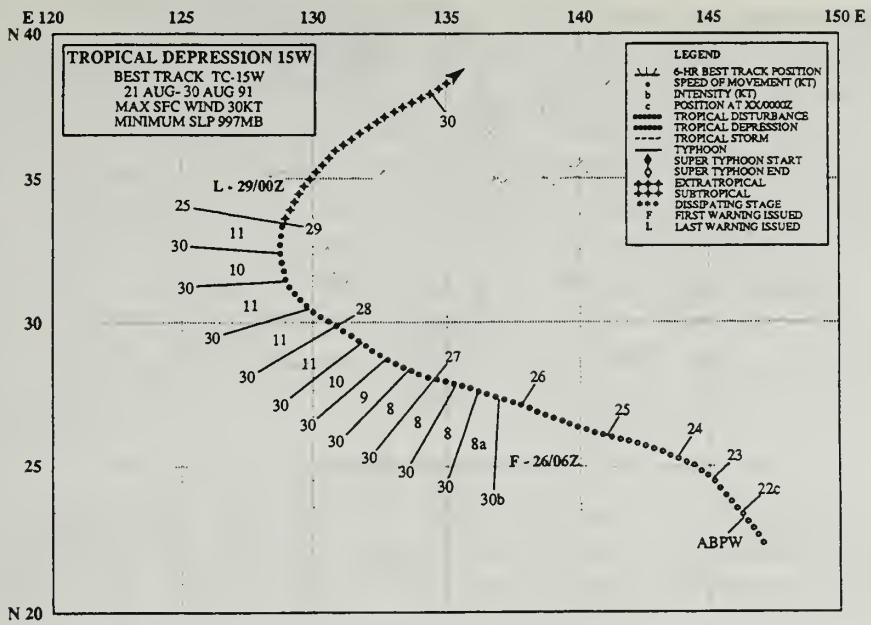

Fig. 4.5(e) Best track for TD 15W during 21-30 August 1991.

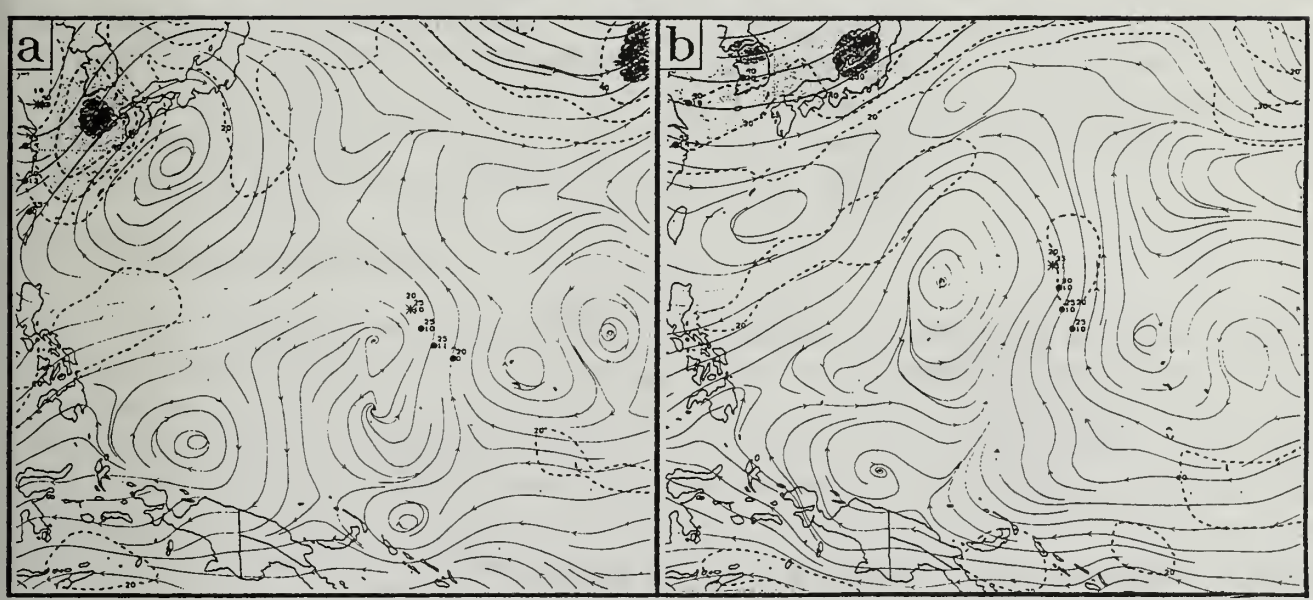

Fig. 4.6 As in Fig. 4.4, except for TS Val during (a) 24, (b) 25, (c) 26, and (d) 27 September 1992.

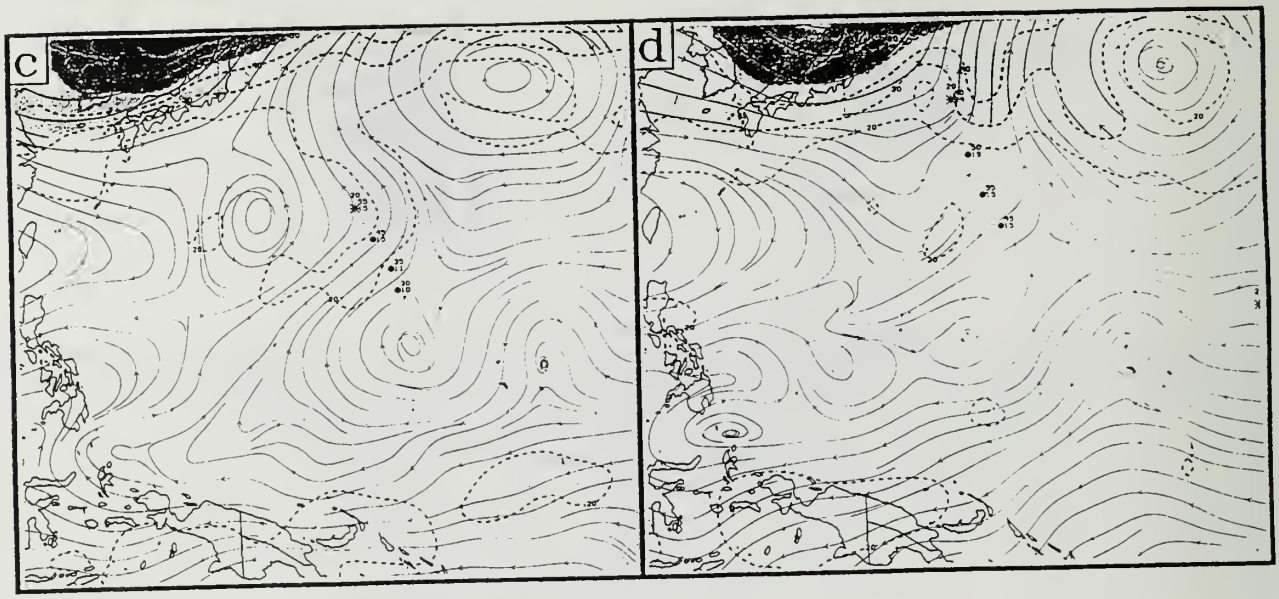

Fig. 4.6 (continued)

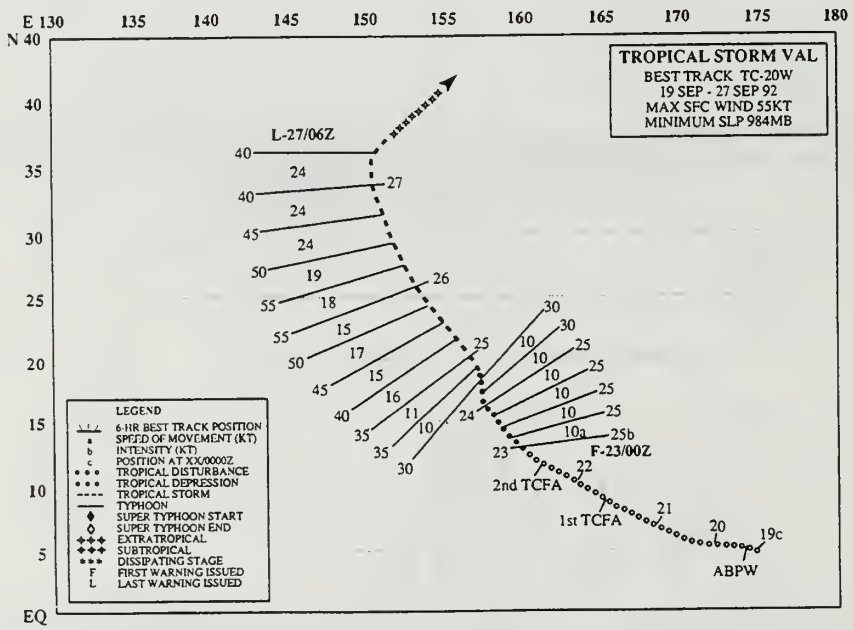

Fig. 4.6(e) Best track of TS Val during 19-27 September 1992.

circulations are often difficult to detect on the basis of NOGAPS 500 mb analyses alone, a refinement to the G Pattern model is discussed here with some examples to improve detection of MGF based on interpretation of satellite imagery. Two distinct ways that cloud patterns manifest the formation and movement of the MGs will be discussed for the cases of TD 15W and Tropical Storm Val in Figs. 4.5a-e and 4.6a-e, respectively.

In the TD 15W case, the initial (Fig. 4.7a) cloud pattern has a more linear appearance characteristic of a reverse-oriented trough to the southeast of the large Typhoon Gladys. During the next three days (Figs. 4.7b-d), cyclonic curvature of the reverse-oriented monsoon cloud band becomes more evident. The circulation of incipient TD 15W (using the best track in Fig. 4.5e to confirm the location) appears in the cumulus cloud lines at the northeast end of the main band of deep convective clouds. One key indicator from the satellite imagery that TD 15W is embedded in a concurrently-developing MG circulation is the development of a relatively cloud-free "moat" between the circulation of TD 15W and the main band of convection to the southeast (Fig. 4.7d). The next four satellite images (Figs. 4.7e-h) are during the same period as the NOGAPS analyses in Figs. 4.5a-d, and confirm the rough correlation between the center of the cloud moat and the MG circulation center in the analyses.

In the Tropical Storm Val case, the MGF takes on a rather different appearance in the satellite visible imagery. Initially, a broad area of loosely-organized convective activity that does not exhibit any reverse-oriented character is present near 8°N, 170°E (Fig. 4.8a). During the next three days (Figs. 4.8b-d), the broad area of cloudiness drifts northwest with some increase in organization evident. Notice the cloud-ringed area of minimum cloudiness near 14°N, 154°E on 23 September (Fig. 4.8d), which is significantly west of the best-track position for Val (Fig. 4.6e). The next four images (Figs. 4.8e-h) are for the same period as the NOGAPS analyses in Figs. 4.6a-d. The key indicator from the imagery that a MG is forming in conjunction with Tropical Storm Val is the semi-circular convective activity (including the convective cloud mass of Val) that defines the eastern periphery of a broad and roughly circular minimum cloud area. This center of the circular cloud minimum area is roughly correlated with the (northward-moving) MG circulation center in the NOGAPS analyses (when present) for the four days. In the last image (Fig. 4.8h), the cyclonic swirl of cumulus clouds near 26°N, 147°E, which manifests the center of the MG circulation, is clearly distinct from the cloud swirl of Val near 33°N, 150°E.

4.6 TCI-related refinements

4.6.1 Relative frequency of TCIs. CE defined six modes of Multiple Tropical Cyclone Interaction (TCI) that were numbered according to the estimated frequency of occurrence. For example, TCI1 (which acts to form a M Pattern) was expected to be the most likely interaction and TCI6 involving a true Fujiwhara interaction to be the least likely. The actual frequencies of occurrence of the various modes of TCIs based on the five-year climatology are listed in Table 4-1. Notice that the numbers of TCI1W and TCI1E case are larger than the number of SF Region and NF Region tracks in Figs. 2.4a and b, which is explained in Note 1 of Table 4-1. The estimated yearly frequencies given in Table 4-1 suggest that TC forecasters should expect multiple cases of TCI1E/W, and TCI3W, and TCI4 during a typical western North Pacific season. The other TCI modes occur less often than once a season, and thus are rare.

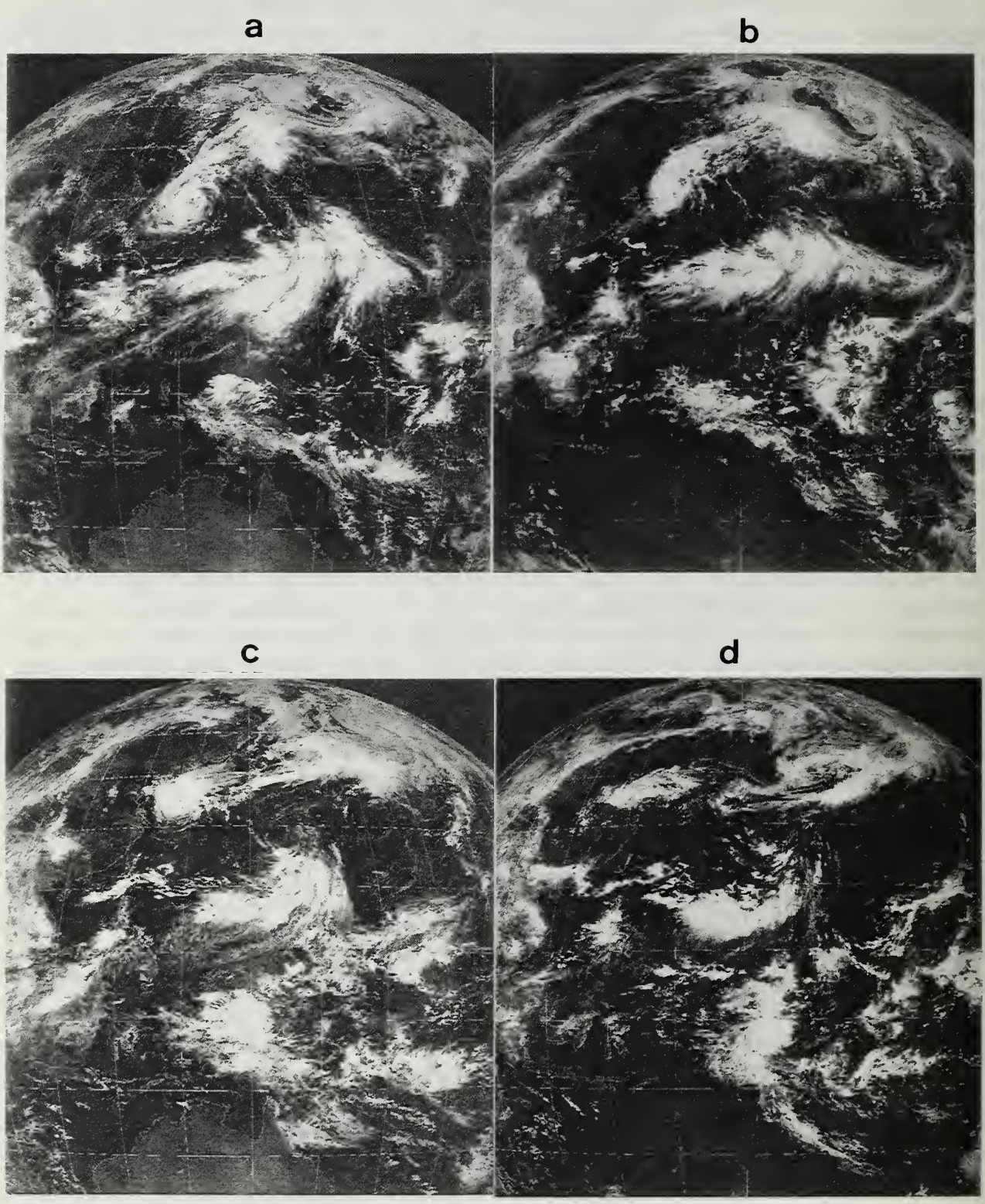

Fig. 4.7 Satellite visible imagery at 03 UTC on (a) 21, (b) 22, (c) 23, and (d) 24 August 1991 of the evolution of a cloud pattern southeast of Typhoon Gladys.

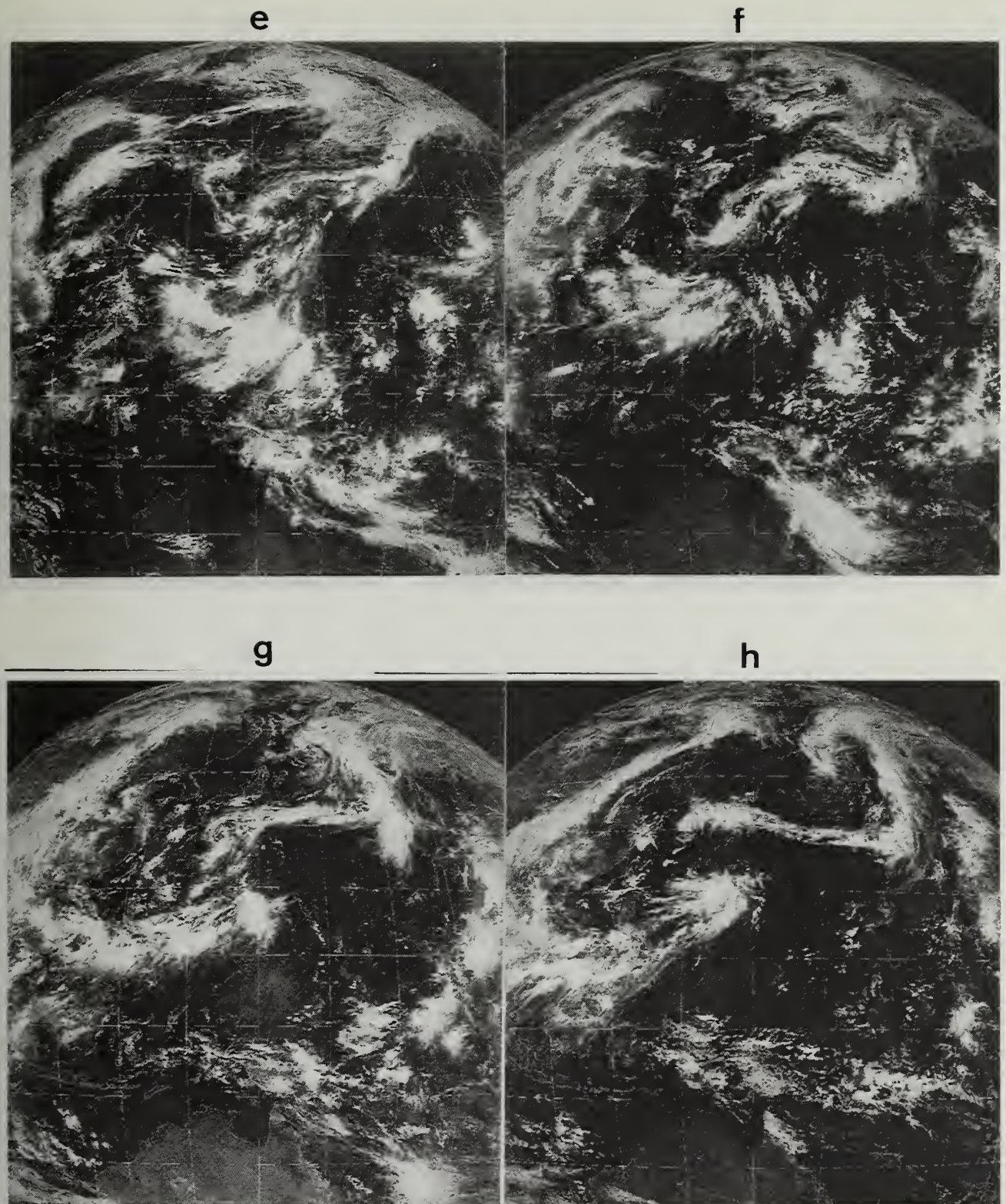

Fig. 4.7 (continued) Satellite visible imagery at 03 UTC on (e) 25, (f) 26, (g) 27, and (h) 28 August 1991 illustrating the formation of a monsoon gyre coincident with formation of TD 15W.

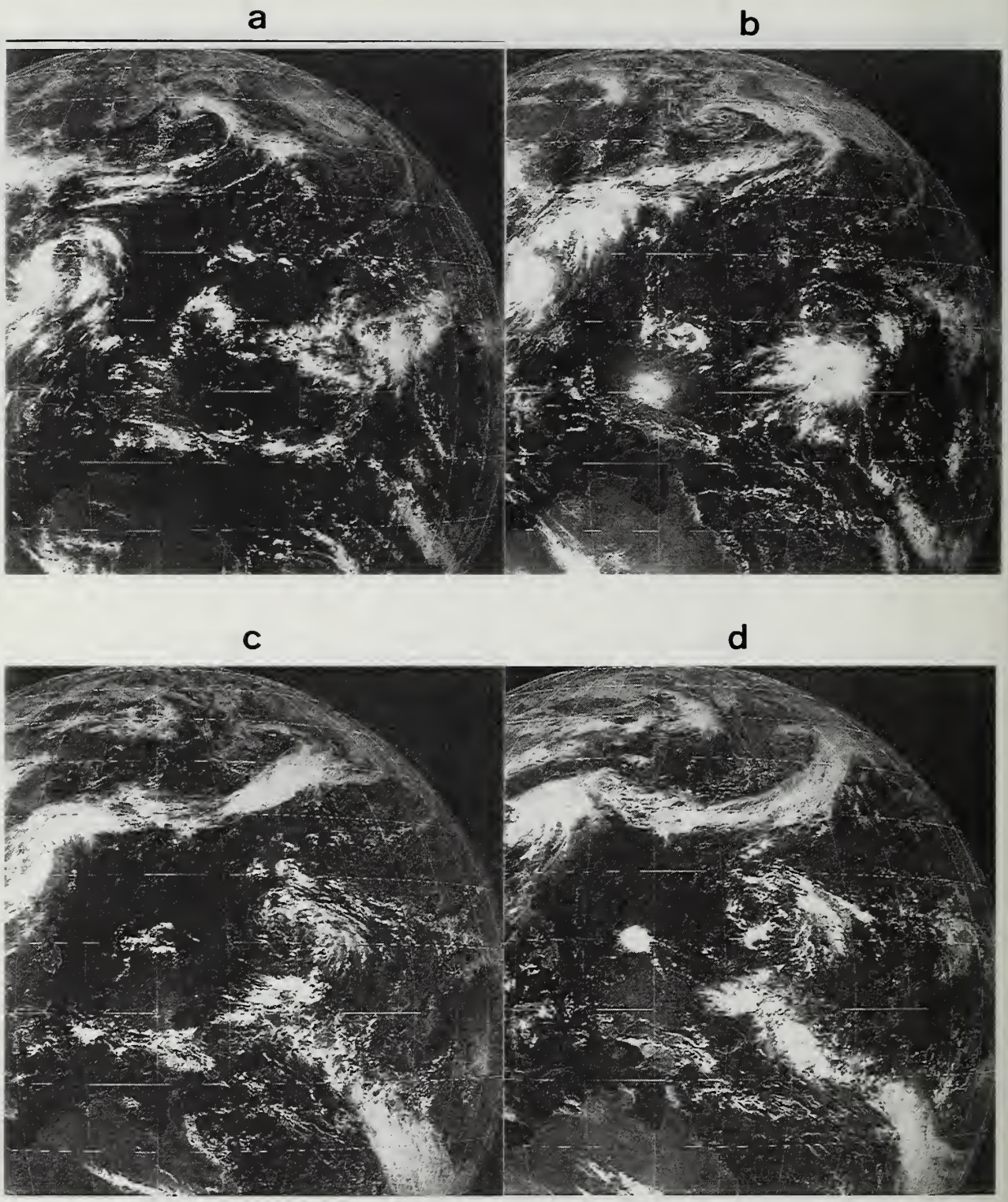

Fig. 4.8 Satellite visible imagery at 03 UTC on (a) 20, (b) 21, (c) 22, and (d) 23 September 1992 illustrating the formation near 8°N, 170°E and subsequent evolution of monsoon gyre cloud pattern.

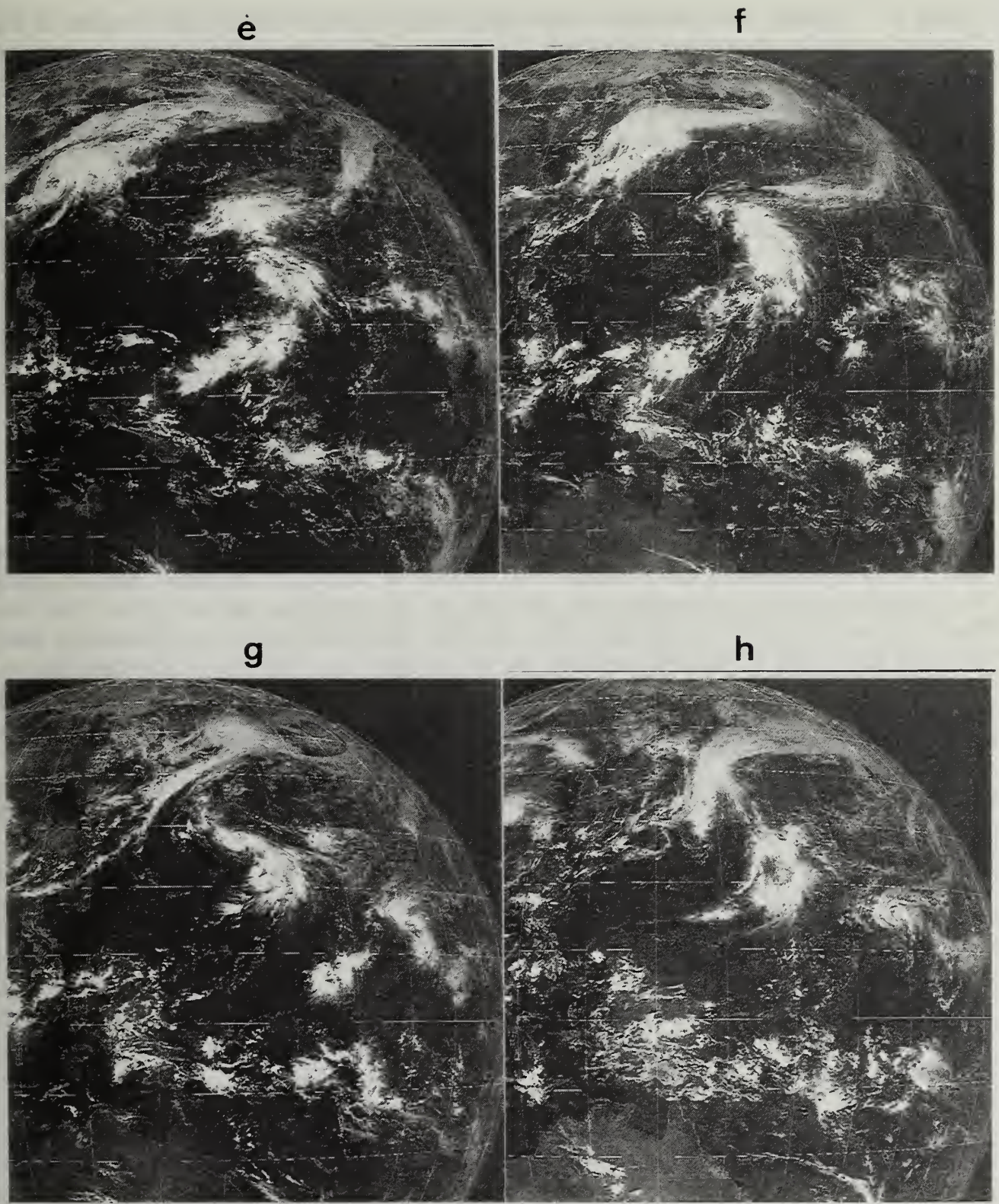

Fig. 4.8 (continued) Satellite visible imagery at 03 UTC on (e) 24, (f) 25, (g) 26, and (h) 27 September 1992 illustrating the coincidence of the monsoon gyre cloud pattern and TS Val.

Table 4-1 Number of occurrences and yearly frequencies for the various modes of TC Interaction during the period 1989-1993. See Carr and Elsberry (1994) for the description of the TCI modes.

Mode of TC Interaction	Total Number of Cases (TCs)	Yearly frequency
TCI4	25	5
TCI1W	16[1]	3
TCI1E	11[1]	2
TCI1W and/or TCI1E	19[2]	4
TCI3[3]	14	4
TCI2	4	1
TCI6	2	<1
TCI5	3	<<1[4]

Notes: [1] Notice that these numbers exceed the number of corresponding tracks in Fig. 2.4a and b. These differences arise because the number of TCI's here includes cases in which the transformational mechanism was deemed to be operative to the extent that the Environment Structure surrounding the TC was transformed into a transitional state between the S and M Patterns for some period of time (e.g., Pattern = S/M and Region = DR/SF or DR/NF). However, a complete transition to the SF or NF Region of the M Pattern was not observed. By contrast, the track segments in Fig. 2.4 represents only periods when the TC Region was given a definite assignment of SF or NF.

[2] This number represents the sum of the TCI1W and TCI1E cases minus the number of times (8) when TCI1W and TCI1E occurred concomitantly. Alternately, there were 11 (19-8) cases when either TCI1W or TCI1E occurred, but not both.

[3] Recall in CE reference was made to TCI3W and TCI3E. It has been determined that TCI3E (i.e., the influence on the peripheral ridge of a western TC from a TC to the east) is essentially just an element of the Reverse-oriented Trough Formation (RTF) model that will be discussed in Chapter 4.7.2 below. Thus, the term TCI3E will be dropped and the designator TCI3 will henceforth represent the phenomenon that CE termed TCI3W, in which a TC track is influenced by the peripheral ridge of the TC to the west. This requires modifications of CE Table 3.9. Replace S/AW by N/AW from 12 UTC 17 September to 00 UTC 21 September and replace S/DR by N/NO from 00 UTC 26 September to 00 UTC 27 September, and replace TCI3E by RTF in the Transformation column.

[4] All three of the TCs experiencing TCI5 were associated with the same MG, which is the Nancy-Owen-Peggy case of 1989 (see CE p. 147-161). Thus, only one unique period of TCI5 occurred in the five-year period. The only other apparent cases of TCI5 are the Odessa-Ruby-Pat case of 1985 (see CE Fig. 3.98) and the recent case of Pat-Ruth in 1994, which also involved a full TCI6 merger. Thus, a frequency on the order of once per five years is suggested.

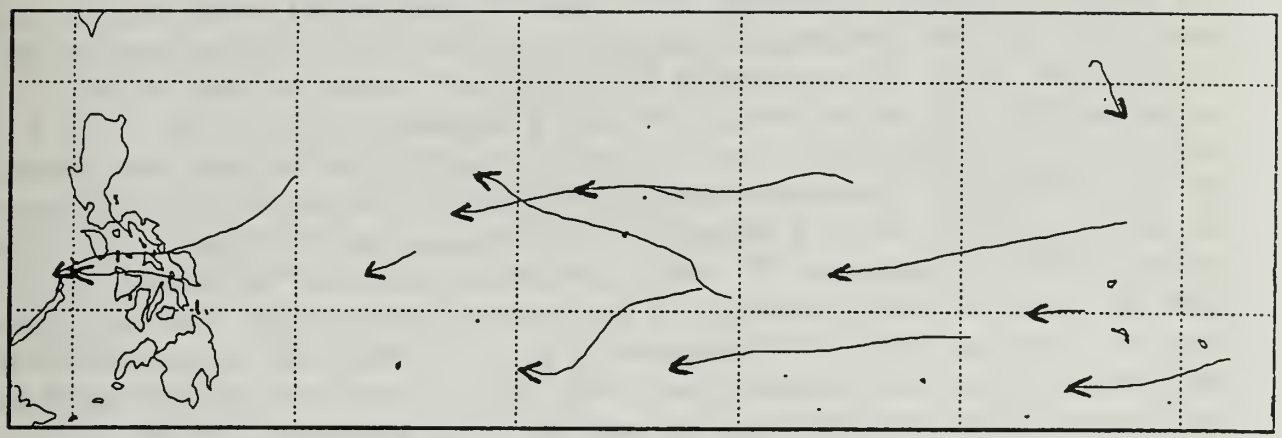

Fig. 4.9 Track segments of storms during 1989-1993 that were in a S/DR combination and were experiencing a TCI3 influence.

4.6.2 TCI3 track characteristics. Track segments corresponding to the 14 cases of TCI3 from a TC to the west (CE's TCI3W) listed in Table 4-1 are shown in Fig. 4.9. Notice that all but one of the track segments are south of west, or are primarily westward. The only significant exception is the sustained west-northwestward track segment of Typhoon Omar (1992) that subsequently passed over Guam. In this case, the impact of the TCI3 from Tropical Storm Polly to the west (CE Fig. E.7b) was to slow the translation speed of Omar (see CE Fig. E.7a) compared to the translation speed before and after the period when TCI3 was occurring. Given that the Typhoon Omar case appears to be an anomaly, the remaining tracks in Fig. 4.9 suggest that the forecaster may anticipate a rather predictable TC track direction once TCI3 commences. As a case study in the next subsection will demonstrate, TCI3 and TCI4 tend to occur concomitantly, which results in feedback that may make the anticipation of the onset and cessation of TCI3 (and hence TCI4 also) rather unpredictable.

4.6.3 TCI4-induced transitions. CE only briefly mentioned TCI4, and then only in the context of precluding a S/DR to N/NO transition by preventing the development of significant -induced ridging to the southeast of the TC undergoing TCI4 (i.e., from a TC to the east). Based on the five-year climatology, about two times per year a TCI4 seemed to precipitate, or at least contribute to, a N/NO to S/DR transition (recall Fig. 2.8) via erosion of the north-oriented ridge. Thus, the subtropical ridge on the poleward side becomes the Dominant Ridge in a S Pattern.

Two examples of TC track changes associated with the TCI4-induced N/NO to S/DR transition are shown in Figs. 4.10a-b. In the case of TY Brian (Fig. 4.10a), the N/NO to S/DR transition occurred immediately following a S/DR to N/NO transition, which resulted in a very sharp track kink from 0000 UTC 30 September to 0000 UTC 1 October 1989. In the case of TY Ryan (Fig. 4.10b), TCI4 from TY Sybil (18 W) to the east resulted in a major turn from a northeastward to a west-northwestward track beginning around 1200 UTC 7 September 1992. The transition in Environment Structure from N/NO to S/DR associated with a major left turn of TY Ryan is illustrated with analyses in Fig. 4.11. At 0000 UTC 6 September (Fig. 4.11a), a peripheral ridge and an associated isotach maximum are clearly evident to the southeast of Ryan, and Ryan is to the east of the circulation center for the TC. All of these are indicators that Ryan is in the NO Region of a N Pattern. Notice that the circulation of TY Sybil to the east separates the peripheral ridge of Ryan from the subtropical ridge circulation to the north-northeast of Sybil. Essentially the same situation prevails at 0000 UTC 7 September (Fig. 4.11b), except that the previous northward motion of Sybil has been arrested, presumably due to a cancellation between BEP and the northwesterly flow over Sybil from the peripheral ridge generated by Ryan.

By 0000 UTC 8 September (Fig. 4.11c), Sybil is actually moving to the south in response to the peripheral ridging from Ryan. As the position of Sybil shifts to the southeast of Ryan, the circulation of Sybil continues to separate Ryan's peripheral ridge from linking with the subtropical ridge to the north. An increasingly deleterious effect on the strength of the peripheral ridge is suggested by the indentations in the 20- and 30 kt isotachs and associated diffluent region to the southeast of Ryan near 23°N, 158°E. Notice also the appearance of a 30-kt isotach maximum to the northwest of Ryan, which in combination with the isotach maximum to the southeast indicates weakening in the environmental steering flow. In the previous 24-h period, the translation of Ryan began to decrease and then turned toward the west-northwest (Fig. 4.10b), which is an indication that a Environment Structure transition from N/NO to S/DR is in progress.

By 0000 UTC 9 September (Fig. 4.11d), as in the intervention of Sybil to the east continues and Ryan approaches the subtropical ridge axis, the Environmental Structure in the vicinity of Ryan has fully transitioned to S/DR. Completion of the transition is indicated by the weakening of the isotach maximum to the southeast of Ryan, the shift of the highest wind speeds to the north-northeast, and an increase in Ryan's translation speed from 6 to 9 kt over the previous 24 h (Fig. 4.10b). Although the impact of Sybil's circulation on the peripheral ridging of Ryan evidently plays a key role in the Pattern/Region transition, strengthening of the subtropical ridge to the northeast of Ryan also seems to have occurred between Fig. 4.11c and 4.11d. Thus, subtropical ridge modulation (SRM) by midlatitude waves (to be described in Chapter 4.8) seems to have contributed to the transition.

The equatorward displacement of TY Sybil between 0000 UTC 7 September is attributed to TCI3 from the peripheral ridge of TY Ryan to the west. This case

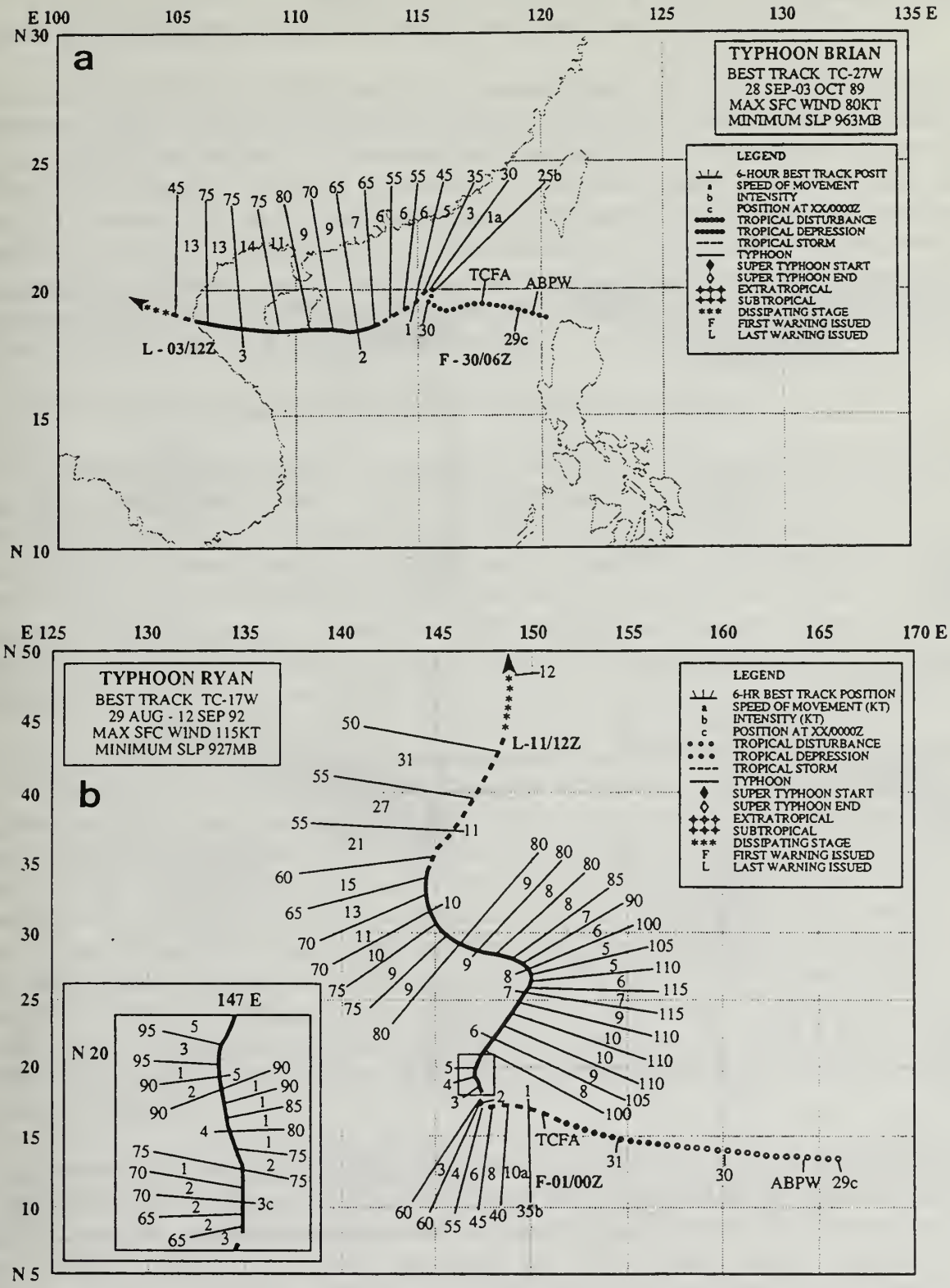

Fig. 4.10 Best tracks of (a) TY Brian from 28 September to 3 October 1989 and (b) TY Ryan from 29 August to 12 September 1992.

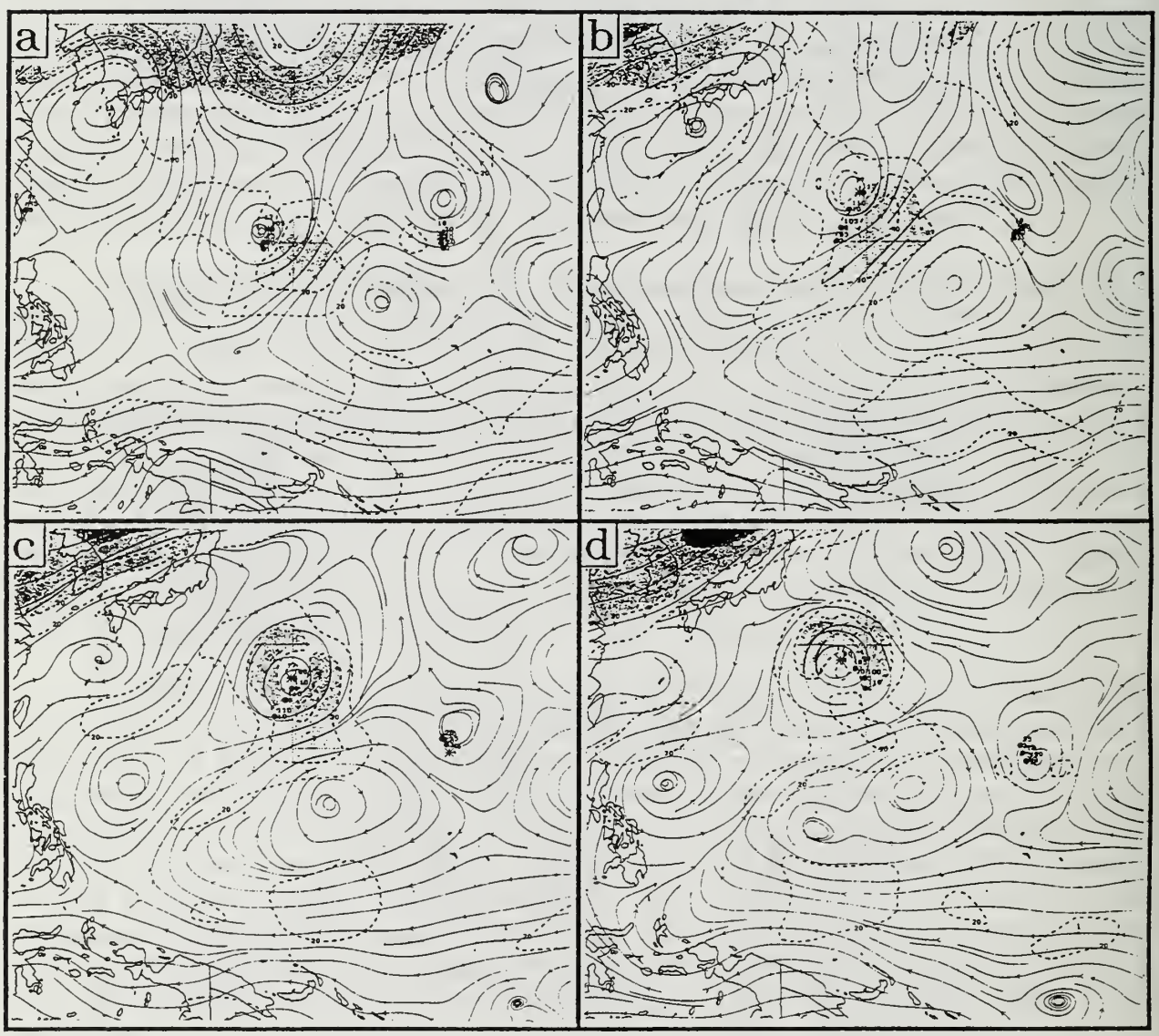

Fig. 4.11 Analyses as in Fig. 4.1, except for (a) 6, (b) 7, (c) 8, and (d) 9 September 1992. TY Ryan is the western storm and TY Sybil is the quasi-stationary storm to the east.

Fig. 4.11 Analyses as in Fig. 4.1, except for (a) 6, (b) 7, (c) 8, and (d) 9 September 1992. TY Ryan is the western storm and TY Sybil is the quasi-stationary storm to the east.

study illustrates how TCI4 and TCI3 may occur concomitantly, and then a "tug of war" may be established. That is, the circulation of a western TC induces a peripheral ridge that is tending to displace the western TC poleward and the eastern TC equatorward, while the circulation of the eastern TC tends to erode the peripheral ridge, which mitigates the tendency of the eastern TC to be displaced equatorward and also diminishes the tendency for poleward movement of the western TC. Such an interaction depends sensitively on the sizes, separation distance, and directional orientation of the two TC circulations. Consequently, it is anticipated that the onset, duration, and cessation of TCI3- and TCI4-related track changes will have a low predictability.

4.7 Reverse-oriented Trough Formation (RTF) transformation model

4.7.1 RTF Model description. According to CE, the key dynamical processes in the subtropical Ridge Modification by a "Large" TC (RMT) transformation and the associated S/DR to N/NO transition are the negative vorticity advection (NVA) tending to build a peripheral ridge to the south and east of the TC and the positive vorticity advection (PVA) tending to erode the subtropical ridge to the north and west of the TC. These nonlinear NVA and PVA contributions arise from the -induced distortion of the TC circulation away from axisymmetry, and the magnitude of the advections is proportional to the horizontal scale of the TC.

This RMT transformation conceptual model is extended here to consider the case of two TCs that are oriented roughly east-west and are sufficiently close (less than about 20° lat.) so that no significant ridge exists between them. If the combination of these TCs is sufficiently large, and particularly if the eastern TC is at a higher latitude than the western TC, then the RMT process associated with each TC may constructively superpose. Such a superposition may lead to an extensive peripheral ridge extending south and east of the two TCs, and to an extended PVA area that may erode the subtropical ridge poleward of the TC pair. As a result, a reverse-oriented trough consisting of the two TCs may be formed that results in the establishment of a N Pattern in which the TCs tend to move northeastward in conjunction with the steering from the large peripheral ridge to the southeast. This scenario is the essence of the Reverse-oriented Trough Formation (RTF) transformation model.

In the five-year sample, the RTF transformation model was assigned to both S-to-N and M-to-N Pattern transitions. The key difference was whether the two TCs were close enough and properly oriented to satisfy the M Pattern criteria before the transition to N occurred. The following case study illustrates the RTF transformation inducing the Environment Structure transition M/NF to N/NO and M/SF to N/NO, which were not anticipated by CE, but were found to recur in the five-year sample (see Figs. 2.8 and 2.9).

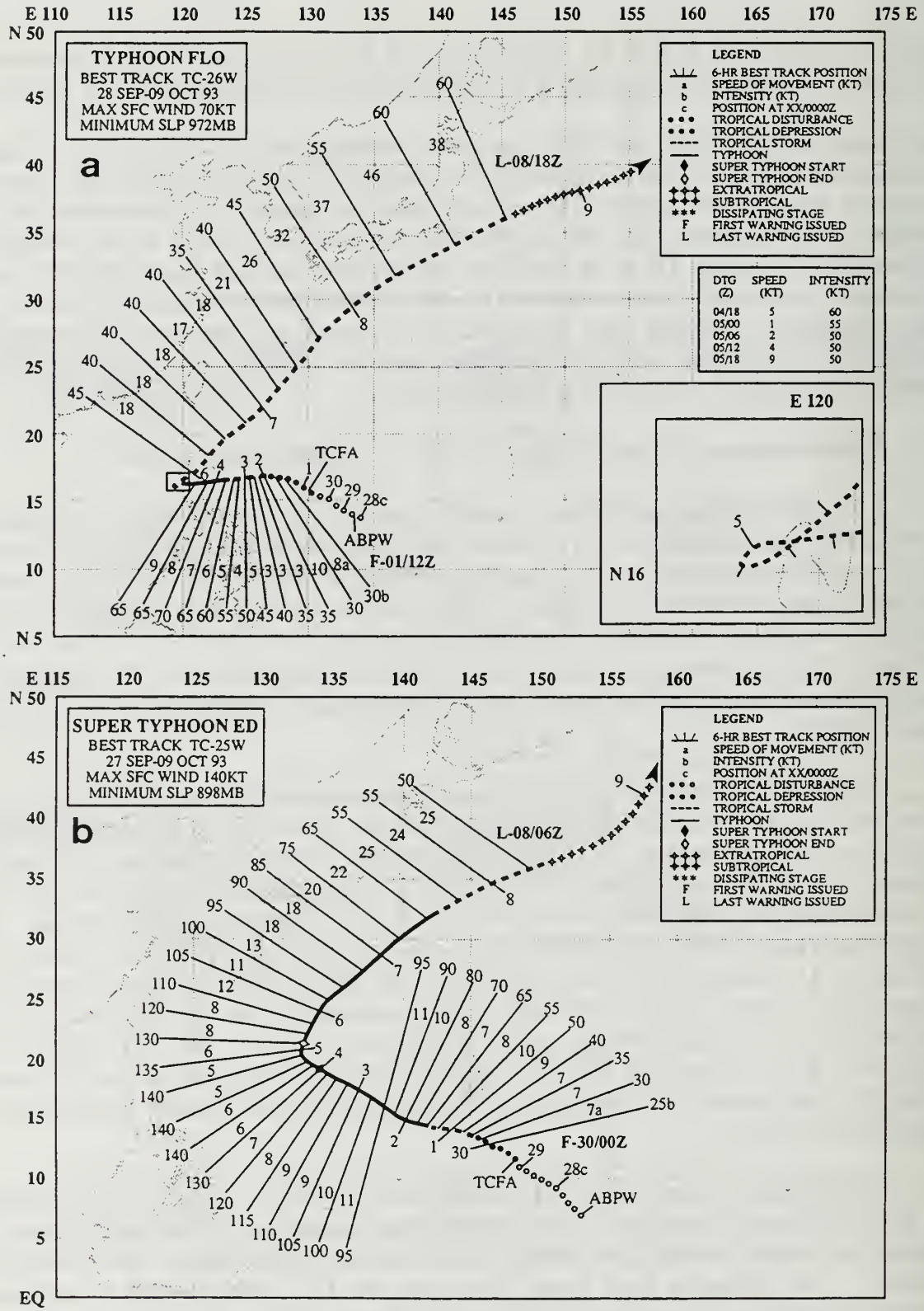

Fig. 4.12 Best tracks for (a) TY Flo from 28 September to 9 October 1993 and (b) ST Ed from 27 September to 9 October 1993.

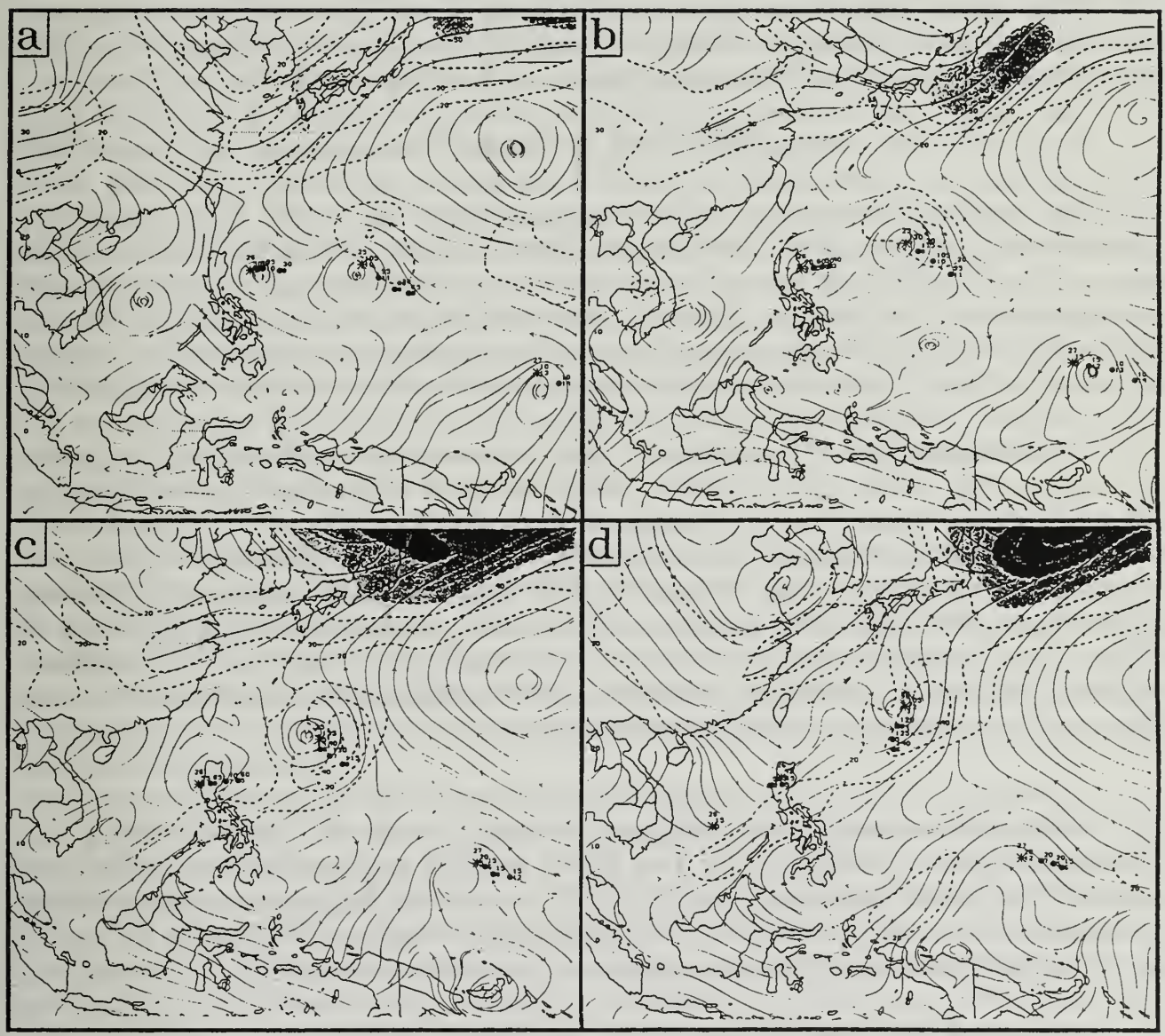

Fig. 4.13 Analyses as in Fig. 4.1, except for (a) 3, (b) 4, (c) 5, and (d) 6 October 1993. TY Flo is the western TC and ST Ed is the eastern TC in the central portion of the domain, TS Gene is in the lower-right corner, and TD 28W is forming in the South China Sea in panel (d).

(i) a disturbance, which will become TD 28W, located in the South China Sea just off the coast of Vietnam; (ii) Typhoon Flo just east of Luzon, RP; (iii) Typhoon Ed near 18°N, 137°E; and (vi) Tropical Storm Gene near 6°N, 155°E. Notice that the axis of the monsoon trough has a slight reverse orientation from TD 28W in the South China to Flo, an essentially zonal orientation from Flo to Ed, and a climatologically normal orientation from Ed to Gene. A prominent ridge is to the southeast of TD 28 W and Flo, but not to the southeast of Ed. The orientation of Ed and Flo to the subtropical ridge suggests that Flo is the western TC in a M/NF Pattern, and that Ed is beginning a transition from S/DR to M/SF. The slightly south of west motion of Flo at this time (Fig. 4.12b) is consistent with the assignment of the NF Region, although the west-southwest to east-northeast slope of the subtropical ridge axis may also be contributing to the south of west motion of Flo.

In the 4 October analysis (Fig. 4.13b), the South China Sea disturbance has drifted southward, Flo has moved westward, and Ed has moved northward. Thus, the three circulations produce a reverse tilt to the monsoon trough axis. Notice that a prominent ridge has developed (near 9°N, 137°E) to the south-southeast of Ed. A combination of the reverse-oriented trough and the peripheral ridge to the southeast would be consistent with an assignment of a N Pattern. However, a continued assignment as a M Pattern is supported by the isotach maximum positions to the northwest and northeast of Flo and Ed, respectively, and by a continued westward component of motion for both Ed and Flo.

On 5 October, both TCs undergo a major turn toward the northeast (Figs. 4.12a-b). The analysis (Fig. 4.13c) has an isotach maximum to the southeast of each TC, and a continuous band of greater than 20 kt winds along the southeast sides of the TCs and to the northwest of the well-established peripheral ridge. All of these factors are indicative of a transition to a N Pattern for Ed, Flo, and TD 28W (with the South China Sea disturbance having become TD 28W). By 6 October (Fig. 4.13d), the transition to a N Pattern is confirmed by the northeastward movement of all three cyclones in response to the extensive peripheral ridge to the southeast. Meanwhile, the subtropical ridge to the northwest has been completely eroded, and replaced with a trough.

In summary, the new RTF transformation conceptual model is an adaptation of the RMT transformation model, and addresses transitions to the N Pattern involving the combined influence of multiple TCs. The RTF is involved in three M/NF to N/NO and three M/SF to N/NO transitions (Fig. 2.8). RTF may be contributing to a small (probably less than 10) number of the S/DR to N/NO transitions, in which two TCs that do not satisfy the M Pattern criteria nevertheless are sufficiently close to trigger a RTF.

4.8 Subtropical Ridge Modulation (SRM) conceptual model

4.8.1 SRM model description. In CE, a midlatitude trough was included in the S Pattern schematic (CE Fig. 3.5). The presence of this trough (and by implication, the accompanying upstream and downstream midlatitude ridges) was said to "modulate" the structure of the mid-tropospheric subtropical ridge. That is, the north-south extent of the

subtropical ridge is reduced equatorward of the midlatitude trough, which results in a "weakness" through which a TC may pass, especially for larger TCs for which Beta Effect Propagation (BEP) is a significant factor. Superposition of a midlatitude ridge and the subtropical ridge tends to inhibit recurvature, or at least defer recurvature until the TC approaches a midlatitude trough-induced weakness in the subtropical ridge.

The SRM transitional mechanism may account for a transition in the Environment Structure of the TC by either weakening or strengthening the subtropical ridge. For example, the SRM model appears in Fig. 2.8 as a contributor to some of the DR to WR and WR to AW Region transitions in the S Pattern via a weakening of the subtropical ridge by a midlatitude trough. Conversely, a ridge-strengthening modulation is implied by the WR to DR transition. A strengthening of the subtropical ridge via SRM also contributes to the Environment Structure transition from N/NO to S/DR in Fig. 2.8.

Since either the trough or the ridge portion of a midlatitude wave may affect the structure of the subtropical ridge, accurate prediction of an associated Environment Structure transition is complicated by several factors. Because the TC is typically moving west-northwestward and the midlatitude wave is moving eastward, this relative motion creates a delicate timing problem. Interaction between the TC circulation and the midlatitude wave may cause TC structure changes. For example, the TC may be weakened as it approaches the mid-latitude trough owing to large vertical wind shear, and thus may undergo a significant reduction in steering level. In addition, the midlatitude wave may be undergoing either amplification or weakening.

4.8.2 SRM model illustration. The SRM entries in Fig. 2.8 are related to three potential scenarios: (i) aiding TC recurvature in the S Pattern; (ii) precluding or delaying TC recurvature in the S Pattern; and (iii) contributing to an Environment Structure transition from N/NO to S/DR. Because the scenario of a midlatitude trough aiding TC recurvature is very familiar to TC forecasters, a separate case study is not included. Rather, the first case study will illustrate both scenarios (i) and (ii) above, and the second case study will illustrate scenario (iii).

Case Study #1: The case of Typhoon Dan (27W) during October 1992 is illustrated with 12-hourly analyses (Fig. 4.14), the JTWC best track (Fig. 4.15), and geostationary satellite infrared imagery (Fig. 4.16). At 0000 UTC 28 October (Fig. 4.14a), Dan is in the DR region of a S Pattern (note isotach maximum to the northeast), and is propagating significantly (note peripheral ridging to the southeast is an indication of BEP). These assessments are consistent with the steady northwestward track of Dan at this time (Fig. 4.15). However, a midlatitude trough that is approaching Dan from the northwest is producing a weakness in the subtropical ridge. By 1200 UTC 28 October (Fig.4.14b), the ridge to the northwest of Dan has weakened further as the trough approaches, and the translation speed of Dan has begun to decrease (Fig. 4.15), which suggests that Dan is in the DR/WR transition zone of the S Pattern. By 0000 UTC 29 October (Fig. 4.14c), the proximity of Dan to the ridge axis and the shift of the isotach maximum to the east suggests

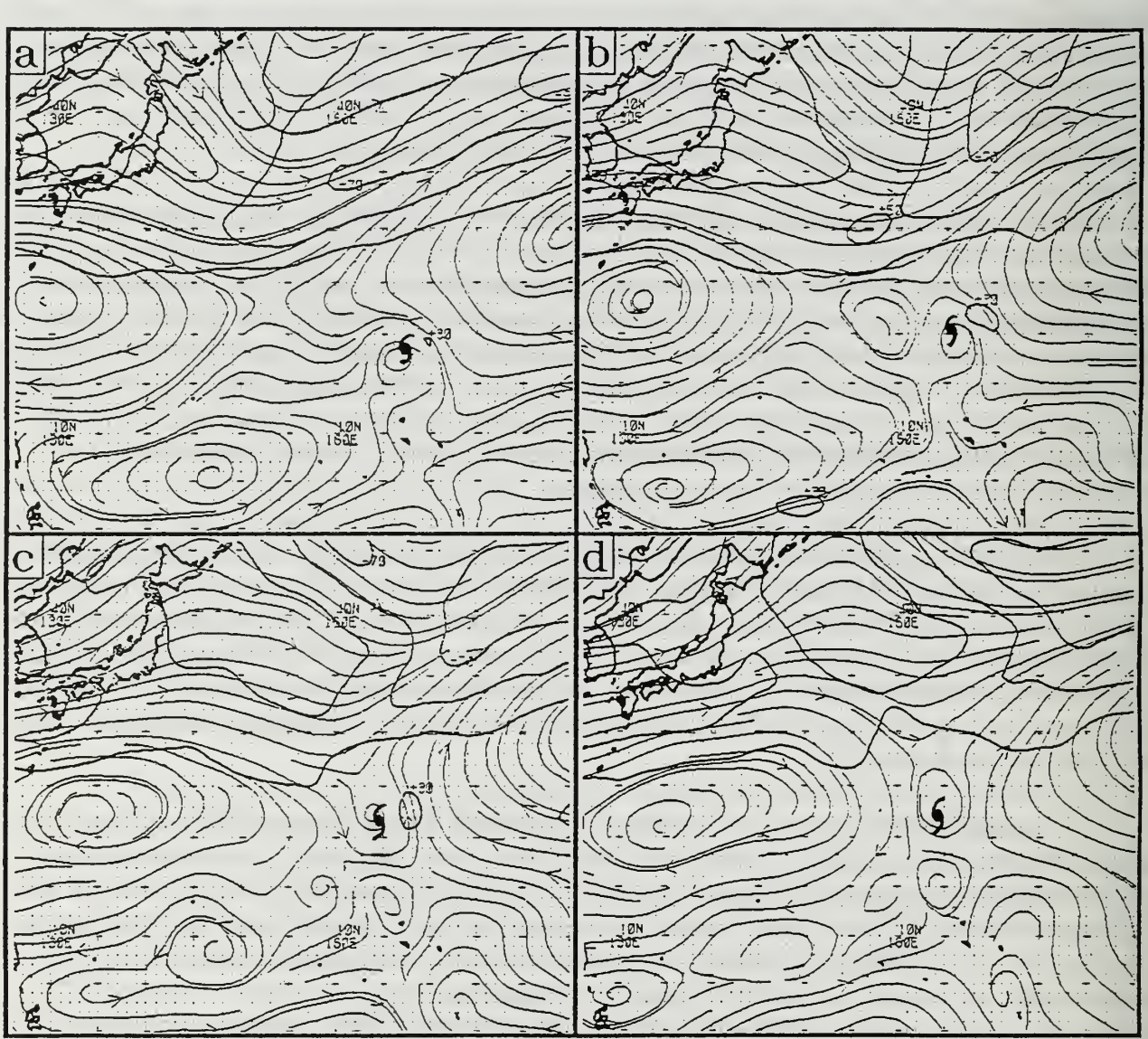

Fig. 4.14 Analyses as in Fig. 4.1, except for (a) 0000 UTC and (b) 1200 UTC 28 October 1992 and (c) 0000 UTC and (d) 1200 UTC 29 October. TY Dan is indicated by the TC symbol.

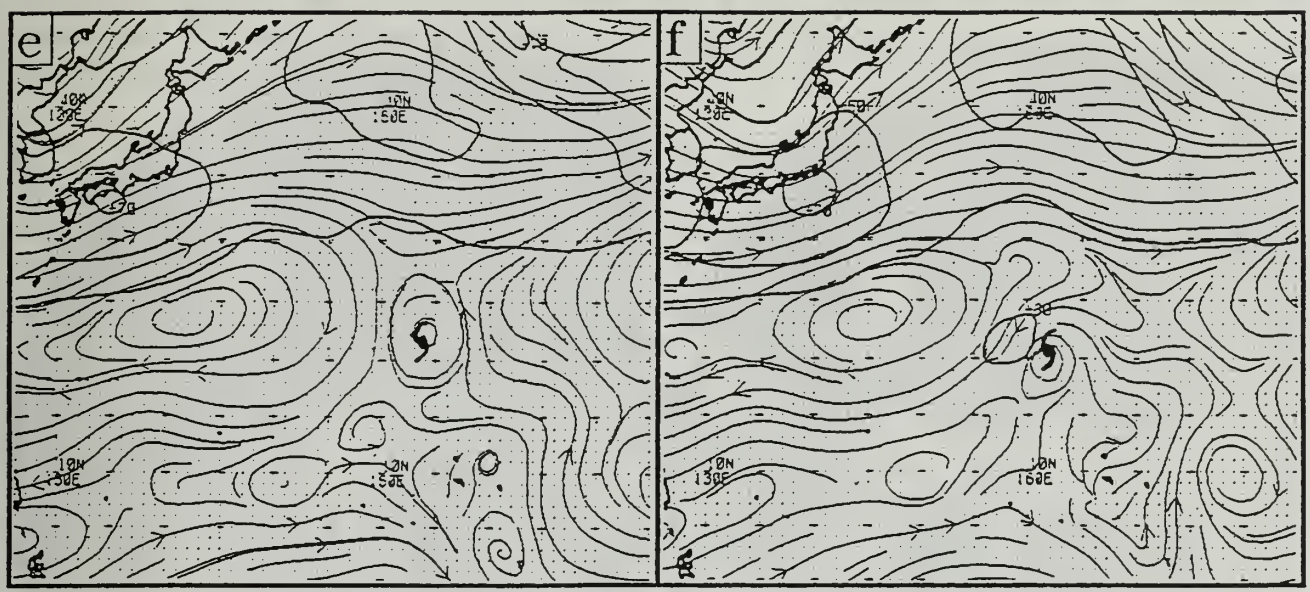

Fig. 4.14 Analyses for (e) 0000 UTC and (f) 1200 UTC 30 October 1992.

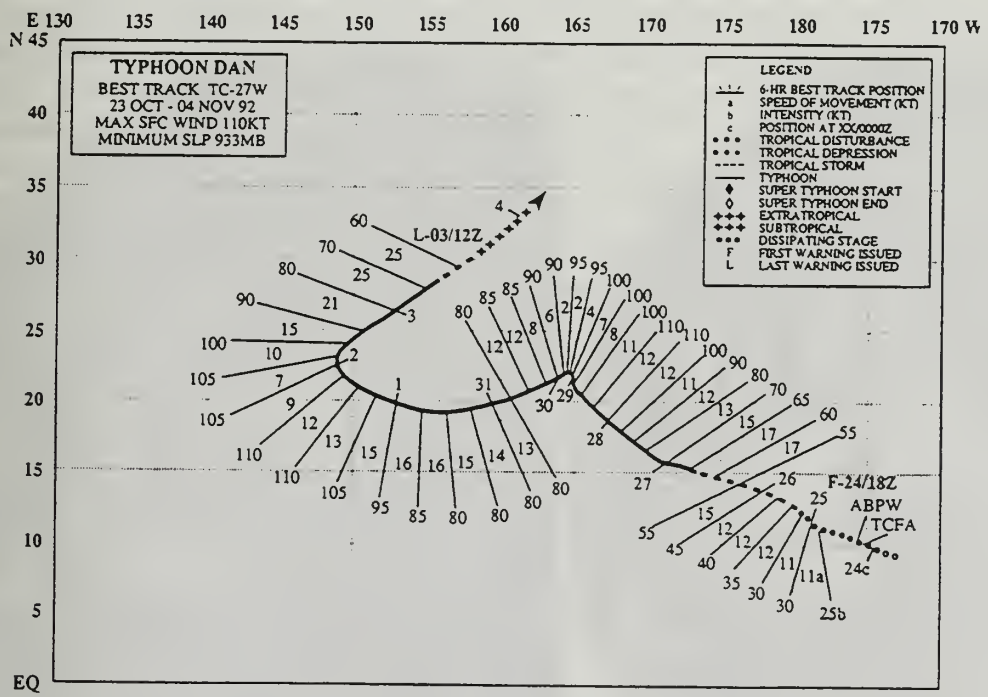

Fig. 4.15 Best track for TY Dan from 23 October to 4 November 1992.

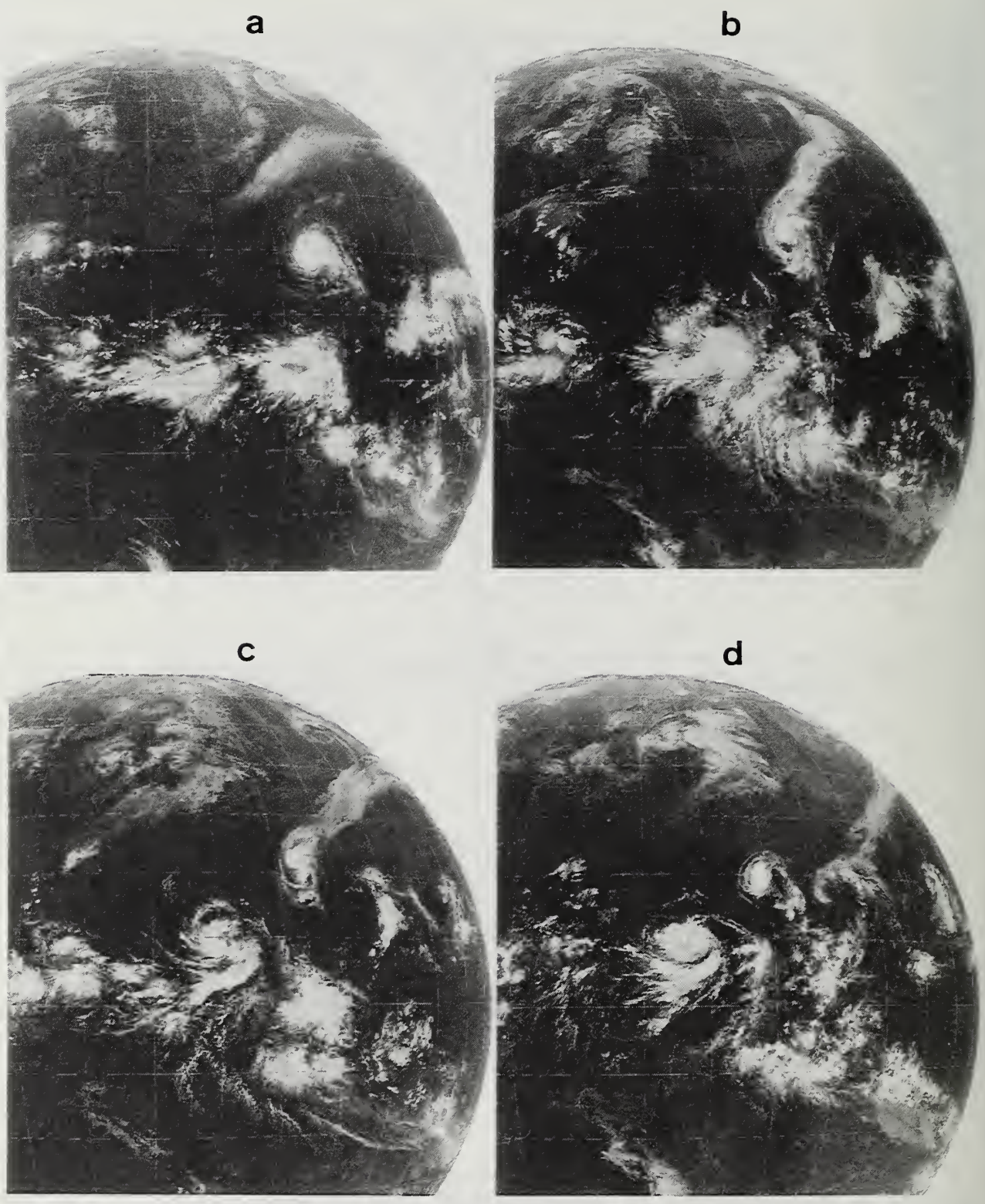

Fig. 4.16 Geostationary satellite infrared imagery at 0300 UTC for (a) 28, (b) 29, (c) 30, and (d) 31 October 1992 including TY Dan.

that Dan has transitioned to the WR Region. This assessment is consistent with the slowly, poleward-turning track of Dan at this time (Fig. 4.15). The scenario thus far illustrates the combined effects of BEP and SRM (i.e., the ridge-weakening mode) leading to a S/DR to S/WR transition as depicted in Fig. 2.8.

By 1200 UTC 29 October (Fig. 4.14d), the midlatitude trough is well east of Dan, and a midlatitude ridge is approaching from the northwest. Notice also the increased north-south extent of the subtropical ridge on the western periphery of Dan compared to 24 h previously (Fig. 4.14b). This increase reflects the ridge-strengthening mode of the SRM conceptual model. A steering component tends to offset the normal northwestward BEP of Dan, which is reflected in the rapid decrease in translation speed and a left turn (Fig. 4.15). Such a track change suggests that Dan is in transition from S/WR to S/DR.

As a midlatitude ridge approaches to the north of Dan over the next 12 h, the analyses (Figs. 4.14e-f) indicate building of the subtropical ridge. By 1200 UTC 30 October (Fig. 4.14f), a prominent subtropical ridge is present poleward of Dan and the 30-kt isotach maximum is now to the northwest of Dan. In conjunction with the translation speed increase to 12 kt, Dan is assigned in the DR Region of a S Pattern. Thus, transition from S/WR to S/DR has been accomplished via the SRM transformation.

Geostationary satellite infrared imagery during the period (Fig. 4.16) illustrates the significant changes in upper-level cloud patterns that accompany the DR-to-WR-to-DR transition sequence. Whereas little TC cirrus outflow to the northeast is evident on 28 October (Fig. 4.16a) when the midlatitude trough is approaching from the northwest, northeastward outflow is enhanced as Dan enters the WR Region on 29 October (Fig. 4.16b). The appearance, and increase with time, of such a bright, unbroken cirrus plume streaming to the northeast is generally considered to be a good indicator that recurvature is imminent. However, a distinct thinning or break has appeared in the cirrus outflow plume to the northeast of Dan on 30 October (Fig. 4.16c), and the degree of this break increases with time (Fig. 4.16d). Such a change in the cirrus plume, combined with the translation speed decrease to an unusually slow 2-4 kt near the ridge axis, provide important indicators that a delayed recurvature or stair-step track is likely to occur.[2]

Case Study #2. The TS Jack (05W) case during May 1993 is illustrated by analyses (Fig. 4.17) and the JTWC best track (Fig. 4.18). On 16 May (Fig. 4.17a), Jack is in a N

---

[2] Admittedly, severe track changes such as in this case are expected to have low predictability. By closely following the track, analyses, and satellite imagery clues summarized above, the forecaster may reduce the delay in modifying the official forecast to reflect such sudden track changes. In addition, such key indicators can alert the forecaster that a low predictability scenario is possible, and thus insert alternate scenarios in the Prognostic Reasoning Message. This concept will be addressed in some detail in a subsequent report that demonstrates the application of the Systematic Approach.

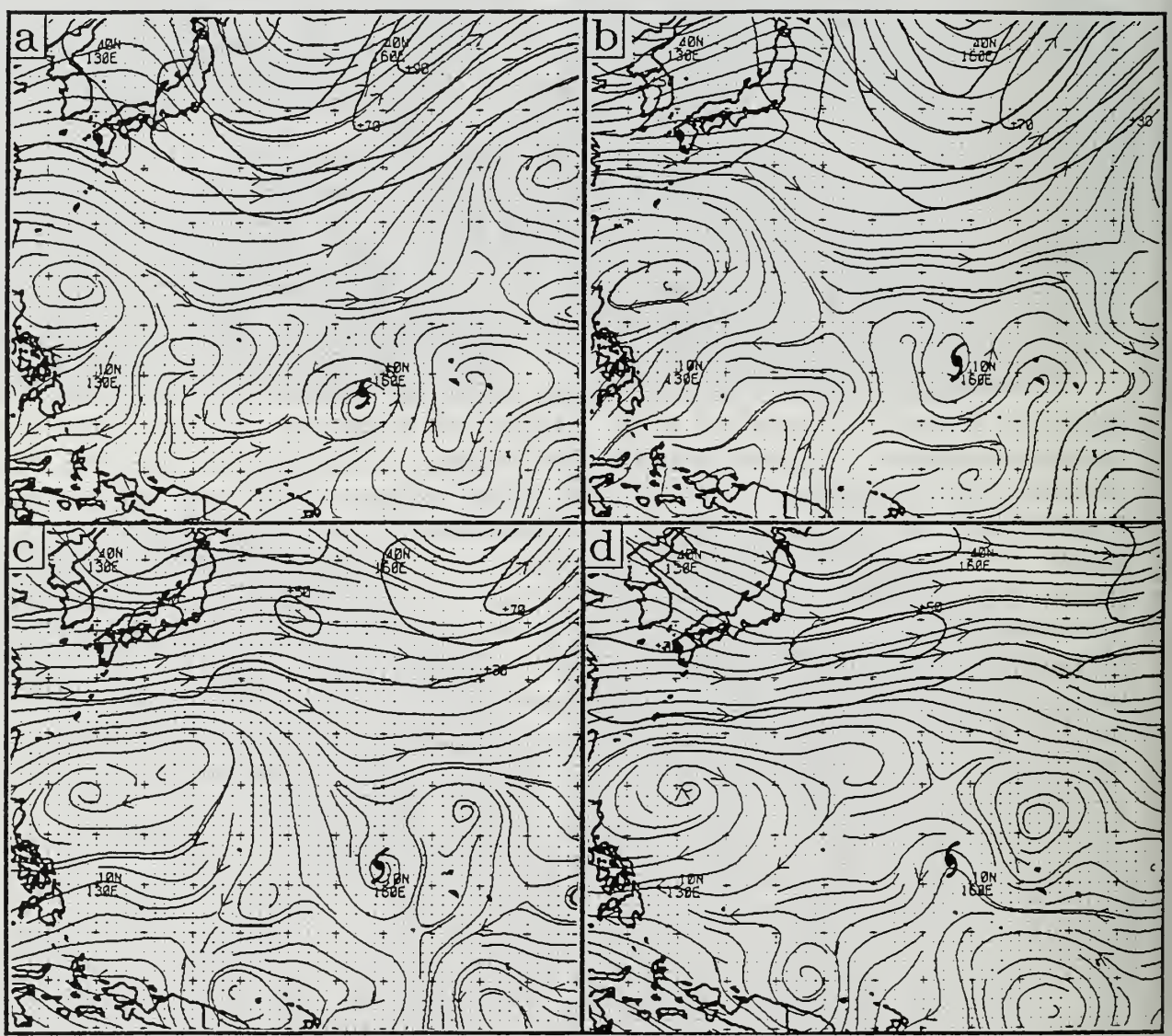

Fig. 4.17 Analyses as in Fig. 4.1, except for (a) 16, (b) 17, (c) 18, and (d) 19 May 1993 during TS Jack.

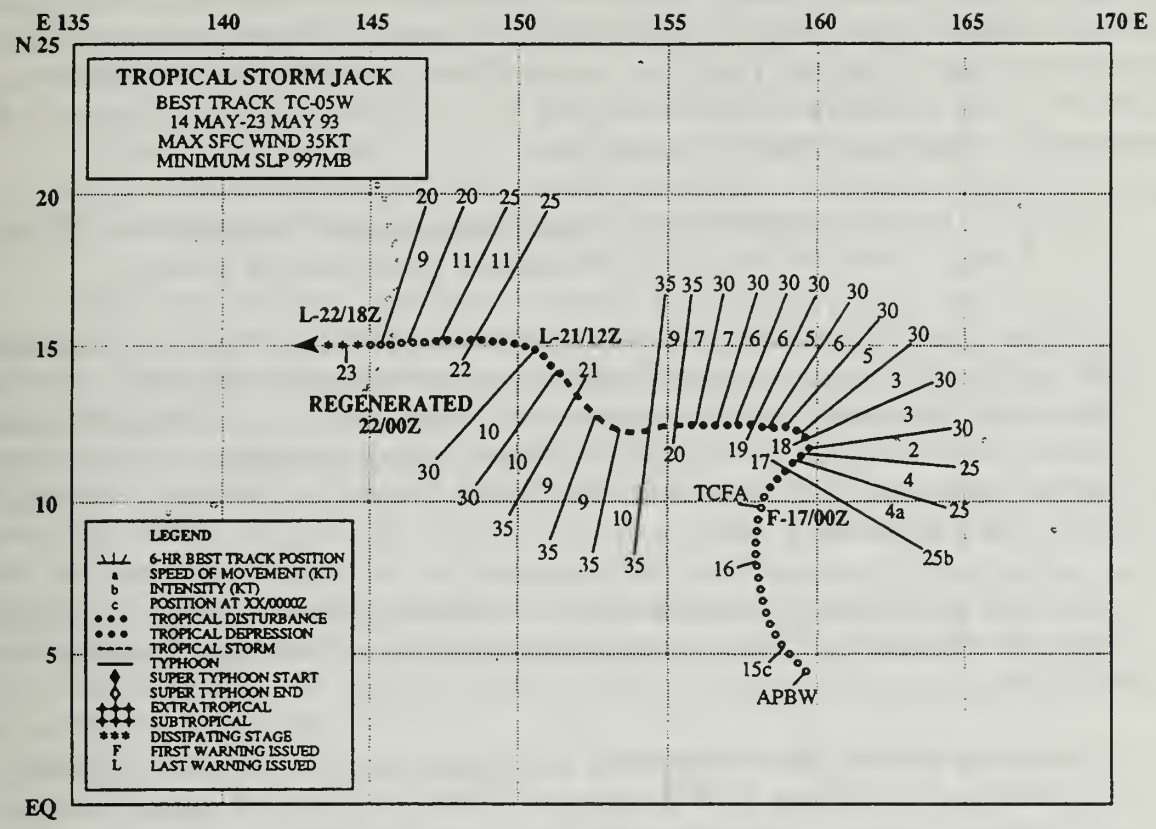

Fig. 4.18 Best track for TS Jack during 14-23 May 1993.

Pattern with a prominent peripheral ridge to the southeast and a break in the subtropical ridge to the north. As expected, Jack is moving on a poleward-oriented track (Fig. 4.18). The deep midlatitude trough that protrudes remarkably far equatorward (to nearly 15°N in the vicinity of Jack) represents a ridge-eroding mode of SRM.

Over the next three days (Figs. 4.17b-d), the deep midlatitude trough is replaced by much more zonal flow, so that a distinct subtropical ridge circulation is re-established to the north of Jack. This change, combined with the weakening of the peripheral ridge to the southeast, puts Jack in the DR Region of a S Pattern. Confirmation that a transition from N/NO to S/DR has occurred is provided by the track direction change from northward to westward during the 24-h period centered on 0000 UTC 18 May (Fig. 4.18). Even though weakening of the peripheral ridge is certainly a contributor, the N/NO to S/DR transition is probably most associated with the subtropical ridge-building mode of SRM. This case illustrates that Environment Structure transitions leading to such major track changes may involve more than one transitional mechanism.

4.9 Summary

This section has described a number of refinements to the Systematic Approach meteorological knowledge base that reflect lessons learned from the development of the five-year climatology (Chapter 2) and the results of the reproducibility test (Chapter 3). A summary of these refinements and how they fit into the overall framework of the meteorological knowledge base is given below:

- small TCs may be expected to follow west-southwestward tracks in the DR Region of a S Pattern when the axis of the subtropical ridge has such a slope;

- it is not possible to distinguish consistently between the N1 and N2 Patterns, so that a single N Pattern is adopted, while acknowledging that transitions into the N Pattern can be accomplished in a number of ways including: (i) Ridge Modification by a single "large" TC (RMT); (ii) TC-independent evolutions of the large-scale environment; and (iii) Reverse-oriented Trough Formation (RTF) by the combined RMT effects of multiple TCs;

- variations in N Pattern orientations (as defined by the slope of the peripheral ridge) can account for TC track directions ranging from northwest clockwise to east-northeast;

- forecasting whether the environment of a certain range of larger than average TCs will undergo a S/DR to S/WR versus a S/DR to N/NO transition as the TC approaches a break in the subtropical ridge will be difficult due to an inherent overlap in the effects of the BEP and RMT TC-Environment transformations;

- the translation speed of monsoon gyres (MGs) may range from quasi-stationary to magnitudes exceeding the translation speed of a TC within the G Pattern, which may result in significant variations in the track of a TC being advected around the translating MG;

- the G Pattern model of CE has been augmented to account for MG formation (MGF) in the vicinity of pre-existing TCs (i.e., N/NO to G/NO and S/DR to G/NO transitions occur), and MG dissipation (MGD) before the TC dissipates or is advected out of the G Pattern;

- the relative frequency of the six modes of TCI has been assessed (Table 4-1);

- TCI3 from the peripheral ridge of a western TC nearly always results in a eastern TC track that is south of west;

- TCI4 not only tends to inhibit the S/DR to N/NO transition, but may also cause (or at least contribute to) a reverse N/NO to S/DR transition by eroding a pre-

existing peripheral ridge associated with the TC being affected;

- a new Reverse-oriented Trough Formation (RTF) TC-Environment transformation conceptual model has been introduced to account for the formation of a N Pattern in association with multiple TCs; and

- a new Subtropical Ridge Modulation (SRM) conceptual model has been introduced to account for Environment Structure transitions in which superposition of a midlatitude trough or ridge plays a major role.

Since several new conceptual models have been added, the depiction of the Systematic Approach provided collectively by CE Tables 3.1-3.3 and CE Figs. 3.4 is deficient. This deficiency is corrected in Fig. 4.19 by combining the content of CE Tables 3.1-3.3 and CE Fig. 3.3 into one illustration of the new structure and content of the meteorological knowledge base. Unlike CE Fig.3.3, the broader concept of transitional mechanisms appears explicitly in Fig. 4.19 with the TC-Environment Transformation conceptual model set and the largely TC-independent Environment Effects conceptual model set now appearing as two sub-groups within the Transitional Mechanisms conceptual model group. The two basic types of Environment Structure transitions that may arise from certain of the Transition Mechanisms is still appropriately illustrated by CE Fig. 3.4. Thus Fig. 4.19 and CE Fig. 3.4 together provide the new conceptual framework of TC motion in the Systematic Approach.

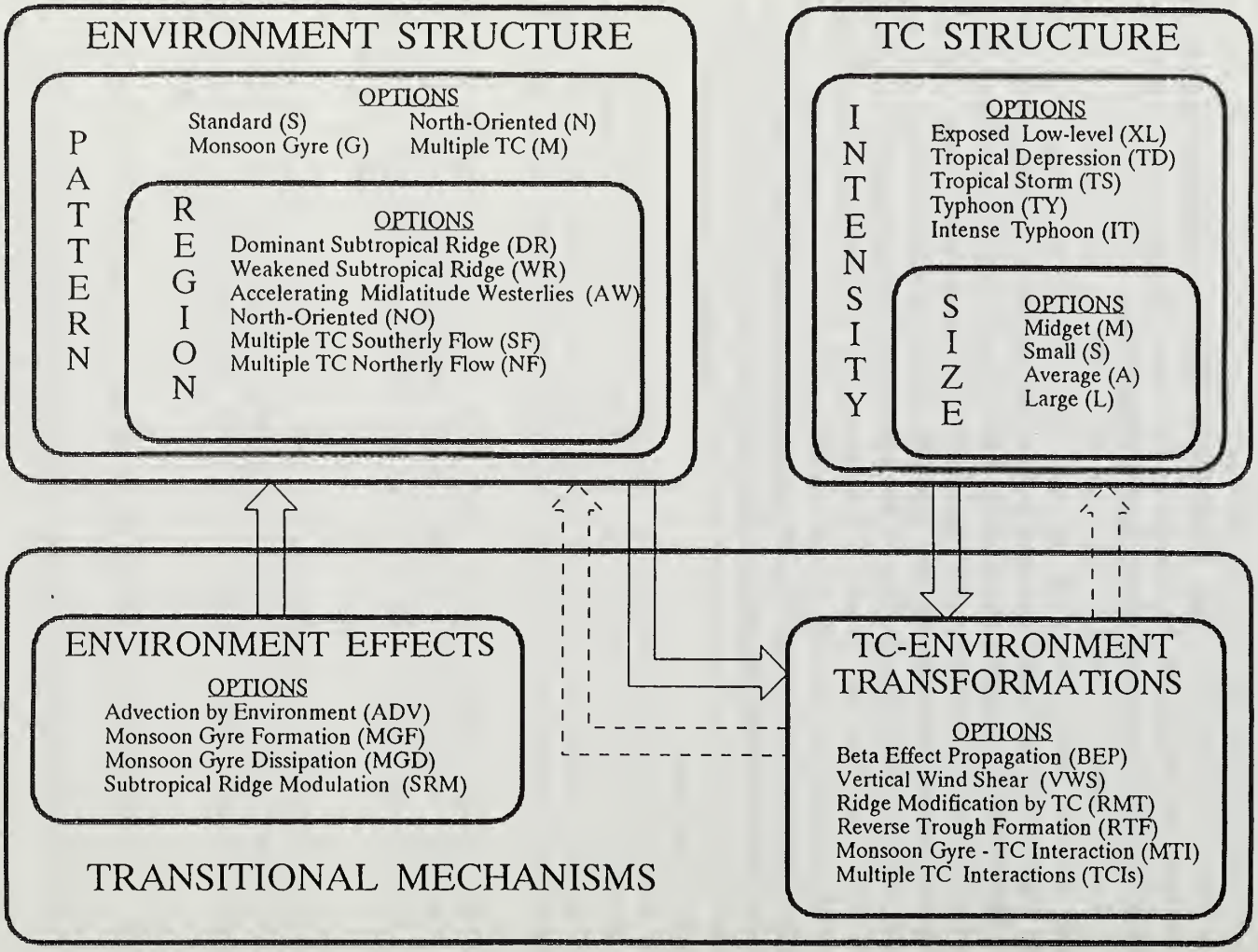

Fig. 4.19 New conceptual framework of TC motion effects of Environmental Structure and TC Structure that expands the list of TC-Environment Transitions to include RTF and separates Environment Effects as a separate subgroup of Transitional Mechanisms. These Environmental Effects include new coneptual models MGF, MGD, and SRM.

5. Application Guidelines for the Meteorological Knowledge Base

5.1 Background

A complex array of Environmental Structure transitions among the ten possible Synoptic Pattern/Region combinations have been observed (Figs. 2.8 and 2.9) to recur in the western North Pacific in response to one or more of eleven identified transitional mechanisms (Table 2-3). One of the key lessons learned from the reproducibility test discussed in Chapter 3 was that the three trainees had significant difficulty in correctly identifying some of the transitions. Although the transition detection rate was high (greater than 80.9% since the "missed" category in Table 3-6 includes "detected but wrong") and the false alarm rate was low (6.1%), only about half (48.3%) of the transitions were correctly identified. In the other 32.7% of the cases, the transition selected by the trainees was "similar" to the correct Pattern/Region combination in the sense that a similar TC track change would result. Often when the transition was S/DR to G/NO, one or more trainees mischaracterized the transition as S/DR to N/NO because they failed to recognize the formation of a MG in the vicinity of the TC. The two transition characterizations are nevertheless similar in that a poleward track change results. As noted in Chapter 4.3, the S/DR to S/WR and S/DR to N/NO transitions are also sometimes difficult to distinguish.

Minimizing the frequency of such incorrect (even though similar) transition assignments is important for two reasons. First, a generally similar TC track change might be followed by quite a variety of track evolutions. For example, a cyclonical TC track around the MG and then toward the northwest would normally be expected following a S/DR to G/NO transition. By contrast, sinuous northward or northeastward motion typically occurs following the S/DR to N/NO transition. Second, numerical TC forecast guidance may be expected to have different forecast traits (biases) following transitions into two different patterns. For example, a transition into a G Pattern typically involves a small TC that, along with the MG, may be poorly resolved in the numerical model, which increases the likelihood of a significant degradation of the TC track forecast. By contrast, a transition from S/DR to N/NO involving a relatively large TC that is more likely to be well represented in the numerical model may result in little or no bias in the track guidance.

Most of the transition mischaracterizations were in part attributable to two key weaknesses in the meteorological data base. The first weakness was the need for refinements to the meteorological knowledge base to address a wider variety of scenarios than CE had anticipated. This weakness has been addressed in Chapter 4. The second weakness was that the trainees needed assistance in considering: (i) which transitions are possible from a given Synoptic Pattern/Region combination, and of those, which are the most probable in various situations; (ii) the one or more key transitional mechanisms that are responsible for each of the possible transitions; and (iii) the key identifying satellite, numerical model, and TC track indicators that are usually associated with each of the possible transitions and transitional mechanisms.

In retrospect, this second weakness may simply reflect the Numerical Guidance Evaluation Process of the Systematic Approach (as represented by the flow chart in CE Fig. 2.1) has not been fully developed. An implementing methodology will be addressed in a forthcoming third technical report of this series. As an interim measure, some Pattern/Region transition recognition guidelines derived from the material in this report and CE are provided here.

5.2 Transition recognition guidelines

Although the transition summary in Fig. 2.9 may be intimidating, it is emphasized that the TC occupies only one Pattern/Region combination in the diagram at a specific time, and a limited set of transitions is possible. Only the specific transition paths leaving that Pattern/Region in Fig. 2.9 need be considered by the forecaster to discern whether: (i) the recent trends in numerical model analyses indicate a transition is imminent or in progress; or (ii) the numerical model forecasts fields *predict* that a transition will occur. To facilitate such considerations, a set of transition path schematics have been extracted from Fig. 2.9 to illustrate the relative probabilities among the possible transitions (including no transition when applicable) for each Synoptic Pattern/Region (Figs. 5.1 - 5.4). In addition to expanding upon the main points of the transition frequency discussion in Chapter 2.5, a number of other important relationships are brought out by these schematics.

To complement the transition probability schematics, Transition Guideline Tables 5-1 through 5-4 have been prepared. Each table is a distillation of information from CE and Chapters 2 and 4 of this report that a forecaster should consider in discerning whether a Environment Structure transition is occurring or will occur. A Transition Guideline table is given for each Synoptic Pattern, and the information is organized by possible transition paths from the highest to the lowest climatological probabilities. The key information is the probability information, seasonal variations, TC structure considerations, and potential indicators of transition and transitional mechanism that may be discerned from satellite imagery, numerical analysis fields, and TC track changes. Although Tables 5-1 to 5-4 are intended primarily for discerning transitions based on analyses, the tables might tentatively be used *with appropriate caution*[3] to discern transitions based on numerical model forecasts. Obviously, the satellite imagery indicators only apply to transitions that are actually in progress.

---

[3] Caution must be used when applying the Transitional Guideline tables as well as the Transition Frequency Schematics to numerical model forecast fields and TC tracks since model biases probably will alter both the relative probabilities of the possible transitions from a particular Pattern/Region combination, and alter the appearance and/or timing of certain model field and TC track indicators when forecast products are being used. The Numerical Model Traits knowledge base, which will be developed in the next technical report, will provide a compilation of such biases.

A TC in the S/DR combination (Fig. 5.1a) has five possible transitions plus the option of "no transition." Because this number of possibilities is significantly higher than for any other Pattern/Region combination (see also Figs. 5.2 - 5.4), evaluating possible Pattern/Region transitions from S/DR is a comparatively difficult task. However, notice that the transitions to N/NO and S/WR plus the "no transition" option account for 76% of all cases. In addition to being relatively rare, the other transition paths require the presence of another TC in the case of the M Pattern, or a MG in the case of a G Pattern. This observation suggests that the key first step in evaluating a potential transition from S/DR is to assess whether either a TC or MG is present or is in the process of developing in the proper location to allow a transition to the M or the G Patterns.

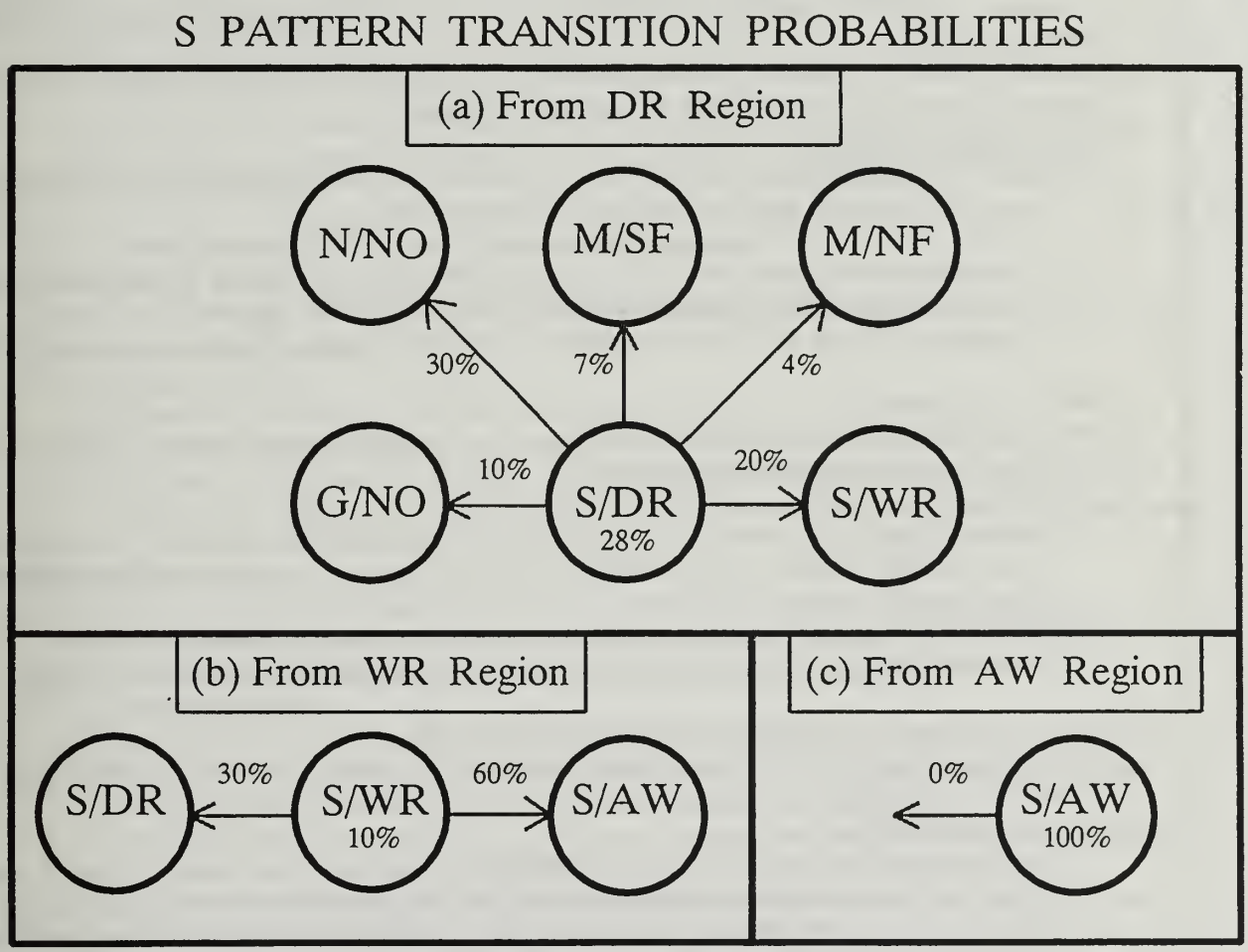

Fig. 5.1 Probabilities of a TC in a Standard (S) Synoptic Pattern either remaining in the present Region (percentage inside the central circle) for the entire life cycle, or transitioning to another Pattern/Region (circles at end of radials; percentages along radials) based on a five-year sample of western North Pacific TCs. Panels (a), (b), and (c) are for a TC presently in the DR, WR, and AW Regions, respectively, of the S Pattern.

Table 5-1 Transition guidelines to be used in conjunction with Fig. 5.1 to evaluate the possible transitions from the Standard (S) Pattern.

S Pattern Transition Guidelines

FROM DR REGION

No Transition: (28% of cases)

(1) More likely in situations involving smaller-than-average TC size (small BEP) and low amplitude midlatitute wave pattern (less SRM).

To N/NO: (30% of cases)

(1) Transition via RMT mechanism is more likely for larger-than-average single TC and relatively weak subtropical ridge.

(2) Transition via RTF mechanism becomes increasingly likely as the trough axis defined by multiple TCs (and/or disturbances) begins to take on a reverse orientation.

(3) Key transition indicators:

(i) building peripheral ridge to SE of TC(s) in NOGAPS 500 mb streamlines (use Streamline Test to assess ridge strength relative to subtropical ridge to north).

(ii) shift of 500 mb isotach maximum from north and east of TC to south and east.

(iii) increasing signs of cloud max-min-max pattern (Min area looks grey in IR imagery). Cloud signature may lead appearance of peripheral ridge in NOGAPS analyses.

(iv) anomalous slowing of TC well equatorward of latitude of pre-existing subtropical ridge axis.

To S/WR: (20% of cases)

(1) More likely for larger TCs (more BEP) at western end of subtropical ridge, especially if high amplitude midlatitude trough approaching (more SRM).

(2) Key transition indicators:

(i) absence of ridging poleward of TC in NOGAPS 500 mb streamlines (Caution: Thin ridges that can preclude/delay transition of small/midget TCs in DR Region are usually under-represented or missed in NOGAPS)

(ii) shift of 500 mb isotach maximum from more northward to more eastward of TC.

(iii) gradual slowing of TC speed that may or may not be accompanied by poleward turning.

To G/NO: (10% of cases-- occurs only during June to November)

(1) Reflects typical case of MG formation (MGF) to west of TC, which is often at disturbance stage (65% of transitions to G/NO).

(2) Key transition indicators:

(i) development of MG cloud pattern in satellite imagery (e.g., see Fig. 4.8 and CE Figs. 3.74a-b).

(ii) MG development usually depicted in NOGAPS 500 mb streamlines as broad cyclonic flow to west of TC, and may eventually appear as a large, closed cyclone. MG circulation development in NOGAPS often lags MG cloud pattern development, and MG center location may be inaccurate.

(iii) gradual turn by TC onto a more poleward track (may be absent if MG moving rapidly westward)

Table 5-1 (continued)

S Pattern Transition Guidelines
(continued)

FROM DR REGION (continued)

To M/SF: (7% of cases; average of 3 per year; favored during August - December)

(1) Key transition indicators:

(i) TC approaching threshold distance and required orientation relative to TC to west and subtropical ridge circulation to northeast.

(ii) Moderate TC translation speed increase, or absence of deceleration expected near ridge axis

To M/NF: (4% of cases; average of 2 per year, favored during August - December)

(1) Key transition indicators:

(i) TC approaching threshold distance and required orientation relative to TC to east and subtropical ridge circulation to northwest.

(ii) shift of 500 mb isotach maximum near TC from northeast quadrant to northwest quadrant

(iii) significant slowing (including stalling) of TC translation speed and potentially sharp equatorward turn.

FROM WR REGION

To S/AW: (60% of cases)

(1) More likely for larger TCs at western end of subtropical ridge with southwesterly flow enhanced by midlatitude trough digging equatorward to latitude of TC.

(2) Key transition indicators:

(i) increasingly prominent, unbroken cirrus outflow to NE of TC in IR imagery.

(ii) TC convective cloud mass not separating from low-level circulation in VIS imagery.

(iii) TC track direction passing through north, and translation speed beginning to show significant increase (may be modest if westerlies are particular weak or if TC is in process of dissipating).

To S/DR: (30% of cases)

(1) Interruption of normal recurvature into S/AW by either ridge-building on poleward side (SRM; 67% of cases) or when approaching mid-latitude trough shears apart TC (westerly VWS; 33% of cases). Westerly VWS favored after late October in vicinity of Northeast Monsoon flow.

(2) Key transition indicators:

(i) In westerly VWS cases, increasing separation of TC convective cloud mass from low-level circulation in VIS imagery. Cirrus plume streaming to NE remains prominent and unbroken as convective cloud mass separates from low-level circulation and recurves.

(ii) Track direction of TC (low-level in VWS cases) changes from northwestward and increasingly poleward to westward or even west-southwestward, and translation speed increases.

(iii) In SRM cases, development of cirrus plume streaming to NE reverses and a break (thinness) begins to develop (see Fig. 4.16c), and NOGAPS 500 mb isotach maximum shifts from the northeast quadrant of the TC to the northwest quadrant.

No Transition: (10% of cases-- TC dissipates before exiting region)

(1) Typically involves TDs or minimal TSs that weaken to <25 kt before transition to AW Region is accomplished.

FROM AW REGION

No Transition: (100% of cases-- TC recurves and dissipates or transitions to extratropical cyclone)

Notice that MGs (and thus G Patterns) developed only during June through November during the five-year period (Fig. 2.3b), and were most prevalent during July through September. Similarly, all but one of the M Patterns occurred during June through December. Thus, it will normally be within these periods that the forecaster must give careful attention to the possibility of transitions from S/DR to G/NO, to M/SF, or to M/NF. As indicated in Table 5-1, satellite imagery will be the primary tool for detecting the formation or approach of a second TC (transition to M Pattern) or formation of a MG (transition to G Pattern) in the vicinity of the TC. Whereas recognizing the formation of a second TC is relatively straightforward, MG cloud patterns are much more subtle and established cloud pattern recognition guidance has not been available. The discussion and examples in Chapter 4.5.2 provides interim guidance until a more complete analysis can be conducted. When a MG formation seems possible based on satellite imagery, a corroborative indicator is a broad turn from a westward direction of motion onto a more poleward-oriented track. As indicated in Chapter 4.5.1, such a turn may not occur if the MG is moving rapidly westward while influencing the TC.

For the relatively infrequent situations in which transition to M/NF must be considered, the key transition indicators from S/DR to M/NF (Table 5-1) for the western TC are a distinct shift of the 500 mb isotach maximum to roughly west of the TC, a deceleration, and a turn onto a west-southwestward track. By contrast, the transition to M/SF is more subtle, with no deceleration as the eastern TC approaches the subtropical ridge axis being an important clue.

Whenever the influence of a MG or another TC can be ruled out, the forecaster must only consider the three more probable options: no transition; transition to S/WR; and transition to N/NO. Although these options have roughly similar probabilities (see Table 5-1), a key factor that favors the "no transition" option is a small TC size, since smaller TCs propagate less and have a weaker, modifying effect on subtropical ridge structure. A transition to N/NO is favored if the TC is larger than average, if a 500 mb peripheral ridge is building to the southeast of the TC, and if the isotach maximum shift is shifting to the south and east. If a TC is approaching a break in the subtropical ridge without being accompanied by an increasingly prominent peripheral ridge to the southeast in NOGAPS, then a S/WR transition is indicated (additional key transition indicators are given in Table 5-1).

The transition possibilities from S/WR (Fig. 5.1b) are only two plus the option of no transition. However, the two possible transition paths from the S/WR combination represent arguably the toughest forecasting challenge that forecasters face -- the recurvature versus stair-step track dilemma. Based on the five-year climatology, recurvature is favored over stair-step by 2-to-1. Notice from Table 5-1 that an important satellite imagery indicator of transition from S/WR is the evolution of the cirrus outflow plume. Whereas plume development tends to confirm the S/AW transition (unless the TC is sheared apart due to VWS!), plume breakup and weakening points to a transition to S/DR. It is also important to notice that once recurvature has occurred, no transitions from the S/AW combination

were observed during the five-year period (Fig. 5.1c).

No TCs during the five-year period remained in the N/NO combination (Fig. 5.2a) for the remainder of the life cycle. Transition to N/AW is favored over transition to S/DR by a ratio of more than 2-to-1. However, recall from Chapter 2.4 that for 8 of the 20 transitions from N/NO to S/DR the presence of another TC to the east was a contributing influence to the erosion of the -induced peripheral ridge (i.e., the TCI4 transformation). If this second TC is not properly positioned to the east, the probability of transition from N/NO to N/AW increases 66% to 80%. The relatively rare (4%) N/NO to G/NO transition via transformation of the reverse-oriented trough into a MG occurs only from June - December. If neither a MG or properly positioned second TC are present, the probability of a transition from N/NO to N/AW rises to 84%, with the remaining 16% to S/DR. As indicated in Table 5-2, the key indicators for a transition to G/NO is the development of the characteristic MG cloud pattern in satellite imagery, and the development (usually delayed relative to the satellite signature) of a large cyclonic circulation to the west of the TC in the 500 mb analysis. Notice that no significant TC track change may occur during a transition from N/NO to G/NO, as the NO Region is common to both patterns. The key transition indicator to S/DR (Table 5-2) is a major shift of the 500 mb isotach maximum from the southeast to the north quadrant of the TC that is accompanied by an accelerating turn of the TC onto a predominantly westward track.

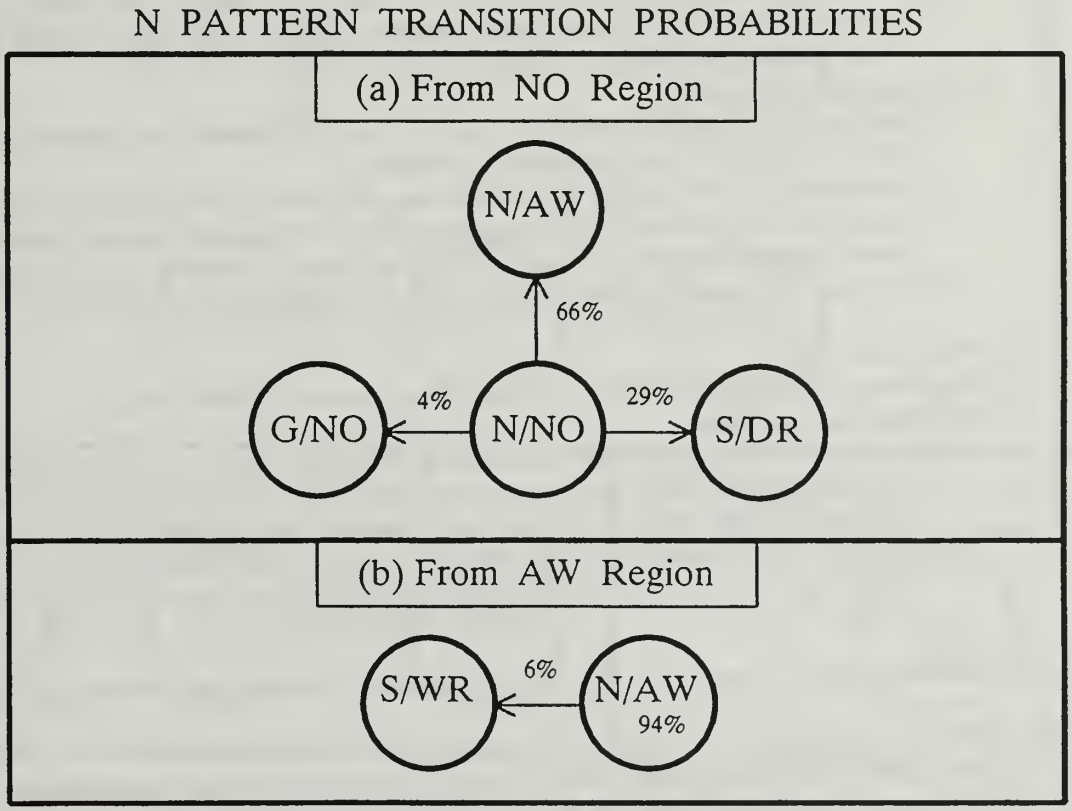

Fig. 5.2 Probabilities of transitions as in Fig. 5.1, except for the (a) NO and (b) AW Regions of the N Pattern.

Table 5-2 Transition guidelines to be used in conjunction with Fig. 5.2 to evaluate possible transitions from the North-oriented (N) Pattern.

N Pattern Transition Guidelines

FROM NO REGION

To N/AW: (66% of cases overall; but likely to be significantly larger if no TC to east (see **To S/DR** below))

(1) Expected result of environmental steering in a persistent N Pattern (assuming TC remains ≥ 25 kt)

(2) May be delayed if peripheral ridge to east of TC moves north with TC.

(3) Key transition indicators:

(i) commencement of accelerating right turn toward the east, particularly following a period of leftward turning.

(ii) Development of a cirrus plume to NE is weak and often delayed when transition occurs without the aid of a significant midlatitude trough to the north (e.g., see CE Figs. 3.56 and 3.58)

To S/DR: (29% of cases overall; but likely to be significantly smaller if no TC to east)

(1) Results from weakening of the peripheral ridge to the southeast and/or strengthening of the subtropical ridge arising from one or more of the following processes:

(i) TCI4 from another TC to east weakening β-induced peripheral ridge (factor in 40% of cases).

(ii) SRM-building of subtropical ridge due to midlatitude ridge passing to north (factor in 25% of cases).

(iii) Westerly VWS-induced change of steering level as TC shears apart (factor in 10% of cases).

(iv) Southwest drift of peripheral ridge to southeast of TC, which causes a break in the connection with the subtropical ridge circulation to the northeast.

(2) Key transition indicators:

(i) Shift of 500 mb isotach maximum near TC from southeast to north quadrant that is closely timed with items (ii) and (iv) under (1) above.

(ii) Weakening of RMT-related cloud max-min-max pattern; particularly when normal convective activity with increasingly cold cloud tops begins to replace the warmer (grey-appearing), and more stratiform mid-level clouds tops that manifest the presence of a strong peripheral ridge.

(iii) Increase in translation speed as track changes from poleward to westward.

To G/NO: (4% of cases)

(1) Represents MG Formation (MGF) in a pre-existing Reverse-oriented Trough.

(2) Key transition indicators:

(i) reverse-oriented cloud pattern that includes TC begins to take on a more curved appearance, and a cloud-minimum "moat" may begin to appear between TC cloud pattern and MG cloud ring if TC is not too far from MG center (see Fig. 4.9 and CE Figs. 3.90 and 3.91)

(ii) See item (2) (ii) under **To G/NO** transition under FROM DR in Table 5-1.

FROM AW REGION

No Transition: (94% of cases-- TC recurves and dissipates or transitions to extratropical cyclone)

To S/WR: (6% of cases)

(1) Associated with ridge building SRM as midlatitude ridge approaches from northwest.

(2) Key transition indicators: Same as for N/NO to S/DR transition above.

By contrast, the probability that a TC will remain in N/AW (Fig. 5.2b) until dissipation/extratropical transition is quite high (94%). However, the forecaster must be aware that a transition to S/WR (usually on the way to S/DR) is a small possibility, and reflects a dissipation of the peripheral ridge to the east of the TC.

Ten percent of the TCs in G/NO (Fig. 5.3a) will dissipate while in that Synoptic Pattern/Region. Transitions from G/NO to G/AW (via advection by MG) or to N/NO (via the MG-TC Interaction (MTI) transformation) are more probable than transitions to G/DR (via advection by MG) or S/DR (via advection by MG or MG dissipation) by a factor of nearly 3-to-1! Key observational indicators of the G/AW and N/NO transitions (Table 5-3) are: (i) the TC cloud pattern is on the periphery of the MG in the G/AW transition, whereas in the latter the TC cloud moves toward the center of the MG cloud pattern; and (ii) the TC motion is steadily poleward in the G/AW, whereas a significant deceleration and possible temporary equatorward turn is an indicator of a transition to N/NO.

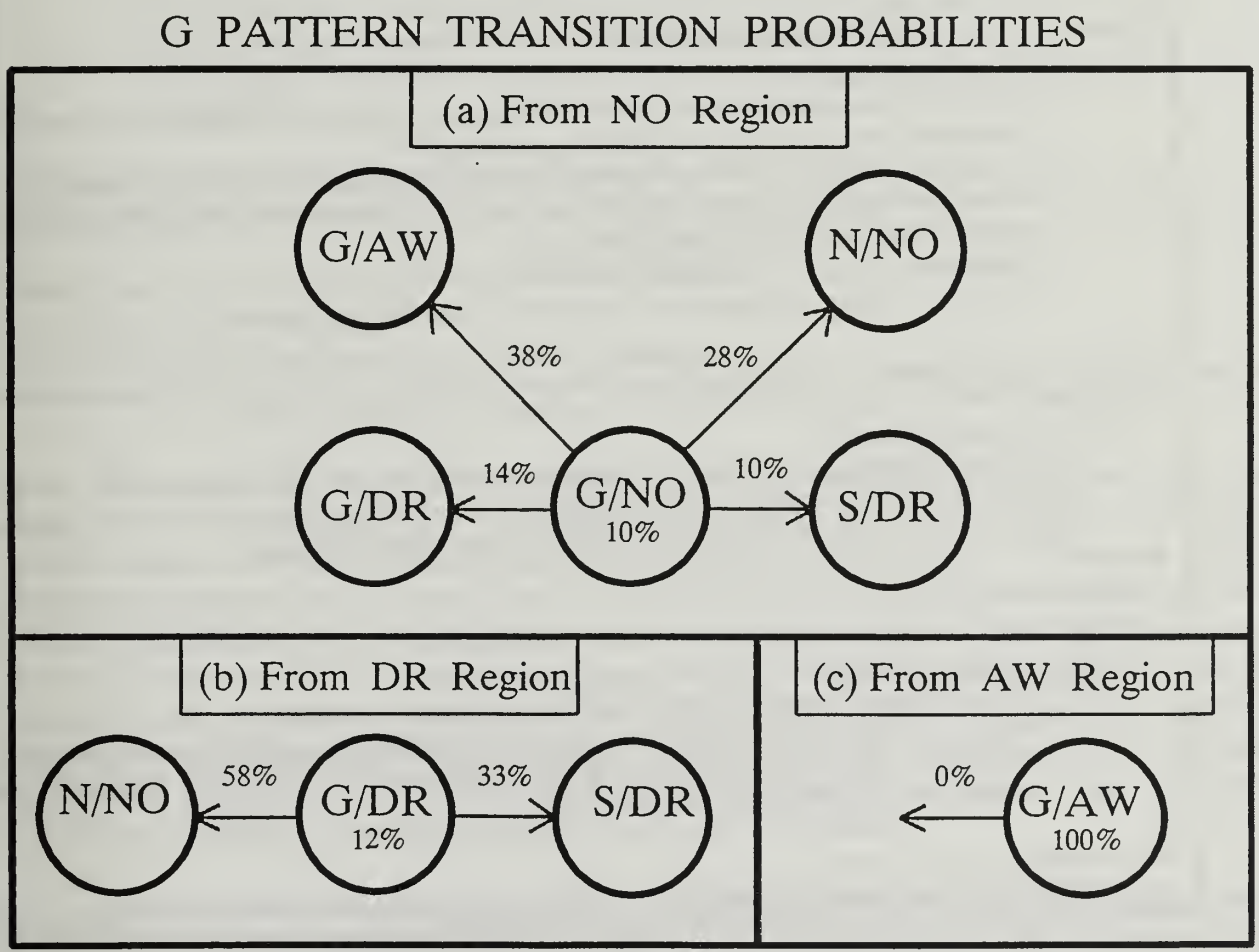

Fig. 5.3 Probabilities of transitions as in Fig. 5.1, except for the (a) NO, (b) DR, and (c) AW Regions of the G Pattern.

Table 5-3 Transition guidelines to be used in conjunction with Fig. 5.3 to evaluate possible transitions from the Monsoon Gyre (G) Pattern.

G Pattern Transition Guidelines

FROM NO REGION

To G/AW: (38% of cases)

(1) Results from advection of TC northwestward by MG circulation through weakness in subtropical ridge.

(2) Favored when TC location is well out on periphery of MG circulation as a subtropical ridge break is approached, so that TC is not drawn into DR Region by inner portion of MG circulation.

(3) Key transition indicators:

(i) TC nearing significant break in subtropical ridge in NOGAPS streamlines just to north of TC .

(ii) TC track becoming increasingly poleward, with minimal deceleration, and perhaps modest acceleration occurring *before* TC direction passes through north.

To N/NO: (28% of cases)

(1) Results from MG-TC Interaction (MTI)

(2) Key transition indicators:

(i) Shift of TC cloud pattern toward center of larger MG cloud pattern. Possible development of crescent-shaped convective cloud mass to southeast of TC.

(ii) Particularly rapid development of peripheral ridge to southeast of MG/TC in NOGAPS 500 mb streamlines, and an associated isotach maximum to southeast of TC. NOGAPS indicators may lag reality in particularly data-sparse areas.

(iii) Sudden slowing of TC translation speed and possible equatorward turn (or tight cyclonic loop), followed by sharp poleward turn and significant translation acceleration.

To G/DR: (14% of cases)

(1) Results from advection of TC by MG from northeast to northwest quadrant.

(2) Key transition indicators:

(i) TC cloud pattern location begins to appear somewhat west of north relative to MG cloud pattern.

(ii) Shift in 500 mb isotach maximum to slightly west of north of TC.

(iii) TC track toward west, usually with a slight equatorward component.

To S/DR: (10% of cases)

(1) Manifests a dissipation of MG while TC is in NO Region.

(2) Key transition indicators:

(i) MG cloud pattern becomes less prominent and eventually dissipates.

(ii) MG/TC circulation in NOGAPS may begin to shrink down to a scale more commensurate with size of TC. Note: Rate of circulation shrinkage depicted in NOGAPS may significantly lag reality, particularly in areas with little data.

No Transition: (10% of cases)

(1) Results from dissipation of TC before TC can be transitioned out of G/NO Pattern/Region combination.

Table 5-3 (continued)

G Pattern Transition Guidelines (continued)
FROM DR REGION
To N/NO: (58% of cases) (1) See (1) under **To N/NO** under FROM G/NO REGION above. (2) See (2) under **To N/NO** under FROM G/NO REGION above. **To S/DR:** (33% of cases) (1) Results from either: (i) MG dissipation while TC is in DR Region; or (ii) advection of TC westward and usually equatorward until TC escapes influence of MG. (2) Key transition indicators: (i) For MG dissipation cases see (2) in **To S/DR** under FROM G/NO REGION above. (ii) For advection of TC westward and away from influence of MG: (a) TC cloud pattern appears increasingly west of, and distinct from, MG cloud pattern. (b) TC circulation in NOGAPS streamlines becomes clearly separated from MG circulation to southeast. **No Transition:** (8% of cases; represents only 1 case in 5 years) (1) Results from dissipation of TC before TC transitioned out of G/DR Pattern/Region combination.
FROM AW REGION
No Transition: (100% of cases) (1) TC recurves and dissipates or transitions to extratropical cyclone.

The transitions to G/DR and S/DR (Table 5-3) are associated with generally gradual changes in TC track from the characteristic poleward direction of the G/NO to the predominantly westward direction in the DR Region of either the S or G Patterns. The key distinction between the two transitions is that G Pattern results from advection of the TC by the circulation of a persistent MG, whereas the S Pattern results from the dissipation of the MG. Since the MG is usually poorly resolved in NOGAPS streamline fields, carefully monitoring the evolution of the MG cloud pattern in the satellite imagery will usually be required to distinguish these two transitions. In particular, MG dissipation may be discerned by carefully looking for a weakening of the MG cloud pattern signature (e.g., less distinct cloud ring; cloud-free moat becoming less evident or absent).

From a G/DR situation (Fig. 5.3b), a transition to N/NO via the MG-TC Interaction (MTI) transformation is nearly twice as probable as a transition to S/DR. Notice in Table 5-3 that a transition from G/DR to S/DR may result from either advection around a persisting MG or dissipation of the MG. As for TCs in G/NO situations, careful monitoring of the MG cloud pattern in satellite imagery is important. When the MG persists,

monitoring the position of the TC cloud pattern relative to the MG cloud pattern can provide an early indication whether a N/NO versus a S/DR transition is in progress. A shift of the TC cloud pattern toward the center of the MG cloud pattern is expected during transitions to N/NO (i.e., manifesting the merger of TC and MG), whereas the TC remains on the periphery of the MG during transitions to S/DR via advection by the MG.

Only one TCS was observed to dissipate before transition from a G/DR situation could be accomplished. As was the case of the AW Region in the S Pattern, transitions from G/AW have not been observed (Fig. 5.3c).

Notice that for a TC in a M/SF situation (Fig. 5.4a), the probability of transition to either S/AW or N/NO are about roughly equal. For a TC in a M/NF situation (Fig.5.4b), the probability of a transition to S/DR or N/NO are equal (Fig. 5.4b).[4] Transitions from the M Pattern to the N Pattern were not anticipated in CE, and have been shown in Chapter 4.7 to result from a TC-Environment transformation called Reverse-oriented Trough Formation (RTF). The key indicator associated with a RTF-induced transition to N/NO (Table 5-4) is the development of a prominent northeast-to-southwest ridge circulation extending along the periphery of the TCs involved. Appearance of this ridge in the 500 mb streamlines with a concomitant shift of the 500 mb isotach maximum to the southeast of both TCs can be a key indicator that the N/NO transition is in progress. Since an accurate depiction (in NOGAPS analyses or forecasts) of the evolution of the peripheral ridge depends on an accurate representation of both TC circulations, the appearance or absence of the peripheral ridge circulation and associated isotach shift in NOGAPS analyses cannot be used as a sole indicator of whether a transition to N/NO is occurring. The appearance in satellite imagery of a cloud max-min-max pattern characteristic of a Rossby wave train extending southeast of the TC pair (or trio) provides probably the best corroborative evidence, although such a pattern is sometimes difficult to discern in real time.

---

[4] Recall from Fig. 2.9 that the number of cases on which these probabilities are based is rather small. Thus, significant changes in the relative probabilities may occur in a larger climatological data base. Nevertheless, the probability of a transition from either region of a M Pattern to a N/NO combination is likely to remain significant, and forecasters must be aware that such situations are possible.

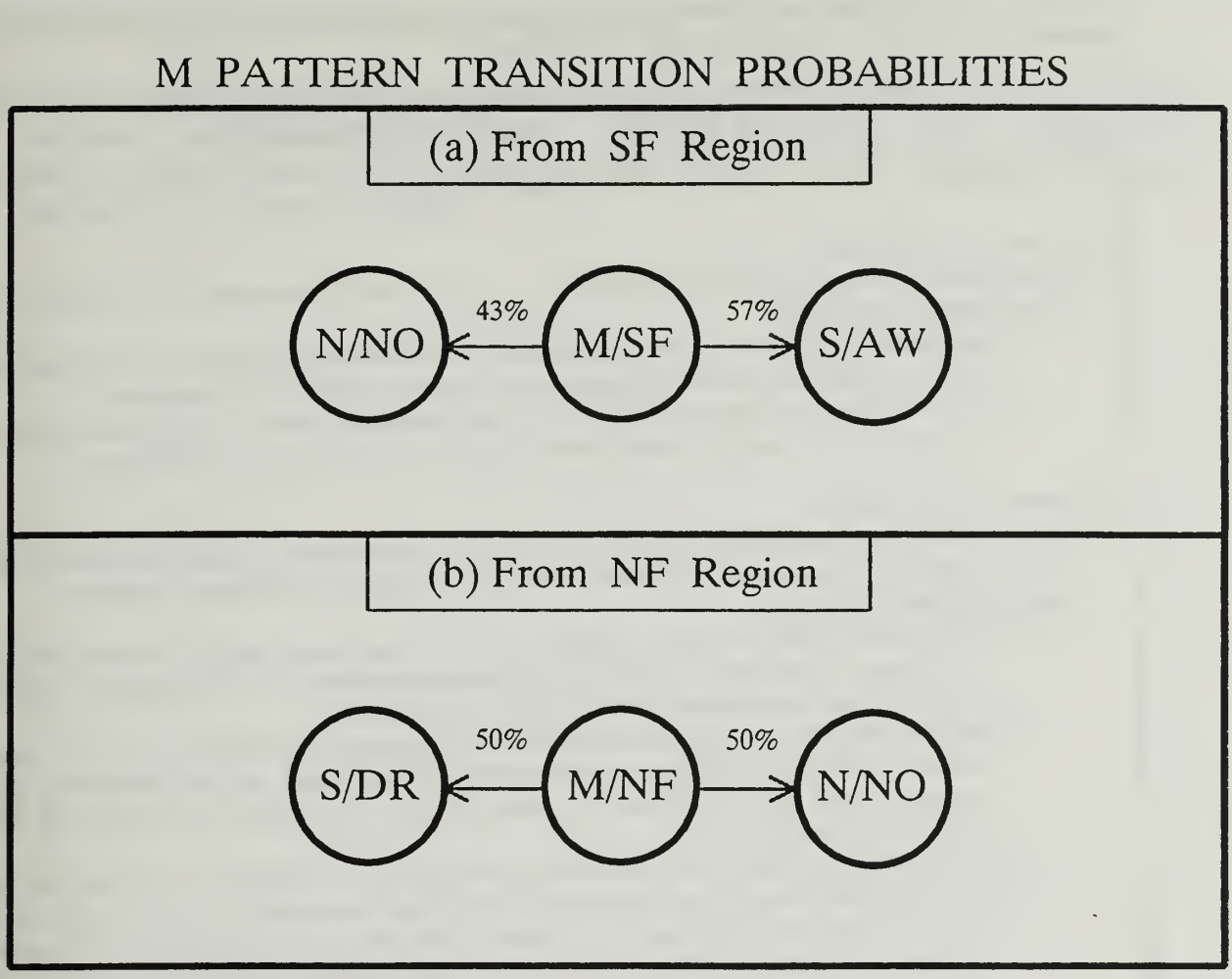

Fig. 5.4 Probabilities of transitions as in Fig. 5.1, except for the (a) Southerly Flow and (b) Northerly Flow of the Multiple (M) TC Pattern.

Table 5-4 Transition guidelines to be used in conjunction with Fig. 5.4 to evaluate possible transitions from the Multiple (M) TC Pattern.

M Pattern Transition Guidelines

FROM SF REGION

To S/AW: (57% of cases)

(1) Results from advection of TC poleward and out of M pattern by environmental steering in SF Region.

(2) Key transition indicators:

(i) Subtropical ridge begins to build to south of TC in NOGAPS streamlines, and isotach maximum begins to shift from northeast quadrant to southeast quadrant of TC circulation.

(ii) TC track direction passes to east of north and translation speed increases (acceleration may be modest initially since TC passed through ridge axis at higher than normal speed).

To N/NO: (43% of cases)

(1) Results from Reverse-oriented Trough Formation (RTF) mechanism building broad peripheral ridge to SE as trough axis defined by TCs begins to take on a southwest-to-northeast orientation.

(2) Key transition indicators:

(i) Development of an increasingly prominent, extensive peripheral ridge to south and east of line of TCs and/or disturbances in NOGAPS 500 mb streamlines. In particular, watch for increasingly poleward orientation of the peripheral ridge axis with time.

(ii) Shift of 500 mb isotach maximum from the northeast quadrant of the eastern TC to southeast quadrant. Look for this shift to be matched by a similar isotach shift for the western TC. In particular, watch for development of a single closed 30-kt isotach that extends along southeast peripheries of both TCs.

(iii) A significant poleward turn and slowing of the eastern TC translation speed that may be matched by a similar and usually more severe track change for the western TC. Look for this track change to occur at about the same time as the isotach shift mentioned in (ii) above. In a relative motion diagram, this collective change of track by the TCs involved may appear as a cessation (or significant slowing) of relative rotation (i.e., as the TCs begin to move on quasi-parallel tracks under the influence of the building peripheral ridge to the southeast.

FROM NF REGION

To S/DR: (50% of cases)

(1) Results from movement of the TC westward and equatorward out of the M Pattern owing to dominance of the environmental steering in NF Region over the northwestward BEP of the TC.

(2) Key transition indicators:

(i) Presence of increased ridging in NOGAPS streamlines to north of TC, and shift of isotach maximum from northwest quadrant of TC to north or northeast quandrant.

(ii) Increase of TC translation speed from 6-8 kt indicative of NF Region to the 10-12 kt typical of DR Region.

To N/NO: (50% of cases)

(1) See (1) under **To N/NO** in the FROM SF REGION above.

(2) Key transition indicators:

(i) See (i) under **To N/NO** in the FROM SF REGION above.

(ii) See (ii) under **To N/NO** in the FROM SF REGION above, except that isotach maximum shift is from the northwest quadrant to southeast quadrant.

(iii) See (iii) under **To N/NO** in the FROM SF REGION above, for comments about western TC.

REFERENCES

Carr, L. E., III, and R. L. Elsberry, 1994: Systematic and integrated approach to tropical cyclone track forecasting. Part I. Approach overview and description of meteorological basis. Tech. Rep. NPS-MR-94-002, Naval Postgraduate School, Monterey, CA 93943, 273 pp.

DISTRIBUTION LIST

Office of Naval Research (Code 322MM) 800 N. Quincy Street Arlington, VA 22217-5000	2
Dr. Robert L. Haney, Chairman Department of Meteorology, Code MR/Hy Naval Postgraduate School 589 Dyer Rd., Room 254 Monterey, CA 93943-5114	1
Dr. Russell L. Elsberry Department of Meteorology, Code MR/Es Naval Postgraduate School 589 Dyer Rd., Room 254 Monterey, CA 93943-5114	157
Library, Code 0142 Naval Postgraduate School Monterey, CA 93943	2
Dean of Research, Code 09 Naval Postgraduate School Monterey, CA 93943	1
Defense Technical Information Center Cameron Station Alexandria, VA 22304-6145	2